W. H. MUNSE
111 Talbot Lab.
University of Illinois
Urbana, Illinois

IL ENGINEERING STUDIES
STRUCTURAL RESEARCH SERIES NO. 218

THE EQUIVALENT FRAME ANALYSIS FOR REINFORCED CONCRETE SLABS

by
W. G. CORLEY
M. A. SOZEN
C. P. SIESS

A Report to
THE REINFORCED CONCRETE RESEARCH COUNCIL
OFFICE OF THE CHIEF OF ENGINEERS, U. S. ARMY
GENERAL SERVICES ADMINISTRATION,
PUBLIC BUILDINGS SERVICE
and
HEADQUARTERS, U. S. AIR FORCE,
DIRECTORATE OF CIVIL ENGINEERING

UNIVERSITY OF ILLINOIS
URBANA, ILLINOIS
June 1961

THE EQUIVALENT FRAME ANALYSIS

FOR REINFORCED CONCRETE SLABS

by

W. G. CORLEY
M. A. SOZEN
C. P. SIESS

A Report on a Research Project
Conducted by the

CIVIL ENGINEERING DEPARTMENT
UNIVERSITY OF ILLINOIS

in cooperation with the

REINFORCED CONCRETE RESEARCH COUNCIL

OFFICE OF THE CHIEF OF ENGINEERS, U. S. ARMY
Contract DA-49-129-eng-393

GENERAL SERVICES ADMINISTRATION, PUBLIC BUILDINGS SERVICE

and

HEADQUARTERS, U. S. AIR FORCE
Contract AF 33 (600) - 31319

UNIVERSITY OF ILLINOIS
URBANA, ILLINOIS

June 1961

TABLE OF CONTENTS

TABLE OF CONTENTS (Cont'd)

LIST OF TABLES

LIST OF FIGURES

LIST OF FIGURES (Cont'd)

LIST OF FIGURES (Cont'd)

1. INTRODUCTION

1.1 Object

The study presented here is concerned with the investigation of methods for determining moments in reinforced concrete slabs by the analysis of equivalent two-dimensional elastic frames. The study is based on the quantitative comparison of moments in slabs as determined from analysis and from tests.

Reinforced concrete as a material for the construction of slabs did not come into widespread use until soon after the beginning of the twentieth century. At this time, the only method available for determining the moments in these structures was that of the theory of flexure for plates. Since it was very difficult to obtain solutions to the plate problem by this method, it was not practical for use as a design procedure.

After a large number of reinforced concrete slab structures had been built and load-tested, an "empirical" method of determining moments was developed. The use of this method was restricted to structures with dimensions similar to those from which it was developed. It was soon recognized that some method was needed for extending the empirical method to structures with more extreme ranges of dimensions. For this reason, an equivalent frame analysis was developed which would give approximately the same results as the empirical design method.

Recently, the development of high speed digital computers has made it possible to obtain more solutions based on the theory of flexure for plates. In addition, more tests are available for use in correlating the theoretical solutions with experimental results. With the additional theoretical solutions and test results it has become possible to reinvestigate

the use of a two-dimensional frame analysis in order to determine its reliability as a method of analysis for reinforced concrete slabs.

The object of this investigation is to make a quantitative comparison of moments determined by the analysis of equivalent two-dimensional elastic frames with those determined from the theory of flexure for plates and from tests on both elastic and reinforced concrete models. After these comparisons are completed, recommendations are made for an equivalent two-dimensional frame analysis which may be used to obtain moments at the design sections in reinforced concrete slabs.

1.2 Scope

The second chapter of this report gives a detailed historical summary of the development of the analysis and design of reinforced concrete flat slabs. This summary gives an insight into the background of the present practice. Next, a number of solutions based on the theory of flexure for plates are presented. These solutions are then compared with moments obtained by the present ACI Code frame analysis. These comparisons include:

1. A typical panel of an infinite array of uniformly loaded square panels supported on circular column capitals.
2. A typical panel of an infinite array of uniformly loaded square panels supported on square column capitals.
3. A typical panel of an infinite array of uniformly loaded rectangular panels supported on square column capitals.
4. A loaded panel of an infinite array of square panels with strip loading for maximum positive moments and supported on square column capitals.
5. A nine-panel structure supported on infinitely rigid square columns and having no edge beams.
6. A nine-panel structure supported on infinitely rigid square columns and having deep edge beams on two adjacent sides and shallow edge beams on the other two sides.

In Chapter 6, a modified equivalent two-dimensional frame analysis is presented. Moments obtained by this method are then compared with those obtained from tests on both elastic and reinforced concrete models. The tests were carried out on the following models:

1. A six-panel aluminum flat slab.
2. A nine-panel Lucite flat plate loaded to simulate an an infinite array of panels.
3. A twenty-five panel Plexiglass flat slab.
4. A nine-panel reinforced concrete flat plate.
5. A nine-panel reinforced concrete flat slab.

Following the comparisons between measured moments and those computed by the proposed frame analysis, a detailed numerical example of this method is presented. For purposes of illustration, the numerical example is presented for the center row of panels of the nine-panel reinforced concrete flat slab model.

1.3 Acknowledgment

The studies presented in this report were made in connection with the investigation of Multiple Panel Reinforced Concrete Floor Slabs conducted in the Structural Research Laboratory of the Civil Engineering Department at the University of Illinois. The investigation is sponsored by the Reinforced Concrete Research Council; Directorate of Civil Engineering, Headquarters, U. S. Air Force; Public Buildings Service, General Services Administration; and the Office of the Chief of Engineers, U. S. Army.

The moments at the design sections of the reinforced concrete flat slab and flat plate test structures of the above investigation were made available by Mr. D. S. Hatcher, Research Assistant in Civil Engineering. Several solutions for plates supported on columns were obtained in the course

of a parallel investigation of slabs under Research Grant NSF-G 6572 from the National Science Foundation. The unpublished solutions were obtained through the courtesy of Dr. A. Ang, Assistant Professor of Civil Engineering. Thanks are due to the staff of the ILLIAC (The University of Illinois Digital Computer) for allowing machine time for portions of this study.

This report was prepared as a thesis under the direction of Professors C. P. Siess and M. A. Sozen.

1.4 Notation

a = one-half the span length measured in the direction of the x-axis

a_{mn} = a constant to be determined

A = the distance from the center of a column, in the direction of the span considered, to the intersection of the mid-depth of the slab and a 45-degree line lying wholly within the concrete

A^* = the distance from the centerline of a column, in the direction of the span considered, to the intersection of the bottom of the slab or drop panel and a 45-degree line lying wholly within the concrete. Maximum of one-eighth of the span length

A_{mn} = a constant to be determined

b = one-half the span length measured in the direction of the y-axis

b_1 = the length (the larger dimension) of each rectangular cross-sectional part of a beam

β = a constant which is a function of the cross section of a beam

c = effective support size

c_1 = effective support size in the direction of the span considered

c_2 = effective support size in the direction perpendicular to that of the span considered

E = modulus of elasticity of the material of a particular member

F = 1.15 - c/L but not less than 1.0

G = shearing modulus of elasticity of the material of a particular member

h = distance between node points of a finite difference network

h_1 = the height (the smaller dimension) of each rectangular cross-sectional part of a beam

H = story height in feet of the column or support of a flat slab

H_f = a ratio of beam flexural stiffness to plate stiffness

I = moment of inertia of a cross section

I_c = moment of inertia of the cross section of a column

I_s = moment of inertia of the cross section of a slab without an edge beam

I_{sb} = moment of inertia of the cross section of a slab including an edge beam

J = a ratio of beam torsional stiffness to plate stiffness

K = stiffness of a member defined as the moment required to rotate the end considered through a unit angle without translation of either end

K_c = stiffness of a column

K_s = stiffness of a slab panel

K_{bc} = stiffness of a beam-column combination

L = length of panel, center to center of columns

L_a = length of panel in direction of the short span

L_b = length of panel in direction of the long span

L_1 = length of panel in direction of the span considered

L_2 = length of panel in direction perpendicular to that of the span considered

m = an integer, 1, 2, 3, ... ∞

m_1 = a distributed torque applied along the axis of a beam

M_n = bending moment at the negative design section

M_o = sum of positive and negative moments in a panel

M_p = bending moment at the centerline of a panel

M_s = total static moment in a panel

M_x = bending moment per unit width of plate in the direction of the x-axis

M_y = bending moment per unit width of plate in the direction of the y-axis

M_{xy} = twisting moment per unit width of plate

$M_{\text{¢}}$ = bending moment at centerline of supports

μ = Poisson's ratio

n = an integer, 1, 2, 3, ... ∞

$N = \frac{Et^3}{12(1-\mu^2)}$ = a measure of the stiffness of the plate

Φ = angle of twist per unit of length

q = distributed load per unit of area

t = thickness of a plate

t_1 = minimum thickness of a flat slab

t_2 = thickness of a flat slab and drop panel

T = twisting moment

θ_f = total angle of rotation (caused by an arbitrary moment) of the end of a column without translation of either end

θ_t = average angle of rotation (due to twisting) of a beam with respect to a column

θ'_t = the reduced average angle of rotation of a beam with respect to a column

v_s = uniformly distributed shear about the perimeter of a column capital

V = total shear at the column centerline (as determined from the equivalent frame analysis)

V_x = vertical shear per unit width of plate

V_y = vertical shear per unit width of plate

w = distributed load per unit of area

w^* = final deflection of a plate, positive downward

W = total load on a panel

W_d = total dead load on a panel

W_L = total live load on a panel

x = coefficient of span length which gives the distance from the center of column to the critical design section

2. THE HISTORICAL DEVELOPMENT OF FRAME ANALYSIS

2.1 Historical Development of Plate Theory*

The earliest studies of the flexure of plates were in connection with sound-producing vibrations. Euler appears to be the first to approach the problem (2)**. After developing his theory of the flexure of beams, he attempted to explain the tone producing vibrations of bells by assuming them to be divided into narrow rings which would act as beams. This method did not prove satisfactory. A few years later Jacques Bernouilli attempted to treat a square plate as a system of crossing beams (3). This theory also proved unsatisfactory when compared with experimental results. Both of these early approaches to the problem involved two-dimensional systems of beams which were used to replace the three-dimensional slab.

In the early part of the nineteenth century, the French Institute offered a prize for a theoretical analysis of the tones of a vibrating plate. After several unsuccessful attempts, Mlle. Sophie Germain won the prize in 1815 with a derivation of a fundamental equation for the flexural vibrations (4). This equation had been suggested by Lagrange in some earlier private correspondence; thus, it became known as Lagrange's equation for the flexure and the vibrations of plates. It was essentially the same as Eq. 5 in Chapter 3.

In the next few years, a great deal of work was done with Lagrange's equation. Navier solved this for the case of a rectangular plate with simply supported edges in a paper presented to the French Academy. A few years later, Poisson offered a derivation based on the stresses and deformations at

---

* For a more detailed historical summary see pp. 417-423 of Ref. 1

** Numbers refer to entries in the List of References.

all points of the plates (5). He also derived a set of general boundary conditions and obtained solutions for circular plates for vibrations and for static flexure under a load symmetrical with respect to the center. Contrary to the case of earlier solutions, Poisson's theoretical results agreed closely with experimental results.

In 1850, Kirchhoff published a paper in which he derived Lagrange's equation and the corresponding boundary conditions by the use of energy methods (6). Kirchhoff found one less boundary condition than had Poisson, but it was later shown that two of Poisson's boundary conditions were inter-related and both solutions were correct (7). At this point, investigators turned to the question of the limitations of the plate theory. Boussinesq's investigations established that the plate theory is applicable to plates of medium thickness (8). He found that when the ratio of thickness to span is either very large or very small, the structure ceases to act as a plate and the plate theory no longer applies.

During this same period, the interest was changing from the problem of sound-producing vibrations to the problem of strength and stresses. This led to the need for numerical results from application of the theory. Several people worked on the problem of a plane boiler bottom supported by stay bolts. Since this is essentially the same problem as that of a homogeneous flat slab under uniform load, these solutions are of interest.

Lavoinne appears to be the first to arrive at a satisfactory solution to the problem of the plane boiler bottom supported by stay bolts (9). He approached the problem by means of a double-infinite Fourier series and solved Lagrange's equation for a uniformly loaded plate consisting of an infinite array of rectangular panels. The supporting forces due to the stay bolts were assumed to be uniformly distributed within small rectangular areas

at the corners of the panels. In 1899, Maurice Levy solved the problem of rectangular plates on various types of supports by means of a single-infinite series depending on hyperbolic functions (10).

At about the same time, some investigators were approaching the problem from a more practical point of view. The most important of these investigations were those of Bach (11,12). In his experimental work, he determined that the line of failure in a simply supported square plate is along its diagonals. The average moment across a diagonal of a simply supported square plate can be computed on the basis of statics. Bach determined some empirical constants which he could multiply the average moment by in order to determine the distribution of the moment along a diagonal. He then approached the problem of the plane boiler bottom supported by stay bolts in the same manner. Thus, Bach arrived at a semi-empirical method of analysis based on the very simple assumptions of statics.

After the turn of the century, an increasing need for numerical solutions to Lagrange's equation became apparent. Modern mathematical methods have opened the way for a number of numerical solutions. In 1909, Ritz published an approximate method for solving the elastic plate problem (13). In this method, a number of functions are chosen with unknown variable coefficients. A finite number of these coefficients are then determined on the basis of energy methods. This method is general and can be applied to any elastic structure.

In 1920, Nielsen published a book in which he solved the elastic plate problem by means of finite differences (14). In this method, differentials of differential equations are replaced by finite differences and the solution reduces to a series of linear algebraic equations. Although this method is also approximate, very good results can be obtained if a sufficient

number of points is chosen. Since Nielsen's book was published, several others have presented solutions by means of finite differences (References 15, 16, and 17).

Yet another approach is that used by Nichols in a paper published in 1914 (18). In this paper, Nichols used basically the same approach that Bach had used earlier. On the basis of elementary statics, he determined the total moment that must be carried in a single panel. This general approach was later accepted by most practicing engineers and was incorporated (in greatly modified form) into a number of building codes. Although Nichols originally developed this for a particular set of conditions, the method is quite general and can be extended to cover all cases of various capital shapes and sizes, various ratios of span length to span width, and various distributions of shear at the supports. An interesting discussion of this method was given in a paper by C. P. Siess published in 1959 (19).

2.2 Construction of Early Slabs

The use of reinforced concrete in the construction of floor slabs dates back to the middle of the nineteenth century. The earliest record of its use is that of a patent granted to William Boutland Wilkinson in Great Britain in the year 1854 (20). This patent called for flat bars or wire rope to be used as reinforcement "where tension is expected in the concrete." In 1865, Wilkinson constructed a house made entirely of reinforced concrete. The first story walls were 12 in. thick and the second story walls were 9 in. thick. The floor of the second story consisted of a grid of beams 26 in. on center and 6.5 in. deep reinforced with 5/16 to 3/8-in. twisted wire rope. Precast plaster panels were placed between the beams and a 1-1/2-in. slab reinforced with 3/16 x 3/8-in. steel flats was cast over the entire area. The slab had a span of about 12 by 12 ft.

The next evidence of the use of this type of construction is that of a patent granted to a Lieutenant Colonel Scott of the British Army Engineers in the year 1867 (21). Sketches indicate that this slab was reinforced with iron bars throughout the bottom with wire mesh embedded in the concrete.

Between 1867 and the turn of the century, several other patents were issued for various types of floor slabs constructed of concrete and metal. These systems were generally of two basic designs. In one system the design was on the basis of a flat tied arch with the reinforcing bars acting as tie rods. The other system was designed on somewhat the same basis as a suspension bridge. The reinforcement was draped from one support to the next in the shape of a catenary and the concrete was used as a filling material. In both cases, the concrete was given only a minor role in the strength of the structure. Neither the flat arch nor the suspension system proved to be an economical basis for the design of reinforced concrete floor systems. Consequently, there was little interest in this type of construction before the development of what is now known as the flat slab.

The first use of flat slab construction can be attributed to C. A. P. Turner. As early as 1903 he made up plans which were very similar to his early type of "Mushroom Floor." These plans were never used, however. Turner's next attempt to incorporate this type of construction into a building met with the disapproval of the Building Department and was also abandoned. In 1905, Turner presented his mushroom system in a discussion to a paper appearing in the Engineering News (22).

In 1905, the first modern flat slab was used in the C. A. Bovey-Johnson building in Minneapolis. The Building Department refused to grant a permit for this building except on the basis of an experimental structure. It was therefore agreed that the floor would be required to stand a test

load of 700 lbs per square foot with a maximum deflection of 5/8 in. at the center of any panel. The entire five-story structure was completed before the load test was performed. Upon completion of the structure, two adjacent panels were loaded with wet sand to a load of 750 psf. The total deflection at this load was only 1/4 in., thus, the first flat slab was a success.

A few years later, 1908, Robert Maillart, apparently unaware of Turner's success, built a model of a modern flat slab and tested it to failure (23). On the basis of this experiment, he quickly saw the advantage of this type of construction. In 1910, Maillart acted as consultant for the Lagerhaus-Gesellschaft building in Zurich. This was the first use of modern flat slab construction in Europe.

Here, for the first time, was a truly economical method of constructing reinforced concrete floor systems. Not only were less materials required, but the cost of formwork was also sharply reduced. The flat slab also offered other advantages such as flat ceilings and reduced over-all height in multi-story buildings. In view of these advantages, this type of construction became popular very quickly. By 1913 over 1000 flat slabs had been constructed.

2.3 Development of Empirical Analysis

Since flat slabs were considered a totally new type of construction and at this time little was known about reinforced concrete as a construction material, a load test was required of all early flat slab structures. However, it was not until 1910 that the first detailed test of a flat slab was made and reported in the literature. This was a load test of the Deere and Webber Building in Minneapolis, Minnesota (24). In this test, nine panels of 60 were loaded and both deflections and strains were reported. After this, many more tests were performed and reported in some detail.

In 1921, Westergaard and Slater presented a paper in which they summarized the most important tests reported up to that time (1). Table 1 shows some of the important features of the tests and the test structures. Steel strains, concrete strains, and deflections were reported for the loaded panels in nearly all of these tests.

In the early load tests, an attempt was made to compute moments from strains using the straight-line theory. On this basis, the flat slab appeared to have an extremely high capacity. It was quickly recognized that the straight-line theory did not properly consider the tension carried by the concrete and should not be used without modification.* Since flat slabs commonly have a very low percentage of steel, the amount of tension carried by the concrete is quite large and cannot be disregarded. Slater approached this problem by first determining relations between steel strain and moment in simple beams and then using these relations to determine the moments in test slabs (1). This procedure proved to be a great help in decreasing the discrepancy between theoretical moments and measured moments. Recent tests at the University of Illinois indicate that the moment carried by tension in the concrete is extremely sensitive to the properties of the concrete (26). Since Slater did not use beams cast of the same materials as those of the test slabs, his adjustment of moments as measured from steel strains cannot be considered rigorous. The tension in the concrete must, therefore, be considered as a major cause of differences between measured results and theoretical results as reported in Reference 1.

There were at least two other sources of error in the interpretation of the early flat slab tests which were not recognized and consequently not

---

* See the discussions of Reference 25.

considered. These can be referred to generally as the neglect of moment carried by adjacent panels and the neglect of the twisting moment around the columns.

The amount of twisting moment carried by the concrete in the vicinity of the columns depends upon the geometry of the supports, the loading pattern, the amount of cracking, and the material properties. The most important of these (for loads less than those which will cause general yielding of the reinforcement) are the geometry of the supports and the loading pattern. For slabs with circular capitals, the twisting moments are quite small although they may still be important. For other shapes of capitals they become more and more important until they reach a maximum for square or rectangular columns. Results of solutions for the nine-panel slab in Reference 17 indicate that, for the case of one strip of panels loaded, twisting moments at the columns may be as much as 15 percent of the total static moment in one panel. Although this large moment would exist only until the concrete began to crack, there is no doubt that a portion of this moment would exist unless the slab were cracked through completely. This accounts for another portion of the discrepancy between the measured and computed results but does not explain it completely.

Another source of error in interpretation is the neglect of moments carried by the panels adjacent to those which were loaded. The error due to neglecting these moments can be quite large. The analysis of the nine-panel slab in Reference 17 indicates that this may be as much as 25 percent of the total moment when only one strip of panels is loaded. Figure 1 shows the computed moments at various sections with the center strip of panels loaded. It can be seen that the sum of the positive and negative moment in the center panel is only about 75 percent of the sum of the positive and negative moments

across the entire width of the structure. Although this is a much more severe case than those of the early slab tests, it indicates that neglecting the effect of adjacent unloaded panels can have a rather large effect on the total moment in a span.

On the basis of the information presented above, it appears that the lack of agreement between theory and the results of early tests is due to an improper consideration of the amount of tension carried by the concrete, neglect of twisting moment at the column capitals, and neglect of the effects of unloaded spans adjacent to the loaded spans. The most important of these appears to be the error in the amount of tension carried by the concrete.

2.4 Development of Empirical Design Method

Prior to the publication of the paper by Westergaard and Slater (1), many engineers believed that flat slabs carried load in some mysterious way and that statics might not apply. Although some engineers recognized that the apparent discrepancy was due to the errors in interpretation cited above, few people were willing to accept this explanation.

In 1914, Nichols derived a relation for the total moment in one panel of a flat slab using simply the principles of statics (18). He then suggested a simple approximate equation for this relation which gives results within less than 1 percent of the static moment. The approximate relation can be stated as:

$$M_o = \frac{WL}{8}\left(1 - \frac{2}{3}\frac{c}{L}\right)^2 \qquad (1)$$

where M_o = sum of positive and negative moments in one panel

W = total load on one panel

L = length of panel, center to center of columns

c = diameter of column capital

The early tests of flat slabs did not appear to verify this. Moments computed from steel strains on the basis of the straight-line formula indicated that much lower moments were presented than Eq. 1 would indicate. On this basis, the 1917 edition of the ACI Building Code permitted an empirical method of design for a total moment given by the relation:

$$M_o = 0.09\ WL\ (1 - \frac{2}{3}\frac{c}{L})^2 \qquad (2)$$

This equation gives moments of approximately 72 percent of the static moment in a panel.

In Reference 1, Slater attempted to give some idea of the capacity of slabs designed by the various methods used at that time. In order to account for the tension carried by the concrete, he took the results of several tests on simple beams and developed relations between measured steel stresses and steel stresses which would exist if no tension were present in the concrete. He then computed moments from the steel strains measured in a number of test structures. These moments averaged about 90 percent of that given by Eq. 1. The scatter of the moments computed for the various test structures indicated that a considerable error was introduced by using beams made of material properties differing from those of the slabs in order to account for the tension in the concrete. Other sources of error are indicated in Section 2.3.

In order to compute the safety factor of the test structures, Slater first determined the average stress in the steel which would exist under the test load if no tension were carried by the concrete. This was done by first using the curves determined from beam tests to convert the measured steel stresses to equivalent stresses with zero tension in the concrete and then adding to this the dead load steel stresses computed by the straight-line theory on the basis of the moment given by Eq. 1. Next, he extrapolated his

beam test results to determine the apparent steel stress when the steel reached its yield point. He then took the ratio of the apparent yield stress of the steel to the stress which was measured under the test load and corrected for tension in the concrete. This gave him the ratio of ultimate load to test load. Although his approach to the problem was correct, the accuracy of the results was limited by the accuracy of the beam test results. This resulted in rather high values of the ratio of ultimate load to test load.

Once the ratio of ultimate load to test load had been determined, factors of safety were determined on the basis of working loads computed by the various design methods. In order to have a consistent comparison, the steel was assumed to have an allowable stress of 16,000 psi at working loads and a yield stress of 40,000 psi. On this basis, Slater arrived at apparent factors of safety of 3 to 6 for structures designed for 100 percent of the static moment and 2 to 4 for structures designed by the 1917 ACI Code (Eq. 2).

The results of this investigation appear to be the primary justification for the empirical design method adopted by the ACI Building Code earlier on a less theoretical basis. It is apparent that, even with a working stress of 16,000 psi in the steel, the empirical method gave a rather low minimum factor of safety. When allowable steel stresses were increased to 20,000 psi, the safety factors were reduced even more.

It should be noted, however, that the safety factors discussed above do not reflect the true capacity of a structure when isolated panels are loaded. It also neglects the fact that most reinforcing bars used in structures will have a yield stress of more than the minimum 40,000 psi.

2.5 Development of Original Elastic Analysis

In early ACI Building Codes, no provision was made for design by any means other than the Empirical Method. Since the ACI Building Code

restricted the use of the Empirical Method to cases similar to those slabs from which it had been developed, it soon became apparent that a method was needed for extending this method.

One of the first attempts to treat a reinforced concrete flat slab structure as a system of equivalent two-dimensional frames was that presented by Taylor, Thompson, and Smulski in Reference 27. In this method, the slab in a typical bay was divided into component parts as determined by assumed lines of contraflexure. Moments were then computed for these individual parts considered as uniformly loaded simple structures. After the moments had been determined they were multiplied by a factor of about two-thirds and the result was taken as the design moment. This reduction was justified because, to quote the text, "the static bending moments do not take into account several factors [sic] which reduce tensile stresses in flat slab construction."

In 1929, a committee working on the California Building Code carried on an investigation to determine the applicability of the Empirical Method as well as to find a suitable method of extending it (28). From this study, a procedure was developed for computing moments in flat slabs by means of an elastic frame analysis. This method consisted of dividing the structure into a system of bents one bay wide. Stiffnesses of the members were found by taking into account all variations in moments of inertia of the members. After moments were determined for alternate span loading, a forty percent reduction in negative moment was allowed. This method was accepted in 1933 for inclusion in Uniform Building Code, California Edition.

At about the same time, an investigation was carried out under the direction of R. L. Bertin to incorporate the frame analysis into the ACI Building Code (29). This investigation was initiated to determine a

method of frame analysis which would give the same results as the empirical analysis. In 1939, Peabody published a paper in which he used essentially the same method later incorporated in the 1941 ACI Code (30). In this procedure, the structure was again broken down into a system of bents, each one bay wide, and consideration was made of increased moments of inertia in the region of the column capitals and drop panels. The moments were then determined and the negative moment was reduced to the value at a distance xL from the centerline of the column. As originally developed, the distance xL was to be determined such that the total moment in a panel was the same as that of the empirical method. Studies indicated that this distance could be found by the equation:

$$x = 0.073 + 0.57 \frac{A^*}{L} \qquad (3)$$

where x = coefficient of span length which gives distance from the center of column to the critical section

A^* = distance from centerline of column, in the direction of the span considered, to the intersection of a 45-degree line, lying wholly within the column and capital, and the bottom of the slab or drop panel. Maximum of one-eighth of the span length

L = span length of slab center to center of columns in direction considered

This relation gave results which were very close to those found in the empirical analysis. These were the basic requirements of the frame analysis incorporated into the 1941 ACI Building Code.

2.6 Present Elastic Frame Analysis

The frame analysis which is specified in the 1956 ACI Building Code (31) appears to be very much like that of the 1941 Code but the apparently minor changes have a large effect in some cases. The procedure is outlined in detail below.

There are no limitations as to when the elastic frame analysis can be used. In practice, however, it would normally be used for structures which do not fall within the limitations for the empirical design method. Consequently, it is used if (a) the structure has less than three spans in each direction, (b) the ratio of panel length to width is greater than 1.33, (c) successive span lengths differ by more than 20 percent, (d) columns are offset more than 10 percent of the span, (e) the structure is more than 125 ft. high, or (f) story height exceeds 12 ft. 6 in. In effect, the frame analysis is used to extend the empirical method to cases that do not fall within the limits of the structures from which the empirical method was developed.

For the analysis, the Code specifies that the structure should be divided into systems of bents in each direction consisting of columns or supports and strips of supported slabs each one bay wide. These beams and columns are assumed to be infinitely rigid within the confines of the column capital where the dimensions of the capital are defined the same as A^* in Section 2.5. The stiffnesses of the various members are to be computed on the basis of the gross concrete cross section. The structure is then to be analyzed for the loads supported where they are definitely known. If the live load is variable, but does not exceed three-quarters of the dead load or if the live load will always be applied to all panels, the structure may be analyzed for uniform live load on all panels. If neither of these conditions are met, the structure must be analyzed for alternate panel loading.

Once the moments are determined, the negative moments are allowed to be reduced to those at a distance A from the centerline of the column. The distance A is defined in ACI 318-56 as the distance from the center of the support to the intersection of the mid-depth of the slab and a 45-degree

line lying wholly within the concrete. This distance replaces the distance xL used in the codes prior to 1956. In addition, both the negative and positive moment can be reduced in each span so that they do not exceed M_o as given by Equation 4:

$$M_o = 0.09\ WLF\ (1 - \frac{2c}{3L})^2 \qquad (4)$$

where M_o = numerical sum of positive and negative design moments in one span

W = total load on one panel

L = span length of slab panel center to center of supports

F = 1.15 - c/L but not less than 1.0

c = effective support size

These assumptions do not represent the action of a flat slab accurately and, in some case, lead to design moments which are considerably in error on the unsafe side. It is shown in later chapters, that the assumption of an infinitely stiff slab over the length of the capital is much too severe. This assumption leads to positive moments which are too low and negative moments which are unrealistically high before the reduction is applied. This assumption also leads to unrealistic relative stiffnesses for the members in a bent. In addition, it precludes the consideration of the torsional resistance of marginal beams and, in effect, assumes that they are infinitely rigid in torsion.

Under some conditions, the combination of assuming excessive stiffness within the column and reducing the negative moments to the value at a distance A from the centerline of the support can result in extremely low design moments. Zweig has shown that, for the case of low live load to dead load ratios, negative moments can be as much as 70 percent less than those found for the Empirical Method and positive moments can be as much as

25 percent less (32). The total moment in the panel for this condition is less than M_o. Since the Code does not state that moments should be increased if the total is less than M_o, there is nothing to prevent a designer from using these extremely low moments.

Although an elastic frame analysis should not be expected to give an exact analysis of a flat slab, it should furnish a relatively simple and reliable method of extending our experience to extreme conditions. It is shown in the following chapters that a two-dimensional analysis can be developed which will give consistent and reliable results.

3. SOLUTIONS FOR PLATES SUPPORTED ON COLUMNS

3.1 Fundamental Equations and Assumptions

All of the solutions in this chapter are based on the theory of flexure for plates. The equations governing these solutions are given below along with their limitations of applicability. Derivations of these equations can be found in Reference 1 and in most testbooks on the theory of plates.

The differential equation governing the deflection, w^*, of a plate can be stated as:

$$\frac{\partial^4 w^*}{\partial x^4} + 2\frac{\partial^4 w^*}{\partial x^2 \partial y^2} + \frac{\partial^4 w^*}{\partial y^4} = \frac{q}{N} \tag{5}$$

This equation is the same as the Lagrange equation with the term depending on motion omitted.

The relations between bending moments, twisting moments, and deflections can be represented by the following equations:

$$M_x = -N\left(\frac{\partial^2 w^*}{\partial x^2} + \mu\frac{\partial^2 w^*}{\partial y^2}\right) \tag{6}$$

$$M_y = -N\left(\frac{\partial^2 w^*}{\partial y^2} + \mu\frac{\partial^2 w^*}{\partial x^2}\right) \tag{7}$$

$$M_{xy} = -N(1-\mu)\frac{\partial^2 w^*}{\partial x \partial y} \tag{8}$$

The relations for shear can be stated as follows:

$$V_x = \frac{\partial M_x}{\partial x} + \frac{\partial M_{xy}}{\partial y} \tag{9}$$

$$V_y = \frac{\partial M_y}{\partial y} + \frac{\partial M_{xy}}{\partial x} \tag{10}$$

---

* The Asterisk is used to prevent confusion with w, the unit load, used in other chapters of this report.

The derivation of these equations is based on several basic assumptions in addition to the ordinary assumptions about equilibrium and geometry. These assumptions apply to all solutions presented here and may be stated as follows:

(a) All forces are perpendicular to the plane of the plate.

(b) The plate is medium-thick; that is, an appreciable portion of the energy of deformation is contributed neither by the vertical stresses nor by the stretching or shortening of its middle plane.

(c) The plate is of a homogeneous, linearly elastic, and isotropic material.

(d) A straight line drawn through the plate before bending remains straight after bending.

The natural boundary conditions which were originally derived by Poisson (5) and later explained by Kirchhoff (6) must be satisfied for a given solution to Equation 5. These may be stated as follows:

(1) The shearing forces must be equal to the corresponding quantities furnished by the forces applied at an edge.

(2) The bending moments must be equal to the corresponding quantities furnished by the forces applied at an edge.

In addition, the individual solutions given below require assumptions regarding reactions, stiffnesses of the capitals and drop panels, and stiffnesses of the columns. These are stated in connection with the solutions to which they apply.

3.2 Solutions by Use of Fourier Series

In Reference 33, Lewe presents solutions for moments in flat slabs which he found by means of a double infinite Fourier Series. In this study, he considered a large number of cases commonly encountered in flat slab construction. Tables are provided which give deflections and curvatures at a finite number of points for each case considered. Although his solutions

are for the case of Poisson's ratio, μ, equal to zero, these can be converted to solutions for other values of this ratio by means of equations 6, 7, and 8. The total moment in a panel is unaffected by the value of μ.

In order to arrive at solutions to Equation 5, it was necessary for Lewe to make seveal assumptions (in addition to the general assumptions listed in Section 3.1) regarding the distribution of reactions, stiffness of the plate in the vicinity of the supports, and type of load applied. The results of all solutions listed below are based on the following assumptions:

(a) Reactions are distributed uniformly over the rectangular areas of the supports.

(b) The plate is of infinite extent.

(c) The plate is of uniform thickness.

(d) Loads are uniform over the entire plate.

From the above assumptions, the boundary conditions can be determined for the case of uniform load over the entire plate. The boundary conditions are that on lines of symmetry (centerlines of reactions and centerlines of panels) the shear is zero and a tangent to the plate in a direction perpendicular to the centerline has zero slope.

The problem is now reduced to that of selecting a Fourier Series that will satisfy the boundary conditions and Equation 5. The expression which represents the load as a function of the coordinates x and y can be expressed as:

$$q = \sum_{m=0}^{\infty} \sum_{n=0}^{\infty} a_{mn} \cos \frac{m\pi x}{a} \cos \frac{n\pi y}{b} \qquad (11)$$

where, the origin for x and y is at the center of a reaction and

q = load as a function of x and y

m = an integer, 1, 2, 3,..... ∞

n = an integer, 1, 2, 3,..... ∞

a_{mn} = a constant to be determined

a = one-half the span length in the x-direction

b = one-half the span length in the y-direction

In a similar manner the expression representing the deflection, w^*, can be expressed as:

$$w^* = \sum_{m=0}^{\infty} \sum_{n=0}^{\infty} A_{mn} \cos \frac{m\pi x}{a} \cos \frac{n\pi y}{b} \qquad (12)$$

where w^* = deflection as a function of x and y

A_{mn} = a constant to be determined.

Other terms in Equation 12 are defined the same as in Equation 11.

Lewe took these relations and determined the constants a_{mn} and A_{mn} such that they satisfied Equation 5, the loading conditions, and the boundary conditions. He then had expressions for the deflections of the plate and, by use of Equations 6 through 10, could determine expressions for moments and shears. By evaluating a sufficient number of terms in these expressions, Lewe arrived at numerical values for deflections and curvatures.

Solutions for plates with alternate strips loaded may be obtained from Lewe's solutions for uniform loading by superposing the results for uniform loading with the results for panels with alternate strips of positive (downward) and negative (upward) uniform load (Fig. 2). Lewe's solutions are for a plate with constant stiffness throughout; thus, the reactions vanish for alternate positive and negative loading. The moments at any point in the panel for this loading condition are the same as the simple beam moment in a direction perpendicular to the loaded strips and are zero in the direction parallel to the loaded strips.

The results of the solutions obtained by Lewe are shown in Figs. 3 to 12. Table 2 shows the dimensions, loading conditions, and other pertinent

information for each of the solutions. The moments given in the figures and in the tables are for Poisson's ratio, μ, equal to zero. Moments are shown for the "design sections" in all cases, i.e., the centerline of the panel for positive moment and a line following the edge of the reactions at the reaction and the centerline of the reactions between them for the negative moment.

The results based on Lewe's work may be divided into three separate categories. These are:

1. Interior panel of infinite array of uniformly loaded square panels (Figs. 3 to 7)
2. Interior panel of infinite array of uniformly loaded rectangular panels (Figs. 8 and 9)
3. Interior panel of infinite array of square panels with alternate strip loading (Figs. 10 to 12)

It can be seen that the scope of these solutions are quite limited. In addition, the assumptions regarding the distribution of reactions and the stiffness of the slab in the vicinity of the reactions are quite different from those which exist in a real structure. For these reasons, Lewe's solutions should not be taken as the moments to be expected in a real slab but should be used only as an indication of what effects the distribution of reaction and slab stiffness have on the moments in a flat slab.

3.3 Solutions by the Method of Finite Differences

Equations 5 through 10 are derived by considering infinitesimally small differentials in setting up the problem. In general, the solutions to these equations are continuous functions. If small finite lengths are considered instead of the differentials, difference equations are obtained which correspond to the differential equations. Solutions obtained by difference equations theoretically approach the exact solutions of the partial

differential equations as the finite length approaches zero. For this reason, the degree of approximation will usually be improved by taking smaller finite lengths.

In general, finite difference operators corresponding to a differential equation may be obtained by the direct substitution of the appropirate difference expressions into the governing differential equations. Boundary conditions are handled by including as many additional equations, as determined from the boundary conditions, as are required to obtain the same number of equations as unknowns.

In many situations, it is convenient to use a physical model of the plate from which the difference equations can be derived directly. N. M. Newmark developed such a model in Reference 34. This model consists of a system of rigid bars connected by elastic hinges with torsion springs connecting adjacent parallel bars (Fig. 14). The model has the following characteristics:

1. The bars are weightless and undeformable.
2. The mass of the plate and the external loads are concentrated at the elastic hinges.
3. The resultants of the direct stresses are bending moments acting at the elastic hinges and at the ends of each bar.
4. The resultant of vertical shearing stresses are shearing forces acting at the elastic hinges and at the ends of each bar.
5. The resultant of the horizontal shearing stresses are twisting moments concentrated in the torsion springs.

The difference equations necessary for the solutions presented below are derived in References 14 and 17. The operator for a general interior point of a plate is shown in Fig. 14. By applying this operator to each point of a network and by determining additional equations from the boundary conditions, a set of simultaneous algebraic equations is obtained.

The solution of these equations gives the deflection of each point of the network. Once the deflection of each point is known, bending moments, twisting moments, and shears may be obtained from the difference equations which correspond to Equations 6 through 10.

In Reference 14, Nielsen has presented solutions to a number of plate problems which he obtained by use of difference equations. The results of these solutions are shown in Fig. 16 through 21. Dimensions and properties of the panels analyzed are indicated in Table 3. In all cases Poisson's ratio, μ, is taken as zero.

All of the solutions presented below are for typical interior panels of an infinite array of uniformly loaded panels. Reactions are considered to be either point supports or square capitals with c/L ratios as high as 0.40. The solution designated NS2 (Talbe 3) is for the case of a slab which has a drop panel and is supported on point supports. The area within the drop panel is assumed to have a stiffness of four times that of the slab. The solution designated NS4 is for the condition of shear linearly distributed around the perimeter of the capital. In all other solutions, the shear is assumed to be uniformly distributed over the area of the capital. Two of the solutions, NS4 and NS5, are for column capitals with varying stiffnesses. In these cases, it is assumed that the stiffness varies from the same as that of the slab at the edge of the capital to the value given in Table 3 at the center of the column.

In general, the results of Nielsen's solutions which are reported here appear to be accurate. In all cases, a sufficient number of points were considered so that the errors due to approximation of the differential equations by difference equations are small. Where direct comparisons are possible, it can be seen that Nielsen's results are in good agreement with those of Lewe.

In Reference 15, Marcus presents the results of some solutions obtained by means of finite differences. These results are summarized in Table 4 and in Figs. 22 through 24. All solutions are given for the case of Poisson's ratio, μ, equal to zero.

The results of Marcus' work which are presented below are for a typical interior panel of an infinite array of uniformly loaded panels. In each case, the stiffness of the panel was assumed to be constant throughout. The capitals were assumed to be non-deflecting at their edges and at their centers. This resulted in a distribution of shear at each capital which was very nearly linear around the perimeter. Square capitals were considered in all cases.

When directly comparable, the results obtained by Marcus are generally in good agreement with those of Lewe and Nielsen. The grid which Marcus used in his solutions contained enough points that errors due to the approximation of the differential equations by difference equations should be small. On this basis, Marcus' results appear to be reliable.

At the University of Illinois, finite difference solutions have been obtained for a number of conditions. Some of the results are reported in References 16 and 17. The results of these investigations are summarized below. In addition, the investigations in References 16 and 17 have been extended to cover some additional cases and the results of this extension are also presented.

In these investigations, the solutions of the simultaneous equations were obtained by use of the ILLIAC (the University of Illinois Digital Computer). Since the ILLIAC has the capacity for solving as many as 143 simultaneous equations, it was possible to use a very fine network of points for the solutions. This resulted in a corresponding reduction in the error of approximation as compared with the results of Nielsen and Marcus.

These investigations can be divided into two categories. The first category is that of one panel of an infinite array of square panels with both uniform loading and alternate strip loading. The second category considers the case of a plate consisting of nine square panels with both uniform loading and strip loading. In all cases, the capitals are assumed to be infinitely stiff. This required that the slope of a tangent to the slab be zero at the intersection of the slab with the capital. When this condition is used, the solution of the problem shows that most of the shear around the supports is concentrated on the corners of the capitals. In cases where non-uniform loads are considered, the columns are again assumed to be infinitely stiff. Where marginal beams are considered to be present in the nine-panel structure, their resistances are assumed to be concentrated along the centerlines of the exterior columns.

Table 5 and Figs. 24 through 28 show the dimensions of the panels analyzed and the moments obtained from the analysis of the interior square panels. For these solutions, c/L ratios vary from 0.10 to 0.25. Moments given in Table 5 are the average moments across the section considered. The negative moments include the twisting moment which exists at the intersection of the column capital and the plate. These twisting moments are on the order of 2 percent of the total moment in panel. They were included here due to the fact that the assumption of infinitely stiff column capitals increases their value enough that they must be considered in order to check statics. In the cases considered previously, twisting moments around the columns were much smaller and could be neglected. Figures 24 through 28 show the variation of moment across the sections indicated.

Table 6 and Figs. 29 through 32 show the results of the investigation of nine-panel slabs. In Table 6, properties of the slabs and loading

arrangements are listed. The first three cases (UI91 through UI93) refer to a structure with no marginal beams and the last case (UI94) refers to a structure with a shallow beam on two sides and a deep beam on the remaining two sides. The ratio of the beam flexural stiffness to the plate stiffness is designated as H_f and the ratio of the beam torsional stiffness to the plate stiffness is designated as J. In the structure analyzed, the deep beam has a flexural stiffness equal to the stiffness of the slab while the torsional stiffness of the shallow beam is one-fourth the stiffness of the slab. In Figs. 29 through 32, the average moments at the design sections of each panel are indicated. These moments are in a direction perpendicular to the loaded strips for all cases of partial loading. Twisting moments around the capitals are not included. For convenience, the average moments across the entire structure are also shown. In all cases moments are given for Poisson's ratio, μ, equal to zero.

Since it was possible to use a large number of unknowns in each of the cases investigated at the University of Illinois, errors due to approximating partial differential equations by the corresponding difference equations are quite small.

3.4 Modified Difference Solutions

In Reference 1, Westergaard presents computed moments for an interior panel of an infinite array of panels with circular column capitals. This analysis is based on the application of ring loads to Nielsen's solutions which were obtained from difference equations (14). Westergaard started with Nielsen's solution for an interior panel supported by point reactions. To this, he applied a linearly distributed upward load on a circle, concentric about the point support, having a diameter of c. At the center of this circle, he applied a load of equal magnitude but opposite in direction. The

nagnitude of this couple was chosen such that a line drawn tangent to the plate at the circle and passing through the center of the reaction would have zero slope. Moments were then determined for the slab under uniform load and acted upon by the ring moments. These were then presented graphically in Reference 1.

The method of analysis used by Westergaard automatically specifies the distribution of reactions and stiffness of column capitals. By the use of ring loads, the shear was required to be linearly distributed about the perimeter of the column capital. In a similar manner, the requirement that the slope of a line tangent to the slab at the ring and passing through the center of reaction be equal to zero can be met, in the practical case, only if the column capital is infinitely rigid.

The results of Westergaard's analysis by modified difference solutions are shown in Table 7 and in Figs. 33 to 36. Moments given in the table are the average across the design sections. The distribution of the moments across these sections are shown in the figures. As in all previous results, solutions are for Poisson's ratio, μ, equal to zero.

3.5 Analysis for Total Static Moment

In 1914, Nichols presented a paper in which he applied the principles of elementary statics to a flat slab in order to determine the total moment in one panel (18). In his original paper, Nichols determined an expression for the total static moment in a panel with circular column capitals. Only three assumptions were made in the development of this expression. These assumptions were:

1. The panel is one of an infinite array of identical panels.
2. All panels are uniformly loaded.

3. The shear is uniformly distributed around the perimeter of the column capital.

On the basis of these assumptions, there is no shear along the centerlines of the columns and panels. A free body diagram of one-half of a square panel can be drawn as illustrated in Fig. 37. The external forces acting on this panel are represented by the total load acting on the slab, $wL^2/2$, and the total reaction, $wL^2/2$, acting at the centerline of the column. The reaction around the capital has a total magnitude of $wL^2/2 - \frac{wc^2\pi}{8}$ and acts at a distance of c/π from the center of the column capital. The remaining portion of the reaction $wc^2\pi/8$, has a center of action at a distance $2c/3\pi$ from the center of the column capital. Resisting these couples are the positive moment at the centerline of the panel, M_p, and the negative moment at the design section M_n. Taking moments about the line AA,

$$M_p + M_n = \frac{wL^2}{2}\frac{L}{4} - \left[\frac{wL^2}{2} - \frac{wc^2\pi}{8}\right] - \frac{c}{\pi} - \frac{wc^2\pi}{8}\frac{c}{\pi} \qquad (13)$$

or

$$M_s = \frac{WL}{8}\left[1 - \frac{4c}{\pi L} + \left(\frac{c}{L}\right)^3\right] \qquad (14)$$

where M_s = total static moment in the panel considered.

W = the total load on the panel considered.

In Referecne 19, it was pointed out that this procedure can be extended to cases of rectangular panels, square or rectangular column capitals, and different assumed distributions of shear around the column capital. The expressions for a number of cases were presented in that paper and are repeated below along with those for other possible cases. These expressions cover nearly every practical combination of dimensions and shear distributions that may be encountered in flat slab structures.

For rectangular panels, and circular capitals with the shear uniformly distributed about the perimeter, the expression becomes:

$$M_s = \frac{WL_1}{8}\left[1 - \frac{4}{\pi}\frac{c}{L_1} + \frac{1}{3}\left(\frac{c}{L_1}\right)^3 \frac{L_1}{L_2}\right] \tag{15}$$

For square panels and square capitals with the shear uniformly distributed about the perimeter:

$$M_s = \frac{WL}{8}\left[1 - \frac{3c}{2L} + \frac{1}{2}\left(\frac{c}{L}\right)^3\right] \tag{16}$$

For rectangular panels and square capitals with the shear uniformly distributed about the perimeter:

$$M_s = \frac{WL_1}{8}\left[1 - \frac{3c}{2L_1} + \frac{1}{2}\left(\frac{c}{L_1}\right)^3 \frac{L_1}{L_2}\right] \tag{17}$$

For rectangular panels and rectangular capitals with the shear uniformly distributed about the perimeter:

$$M_s = \frac{WL_1}{8}\left[1 - \frac{2 + \frac{c_1}{c_2}}{1 + \frac{c_1}{c_2}}\frac{c_1}{L_1} + \frac{1}{1 + \frac{c_1}{L_1}}\frac{c_1^2 c_2}{L_1^2 L_2}\right] \tag{18}$$

For square panels and square capitals with the shear concentrated at the corners of the capital:

$$M_s = \frac{WL}{8}\left[1 - 2\frac{c}{L} + \left(\frac{c}{L}\right)^3\right] \tag{19}$$

For rectangular panels and square capitals with shear concentrated at the corners of the capital:

$$M_s = \frac{WL_1}{8}\left[1 - 2\frac{c}{L_1} + \left(\frac{c}{L_1}\right)^3 \frac{L_1}{L_2}\right] \tag{20}$$

For rectangular panels and rectangular capitals with the shear concentrated at the corners of the capitals:

$$M_s = \frac{WL_1}{8}\left[1 - 2\frac{c_1}{L_1} + \frac{c_1^2 c_2}{L_1^2 L_2}\right] \tag{21}$$

The subscripts 1 and 2 in the above equations refer to dimensions which are respectively parallel and perpendicular to the direction in which moments are considered.

It can be seen that Equations 15, 18, and 21 are general and the others are merely special cases of these three. In Section 2.4 it was noted the Nichols sugested an approximate expression (Eq. 1) for Equation 14. Figure 38 gives a comparison of equations 1 and 14. In addition to these two, Equation 16 is also shown in Fig. 38. From this comparison, it can be seen that, within the ordinary ranges of values for c/L, Equation 1 gives a good approximation of the expression for moment in a slab with circular capitals (Eq. 14) but does not work as well for slabs with square capitals (Eq. 16).

The above equations are correct for the conditions for which they were developed. The conditions assumed for the derivation of these equations may be slightly different in a real structure. The most important of these differences, assuming a large number of panels are loaded uniformly, will be the distribution of shear around the capital. In a real structure, the distribution of shear will be somewhere between the conditions of uniformly distributed about the perimeter of the capital and concentrated at the corners. Since the assumption of uniform shear is conservative, this assumption is to be preferred over the assumption of concentrated shear. The method of approach is theoretically sound and very simple. Although it does not give the distribution of moments, the method presents a simple means of determining the total moment in a panel.

4. COMPARISONS OF COMPUTED MOMENTS

4.1 Typical Panel of Infinite Array of Square Panels with Uniform Load

Each of the investigations mentioned in Chapter 3 has included the case of a typical panel of an infinite array of uniformly loaded square panels. In Sections 3.4 and 3.5, computed moments are presented for the case of circular column capitals. Sections 3.2, 3.3, and 3.5 give moments for the case of square capitals.

Figure 39 shows a comparison of total moment versus c/L for a structure with circular column capitals and no drop panels. The solid line shows the moments that Westergaard obtained by modifying Nielsen's finite difference solutions. By including Nielsen's solution for a plate with point supports (Table 3), it was possible to show the variation of moments for values of c/L ranging from 0 to 0.3. This covers the range of c/L ratios commonly used in flat slab structures.

Since Westergaard's solutions are based on the assumption that shear is uniformly distributed around the perimeter of the capital, Equation 15 was used to compare his moments with the total static moment in the panel. The slight difference between the static moment and that for Westergaard can be attributed to a slight error in the assumed distribution of moment about the column capital in summing up the moments shown graphically by Westergaard.

In addition to the static moment and the moments obtained by Westergaard, design total moments obtained by the ACI Code are included in Figure 39. Moments obtained by the equivalent frame analysis are reduced to the value at a distance A from the centerline of the column. In computing the distance A, the slab was assumed to have the minimum allowable thickness

of L/36. The design moments are not, however, reduced to M_o. In accordance with the requirements of the ACI Code (318-56), the total moment which must be provided for is the smaller of the moments obtained by the two methods. Consequently, if only uniform loading is considered, the empirical moment would govern up to a c/L ratio of 0.3 and the moments obtained by frame analysis would govern for larger values of c/L.

Figure 40 shows the moments at the design sections of the panel considered. The solid line represents moments obtained by Westergaard's modified finite difference solutions (Table 7). The two remaining lines represent moments obtained by use of the ACI Code frame analysis and empirical method. In Figure 40, the negative moments obtained by frame analysis are again reduced to the value at a distance A from the column centerline. According to the ACI Code, the total moment can again be reduced to M_o for values of c/L up to 0.3. Since the Code does not specify how the reduction shall be made, the entire reduction can be applied to either the negative or the positive moment or a proportionate amount can be applied to each. For values of c/L larger than 0.3, the moments obtained by frame analysis can be used without further adjustment.

Figure 41 shows a comparison of total moments in a typical panel of an infinite array of uniformly loaded square panels with square column capitals. The solid line represents all solutions by Lewe, Nielsen, and Marcus for which the shear was assumed to be uniformly distributed over the area of the capital. In addition, Nielsen's solution for a capital with a variable stiffness (NS4) and Marcus' solution for the assumption of shear uniformly distributed about the perimeter of the column capital (MS2) are shown. In order to compare these results with the static moment, a line representing Equation 16 is also shown. This line falls below the one representing the case of shear uniformly distributed over the area of the capital.

The results obtained by Lewe, Nielsen, and Marcus are in good agreement with the static moment as given by Equation 16. Since the assumption of shear uniformly distributed over the area of the capital puts the center of reaction closer to the center of the capital than in the case of shear uniformly distributed about the perimeter of capital, Equation 16 should give moments less than those obtained on the basis of the first assumption. Marcus' solution (MS2), which is based on the same assumption as Equation 16, gives a total moment equal to the static moment. As expected, Nielsen's solution for a plate with a capital of variable stiffness falls between the lines representing the other two assumed shear distributions.

Lines representing Equation 19 and moments obtained by finite differences at the University of Illinois are also shown in Figure 41. It can be seen that the moments found in the University of Illinois investigations are slightly higher than those given by Equation 19. This is again in the proper relation to the other moment if the distribution of shear is considered.

For purposes of comparison, design moments found by the ACI Code are also given. Since the Code makes no explicit distinction between circular capitals and square capitals, these moments are identical to those shown in Fig. 39.

Figure 42 shows the moments at the positive and negative design sections. This illustration indicates that the negative moment is not greatly influenced by the distribution of shear in the vicinity of the reaction but there is a large effect on the positive moment. Although Fig. 41 indicated that the rigidity of the column capital does not greatly change the sum of the moments in a panel, Fig. 42 shows that there is an increase in negative moment and a decrease in positive moment as the rigidity of the capital increases. However, these changes in distribution of moment are not large.

The comparisons shown in Figs. 39 through 42 show the affects of the size, shape, and stiffness of the column capital and the distribution of shear around the capital. They also indicate that the solutions give consistent and reliable results for the assumed conditions. There is still a question, however, as to how well the assumed conditions represent those present in a reinforced concrete flat slab. The size and shape of the capitals are known quantities and require no further discussion. The stiffness of the capital and the distribution of shear in the vicinity of the capital are not, however, always known. Since cracks are likely to form around the capitals, there may be very large differences in the relative stiffness of the capital and the slab from those assumed in the analysis. This will influence the amount of moment carried at the negative design section and the positive design section but will not change the total moments in the panel so long as the distribution of shear is not changed. For this reason, the most important assumption is that of the distribution of shear around the capital.

When the slab is supported by circular capitals, the shear should be very nearly uniformly distributed about the perimeter. Any variation from this distribution will be small and will not change significantly the total moment in the span. If square capitals are used to support the slab, the centroid of the shear forces at the design section (perimeter of one-half the capital) should be between those corresponding to shear distributed uniformly along the perimeter and shear concentrated at the corners. Test results presented in Reference 26 indicated that the assumption of shear uniformly distributed about the perimeter may be close to reality in the case of flat slabs. This assumption is conservative and appears to agree with test results.

If the uniform distribution of shear is assumed to be correct, comparisons can be made between design moments and theoretical moments in flat

slabs. Figures 39 and 40 show that design moments are considerably smaller than theoretical moments in all cases of slabs supported on circular column capitals. The primary reason for this is the misinterpretation of the results of early tests on flat slabs as explained in Chapter 2. It is significant, however, that the ACI frame analysis predicts the proper trend in the moments. For slabs supported on square column capitals the positive and total design moments computed by frame analysis are considerably lower than the theoretical moments. The negative moments computed by the equivalent frame analysis are in good agreement with the theoretical moments. The empirical method gives design moments which are too low for small values of c/L but are larger than the theoretical moments for extremely high values of c/L. Again, the moments obtained by frame analysis show the proper trend.

4.2 Typical Panel of Infinite Array of Rectangular Panels with Uniform Load

In this section, moments in an interior panel of an infinite array of rectangular panels are compared. In Sections 3.2, 3.3, and 3.5, solutions for this case were cited. Although available solutions based on the theory of flexure for plates are quite limited, the equations presented in Section 3.5 present a means of extrapolating the results to determine the effects of changes in the ratio of the lengths of sides.

Figure 43 shows a comparison of total moment versus the ratio of span lengths for the solutions presented in Tables 2, 3, and 4. The solid lines represent the total static moment in terms of WL_1 as computed by Equation 17. The moments given by Equation 17 are in good agreement with those obtained by Lewe, Nielsen, and Marcus. Where differences do exist, they can be attributed to the slight errors in determining the average theoretical moment across the design sections of the plates from the values given at a finite number of points.

The average moments at the design sections are shown in Figs. 44 through 46. Figure 44 shows moments in the long span for $c/L_b = 1/8$. Figures 45 and 46 show comparisons of moments in the short span for ratios of c/L_a equal to 1/6 and 1/4, respectively. In addition to solutions obtained by Lewe and Marcus, these three figures include design moments based on the provisions of the ACI Code. It can be seen that there is very little change in the average moment at the design sections as the ratio of length of panel to width of panel increases. In all cases, the ACI positive design moment is considerably less than that obtained by the theory of flexure for plates. The negative design moments are also low but not as far below the theoretical moment as in the case of positive moments. The reasons for this were cited in the discussion of square panels. The ACI frame analysis again predicts the proper trend in the positive moments but indicates that negative moments in the short span decrease as the ratio of length to width increases. This is a result of the unrealistic method of reducing the negative moment. In proportioning a slab, thickness is governed by the longer span of the slab. For this reason, the distance A is proportionately larger in the direction of the short span and an incorrect trend is obtained in the negative design moments.

In order to determine the influence of more extreme values of the ratio of span length to span width on the moments in rectangular panels, the results of Equation 17 for various ratios of L_b/L_a are shown in Fig. 47. The moments and the c/L_1 ratios in this figure are given in terms of the length of span considered. The line marked $L_b/L_a = 1$ indicates the total static moment in either span of a square panel. Lines above this, show moments in the long span and lines below show moments in the short span of rectangular panels with various L_b/L_a ratios. Since only square column capitals are

considered, geometry places limitations on the size capital that can exist for a given ratio of L_b/L_a. When the ratio of L_a/L_b becomes equal to the ratio of c/L_a, the physical structure becomes a slab supported on a wall and the moment in the short span is zero.

The above comparisons indicate that the total moments and average moments at the design sections are practically unaffected by the ratio of span length to span width. However, the distribution of moment along the design section does not remain the same. Comparisons of the distributions shown in Figs. 8, 9, 20, and 23 with those for square panels indicates how the distribution of moment is changed. In general, moment in the long span tends to become uniformly distributed along the design section as the ratio of the two span lengths increases, while the moment in the short span tends to increase in the column strip and decrease in the middle strip of the panel.

4.3 Typical Panel of Infinite Array of Square Panels with Strip Loading for Maximum Positive Moment

In Sections 3.2 and 3.3, moments were presented for slabs with alternate strips loaded in order to produce maximum positive moment along the centerline of the panel. The moments computed by Lewe (Section 3.2) represent the case of columns with no flexural stiffness. The investigations carried out at the University of Illinois consider the case of a slab supported on columns with infinite flexural stiffness.

Figure 48a shows a comparison between moments based on the theory of flexure for plates and design moments computed by the ACI Code frame analysis. In computing these moments, the columns were assumed to have zero flexural stiffness. The solutions based on plate theory include the assumption that the reaction is uniformly distributed over the area of the capital. In

addition, the plate is assumed to have the same stiffness over the reaction as it has at points outside the reaction. As was indicated in Section 4.1, these assumptions tend to give computed positive moments which are higher than those found on the basis of other assumptions. Since the ACI Code allows the sum of the maximum positive and negative moments to be reduced to M_o, the moments based on the frame analysis are higher than what would be generally used in design.

No solutions based on the theory of flexure for plates are available for a slab supported on columns with a finite flexural stiffness and having alternate strips loaded for maximum positive moment. In order to obtain some idea of the effects of column stiffness, one solution was obtained for a slab supported on columns with infinite flexural stiffness (Table 5). This solution was for a flat plate without drop panels and with square capitals having a c/L ratio of 0.2. As mentioned in Section 3.3, the assumption of infinitely stiff columns and capitals results in most of the shear being concentrated at the corners of the capitals. It was shown in Fig. 42 that this also results in positive moments which are slightly lower than those obtained on the basis of other assumptions.

Figure 48b shows a comparison of this solution with moments obtained by the ACI frame analysis. It can be seen that, for a c/L ratio of 0.2, the frame analysis predicts a maximum positive moment which is smaller than that computed by plate theory. This discrepancy can be ascribed to the fact that the ACI frame analysis assigns too much stiffness to the slab in the vicinity of the column capital. It was previously shown that, even for uniform loads, the ACI frame analysis predicts positive moments which are considerably below those obtained by plate theory.

The values plotted in Fig. 48 should not be interpreted as giving the moments in an actual reinforced concrete flat slab loaded to produce

maximum positive moment. Instead they should serve only to indicate the possible extremes in the values of these moments and show how the moments change as column stiffness changes. In general, it appears that the frame analysis predicts the correct trend in the moments in flat slabs loaded for maximum positive moment as it does in slabs under uniform load.

4.4 Nine-Panel Slab

The comparisons given in Sections 4.1 and 4.2 have all been concerned with one panel of an infinite array of identical panels. In order to approach this case in a real structure, the panel in question would need to be at least the third panel from the edge in any direction. This would require a structure of a minimum of twenty-five panels. This means that the majority of panels in most structures fall into the category of an edge panel, corner panel, or "first interior" panel. A nine-panel structure offers an excellent means of investigating the moments in edge panels and "first interior" panels. The eight panels around the perimeter of this type of structure are edge and corner panels and the center panel is similar to a "first interior" panel in a larger structure. Under all comparable loading conditions, the moments in any panel of a nine-panel structure will be larger than those in the corresponding panel of a larger structure.

In Section 3.3, computed moments were presented for two nine-panel structures. These structures were identical in every respect except that one structure had edge beams. In both structures, all columns were assumed to have a c/L ratio of 0.1 and to be infinitely stiff in flexure. As previously mentioned, this results in the shear being concentrated at the corners of the capital. This assumption results in slightly lower positive moments than would be expected in an actual structure. For the same reason, the negative moments in the edge panels are higher than those in an actual structure. In

the structure with edge beams, the deep beams were assumed to be on two adjacent edges and the shallow beams on the other two edges. This resulted in the structure being symmetrical about one diagonal.

Table 8 shows a comparison of moments due to uniform load in the nine-panel structure without edge beams. In this table, moments based on the theory of flexure for plates are compared with design moments computed on the basis of the provisions of the ACI Code. The empirical moments are based on the assumption that the slab has no drop panels. In order to apply the ACI Code frame analysis, it was necessary to assume that the columns were so short that they were infinitely stiff as compared with the slab. The distance A was computed on the assumption that the thickness of the slab was equal to L/36. On the basis of these assumptions, the positive design moment is the same as that in a uniformly loaded beam fixed at both ends and having an infinite moment of inertia for a distance L/20 from each end.

Table 8 indicates that the design moments based on the empirical method are the same in the exterior rows of panels as in the interior row of panels. At the exterior column, the empirical design moments are larger than those computed on the basis of plate theory. If the twisting moments were included in the moments obtained by plate theory, this difference would not be as large but the empirical design moments would still be greater. At all other design sections, the moments based on plate theory are larger than the empirical design moments. At the exterior column, the design moments based on the ACI Code frame analysis are larger than either empirical moments or the moments based on plate theory. The frame analysis moments fall between the plate theory moments and empirical design moments at the interior column and at the positive moment section of the center panel. The frame analysis gives moments at the center of the edge panels which are considerably lower

than either the empirical design moments or the moments obtained by the theory of flexure for plates.

Table 9 shows moments for the same structure with strip loading. In the first case, the structure is loaded for maximum positive moment in the edge panel and maximum negative negative moment at the exterior column. It can be seen that the frame analysis gives positive moments which are too small and negative moments which are too large. In the second case the structure is loaded for maximum positive moment in the center panel. Again, the frame analysis gives positive moments which are lower than those computed by plate theory. The third case considers loading for maximum negative moment over the first interior column. In this case, the frame analysis again gives moments which are lower than those obtained by plate theory.

The ACI frame analysis gives moments which do not agree with plate theory due to the fact that the frame analysis does not consider properly the manner in which moments are carried in the vicinity of the column capital. The slab on each side of the column will exhibit curvature even if the column capital is infinitely stiff. Neglecting this fact gives negative moments at the edge columns which are too high. At interior columns, the negative moments are still high at the column centerlines. Consequently, the positive moments are lower than indicated by plate theory. Reducing the negative moments to the value at a distance A from the column centerline makes moments at interior columns smaller than indicated by plate theory. At the exterior columns, the moments are so large initially that a reduction to the value at the distance A gives negative moments which are still considerably in excess of those obtained from the theory of flexure for plates.

In Table 10, theoretical moments and design moments are compared for a uniformly loaded nine-panel structure with edge beams. Moments based

on the theory of flexure for plates are not changed greatly except at the exterior columns. At this section, negative moments are increased considerably and are closer to those computed by frame analysis. Since the empirical method requires that the edge beams be designed to carry a specified percentage of the load on the adjacent panel, the required design moment in the exterior panels is increased. Table 10 indicates that, in some cases, this requirement increases the combined design moments of the slab and beam to an amount equal to or greater than the static moment. For the structure considered in Table 10, the static moment given by Equation 16 is 0.106 WL. It can be seen that, in each of the edge strips, the design moment required by the empirical method is equal to or greater than the static moment.

The above comparisons indicate that, in a nine-panel structure without edge beams, design moments obtained by either the ACI Code empirical method or frame analysis will be lower than the static moment in the panel. Design moments at the edge columns are generally higher than those obtained from plate theory. At all other sections, design moments are generally lower than theoretical moments. The only exception to this is in exterior panels which contain edge beams. In these panels the design moments in the edge beams plus those in the panel are greater than the theoretical moments.

In the nine-panel structures considered, the frame analysis does not predict the trend in the moments properly. In the edge panels, it does not even fulfill its original purpose of giving approximately the same design moments as the empirical method. Although the structures considered included unusually stiff columns, this was not the major cause of the differences in the moments. In the following chapters, methods of reducing these differences will be discussed.

5. DISCUSSION OF THE ASSUMPTIONS OF THE ACI FRAME ANALYSIS

5.1 General Remarks

The treatment of a flat slab as an equivalent two-dimensional elastic frame is at best only a good approximation. It is apparent that variations of the slab stiffness, loading arrangement, and support conditions in the third dimension will influence the moments in the direction considered. The influence of these variations can be studied by the use of the theory of flexure for plates, but no rigorous method is available for determining their effects by a two-dimensional analysis.

In the preceding chapters, it has been shown that in most cases the present ACI Code frame analysis predicts the correct trends in the values of moments. This suggests that the frame analysis can be modified to give results which agree with those obtained from both plate theory and test results.

In this chapter, the effects of different assumptions for the stiffness of the slab and columns are investigated to determine which assumptions give the most reasonable results. In addition, possible ranges in stiffness of the various members are investigated in order to determine how different assumptions influence the computed moments.

5.2 Flat Slab with Uniform Load

A flat slab panel differs from a beam in that the curvature in the transverse direction is significant. Although the double curvature has no effect on the total moment in a panel, it does change the distribution of moment between the positive and negative design sections and at the design sections.

Figure 49 shows the deflected shape of one-half of a uniformly loaded flat slab panel. Curvatures exist in the direction of the x-axis as well as in the direction of the y-axis. In Fig. 49b, the deflected shape of one-half of a uniformly loaded flat slab with properties similar to those required by the assumptions of the ACI Code frame analysis is shown. It was pointed out in Chapter 2 that Code frame analysis assumes the slab to be infinitely rigid within the limits of the column capital. In order to meet this requirement the slab must have zero deflection and zero curvature between the supports. As a consequence of this requirement, a uniformly loaded slab will exhibit zero curvature along the x-axis.

Lewe, Nielsen, and Marcus have presented moments for an interior panel of a slab on point supports with all panels loaded (Tables 2, 3, and 4). The average moments at the panel centerline and column centerline for this case can be compared with the moments at the centerline and support of an equivalent uniformly loaded beam fixed at both ends. The values of the moments in the beam would be 0.0833 WL at the support and 0.417 WL at midspan. It can be seen in the tables that, for $\mu = 0$, the moments determined by plate theory are not significantly different from these values. If Poisson's ratio has a finite value, Equations 6 and 7 show that the distribution of moment between the two sections is changed. Specifically, the positive moment is increased and the negative moment decreased. For a slab on point supports and $\mu = 0$, the average moments on the slab are very close to those in an equivalent beam. Consequently, neglecting deflections and double curvature does not influence greatly the ratio of the positive and negative moments.

The moments presented in Table 5 are for a uniformly loaded slab supported on infinitely rigid columns. The positive moments for this case can be compared with positive moments in beams which are fixed at each end

and are infinitely rigid within the limits of the capital. For $\mu = 0$ and c/L equal to 0.1 and 0.2, Table 5 gives positive moments of 0.0386 WL and 0.0316 WL respectively. The equivalent beams give positive moments of 0.0337 WL and 0.0267 WL for the same c/L ratios. For finite values of Poisson's ratio, the positive moments based on plate theory are larger and the differences are even greater. This comparison shows that for slabs supported on real columns the influence of deflections between the supports and curvature in the transverse direction is quite significant. Even for the case of infinitely rigid supports, the equivalent beam gives much lower positive moments than those obtained from plate theory.

The assumption of infinitely rigid column capitals is unrealistic even if double curvature and deflection between supports are accounted for. In the case of a flat slab with column capitals, there will always be significant deflections at the edge of the capital. For flat plates where no capital is used, the deflections at the support are quite small but nevertheless, are present.

The solutions designated NS3 and NS4 in Table 3 along with solution UI3 in Table 5 provide a means of comparing the effects of variations in capital stiffness. All three of these solutions are for equal capitals with a c/L of 0.2 and for $\mu = 0$. The solution designated UI3 is for an infinitely rigid column capital; NS4 is for a capital varying in stiffness from that of the slab at the edge of the support to infinity at the center of the support; and NS3 is for a capital with a stiffness equal to that of the slab throughout. Positive moments determined by these solutions vary as follows:

NS3	0.0401 WL
NS4	0.0358 WL
UI3	0.0316 WL

Since the solutions include three different assumptions for the distribution of shear at the support, negative moment and total moment cannot be compared directly. In general, increased stiffness of the capital appears to concentrate the shear farther from the center of the reaction thereby reducing the total moment in the span. This comparison indicates that the ACI Code assumption of infinitely stiff column capitals will result in positive design moments which are lower than those that may be expected in a real structure. If a finite value of Poisson's ratio is considered, the differences become even greater.

The ACI Code makes no specific recommendation for consideration of the torsional stiffness of edge beams. Indirectly, the Code assumptions assign infinite torsional resistance to the edge beams. This is the result of assuming the equivalent beam to be infinitely rigid within the limits of the column capital. Figure 50a shows the deformed shape of a beam over an infinitely rigid column with a uniform twisting moment applied to it. The ends of the beam rotate with respect to the column. Figure 50b shows a beam which has infinite torsional stiffness and has a uniform twisting moment applied to it. This illustration represents the stiffness assumptions for edge beams as given by the ACI Code. Since the stiffness of a member is defined as the moment per unit of rotation, it is obvious that the beam column combination illustrated in Figure 50a is much less stiff than the one shown in Figure 50b.

The moments for the two nine-panel structures tabulated in Figs. 31 and 32 give an indication of the effects of edge beams. Figure 31 shows that with no edge beams, the moments at the edge of the uniformly loaded nine-panel slab average 0.030 WL (neglecting twisting moment at the columns) over the width of the structure. When edge beams with the torsional and flexural

stiffnesses shown in Table 6 are added, the moment at the exterior columns is increased to an average of 0.048WL on the shallow beam side and 0.049WL on the deep beam side. The stiffness of the edge beams can have a large effect on the moments at the exterior design section of a slab. The ACI Code assumption of infinite torsional stiffness assigns more moment to this section than the section carries in the real structure.

5.3 Flat Slab with Strip Loading for Maximum Positive Moments

If all panels are loaded, the relative stiffnesses of the slab panels and columns are important only in the exterior spans of a structure as long as the span lengths are approximately equal. When adjacent span lengths are considerably different or when strip loading is considered, the relative stiffnesses of the members become important in all spans.

The relative stiffnesses of two adjacent slab panels are not very sensitive to the assumed variation of stiffness within the panels. As long as consistent assumptions are made about the variation in the moment of inertia within each panel, the computed relative stiffnesses of adjacent panels are not affected. To a lesser degree this is also true for determining the relative stiffnesses between the slab panels and the columns. The problem is in determining what assumptions must be made in order to be consistent.

In order to determine the variation in moment of inertia along the axis of a column, the ACI Code requires that the column be considered infinitely rigid within the column capital and that the gross concrete section be used at other points. Where a flat slab with column capitals is used, this assumption is reasonable. It makes little difference in the computed stiffness of the column whether the capital is considered to have an infinite moment of inertia or whether the actual variation in moment of inertia within the capital is considered. For a flat plate where no enlargement is present

at the top of the column, this assumption does not appear to be reasonable.* For this case it would be realistic to base the computed stiffness on the actual moment of inertia of the column. In any case, use of the gross section of the column is reasonable since the columns are usually uncracked at working loads.

The ACI Code also requires that the stiffnesses of the slab panels be based on the gross section of the concrete and that the slab be assumed to have an infinite moment of inertia within the confines of the column capital. Although the use of an uncracked section for the slab may be unrealistic at working loads, any other assumption would require a great deal of guesswork as to what sections should be assumed cracked or uncracked. In addition, it would greatly complicate the computations. Since the relative stiffnesses of the columns with respect to the slabs are not greatly changed by the formation of a few cracks, moments of inertia based on the gross concrete section appear to be the most desirable.

The assumption of an infinite moment of inertia within the limits of the column capital does not appear reasonable. The moment of inertia directly over the column may be infinite, but the moment of inertia of the slab on either side of the column is a finite value. Although the average moment of inertia of the slab may be quite large within the confines of the capital, the effective stiffness of this portion of the equivalent beam should be based on a finite moment of inertia in order to take the curvature of the slab into account. The assumptions necessary for determining the proper equivalent stiffness can be determined from theoretical studies and test results.

---

* The capital is defined to include the largest right circular cone with 90-degree vertex angle that can be included within the outlines of the column.

Figure 51 shows the effect of the relative column stiffness on the positive moment in a flat slab with alternate strip loading. The solid line in this figure represents moments for strip loading based on the theory of flexure for plates. It was obtained by extrapolating the results shown in Fig. 48. The moment for a relative column stiffness of zero was taken from Fig. 48a and the moment for a relative column stiffness of 1.0 was taken from Fig. 48b. It was then assumed that the moment was a linear function of the relative column stiffness and the two points were connected by a straight line. The broken line in Fig. 51 shows the maximum positive moment in a flat slab as determined from the ACI Code frame analysis. It can be seen that the frame analysis and plate theory both predict the same trend in the maximum positive moment with the frame analysis predicting consistently lower values. As stated before, the difference is due primarily to the assumption of infinite stiffness within the limits of the column capital.

It should be noted that the 1956 ACI Code attempts to limit the relative stiffness of columns used in flat slab construction. This is done by requiring a minimum moment of inertia for the columns as given by the following equation:

$$I_c = \frac{t^3 H}{0.5 + \frac{W_D}{W_L}} \qquad (22)$$

where I_c = moment of inertia of the column in in.^{4}

H = story height in feet

t = minimum slab thickness

W_D = total dead load on panel

W_L = total live load on panel

For a W_D/W_L ratio of 1.0 or less, it can be shown that this limitation provides relative column stiffnesses ranging from 0.5 to 1.0

with common values of 0.6 to 0.9. Figure 51 shows that, within these limitations, maximum positive moments do not vary greatly. In addition, it can be seen that an error in the assumed stiffnesses of either the slabs or columns will not appreciably change the computed moments.

6. PROPOSED FRAME ANALYSIS

6.1 Assumptions and Procedure

The comparisons in the preceding chapters have indicated that an equivalent two-dimensional frame analysis can be used to determine moments in flat slabs. It was also shown that several modifications should be made in the procedure presently allowed by the ACI Code. In this chapter, a method is presented for the determination of moments at the critical design sections. Moments obtained by the proposed method are then compared with the results of tests on both elastic models and reinforced concrete models.

In Chapter 5, it was shown that the ACI Code assumption of infinite stiffness of the slab within the limits of the column capital results in unrealistic slab stiffness and fixed end moments. In order to overcome this difficulty, it is necessary to assume an effective depth for the slab over the area of the column capital. When this is done, the moment of inertia of the fictitious section remains finite yet the increased stiffness in the vicinity of the columns is accounted for. Studies have shown that, for square capitals, an assumed thickness over the column capital of twice the thickness of the slab will give positive moments which agree with those found by plate theory.

Figure 52 illustrates the assumptions necessary for determining stiffnesses, carry-over factors, and fixed-end moments for slabs with square column capitals. The moments of inertia at the various sections along the slab are determined on the basis of the dimensions shown for sections AA, BB, and CC. The 1/EI diagram for the equivalent two-dimensional beam is shown at the bottom of Fig. 52. Moment distribution constants can be obtained from this diagram by normal procedures.

For a slab supported on circular column capitals, the above assumption results in an equivalent beam with a variable moment of inertia over the column capitals. In order to simplify the calculations, an equivalent moment of inertia which is constant over the column capital can be used. The errors in relative stiffness which are introduced by this assumption are quite small and will not greatly influence the final moments. For a flat slab supported on circular column capitals, good results can be obtained by using the same equivalent two-dimensional beam as in the case of square capitals but assuming an effective depth of 1.75 t_1 over the capital. Section CC in Fig. 52 would then have a moment of inertia, I_{CC}, based on the dimensions shown except that the effective depth over the column would be 1.75 t_1. The moments of inertia at all other sections and the 1/EI diagram would remain as shown.

Figure 53 shows comparisons of positive moments in an interior panel of a flat plate as determined by the theory of flexure for plates and by both the proposed frame analysis and the ACI Code frame analysis. In Fig. 53a, the solid line represents moments found by means of difference equations (Table 5). These solutions were obtained for a slab supported on infinitely rigid square capitals. For this reason the positive moments obtained in these solutions may be considered a lower bound to those that would be found in a real structure. It can be seen that the positive moments obtained by the proposed frame analysis are in good agreement with those obtained by plate theory. Moments computed by the ACI Code frame analysis are considerably lower for c/L ratios in the common range used in flat slab construction.

In Fig. 53b positive moments obtained by the proposed frame analysis for a slab supported on circular capitals are compared with those obtained from the ACI Code frame analysis and those obtained by Westergaard

(Table 7). Since Westergaard's moments are for infinitely stiff column capitals, they may also be taken as a lower bound to the moments in a real structure. It can be seen that the proposed frame analysis gives positive moments which are in good agreement with those obtained by plate theory while the ACI Code frame analysis gives moments which are considerably lower.

In general, the proposed frame analysis appears to give good results for the positive moment in a panel of an infinite array of uniformly loaded panels supported on either square or circular column capitals. It should be noted that the above comparisons were based on Poisson's ratio equal to zero. As previously noted, finite values of μ would result in slightly higher values of positive moments. Since reinforced concrete flat slabs may be cracked even at working loads, it appears impractical to attempt to consider the quantitative effects of Poisson's ratio. In addition, the use of an equivalent two-dimensional structure is only approximate so that the introduction of μ would only complicate the problem and add very little to the accuracy of the method.

For interior columns, stiffnesses can be based on the moment of inertia of the gross concrete section. In flat plate structures without column capitals, the column will have a constant moment of inertia up to the bottom of the slab. From the bottom of the slab to the mid-depth, the moment of inertia can be considered to be infinite. Figure 54a shows a quantitative $1/EI$ diagram for an interior column of a flat plate. Once this diagram has been obtained, the column stiffness can be computed by ordinary methods.

If a column capital is present at the top of an interior column, the computation of stiffness becomes somewhat more complicated. It is apparent that the moment of inertia, within the enlargement of the capital,

varies along the column. Where the capital intersects the bottom of the slab or the drop panel, if one is present, the moment of inertia becomes infinite. In order to simplify computations, it is sufficiently accurate to assume that the 1/EI diagram varies linearly from that of the column at the base of the enlargement to zero at the intersection of the capital with the bottom of the drop panel or slab. This is shown qualitatively in Fig. 54b. In this figure, the distance H refers to the story height and the distance $t_1/2 + t_2$ refers to either the half depth of the slab or the half depth of the slab plus the depth of the drop panel. Again, after the 1/EI diagram has been obtained, the stiffness of the column can be computed by ordinary methods.

Computation of stiffnesses for exterior columns is a somewhat more involved problem than is the one for interior columns. In order to approach the question of the stiffness of an exterior column, it is first necessary to consider how the moment is transferred into the column from the slab. At the face of the column, the moment is transferred directly from the slab to the column. In addition, a large portion of the moment is first transferred from the slab to the edge beams and then from the edge beams to the columns. It should be noted that the portion of the slab which connects the exterior columns serves the same function as an edge beam if no deepening of the slab is provided.

If the edge beams exhibited an infinite torsional resistance so that there was no rotation of the beam between the columns, the stiffnesses of the exterior columns could be computed in the same manner as those of the interior columns. Since this is not the case, the reduction in relative stiffness of the column due to twisting of the beam must be taken into account. This may be done by considering the exterior beam-column combination as a single element and computing the average stiffness of this member.

For use in the Cross distribution procedure, the stiffness of a member may be defined as the moment required to rotate the end considered through a unit angle without translation of either end (35). For a beam-column combination, this can be represented by the following equation:

$$K_{bc} = \frac{m_1}{\theta_f + \theta_t} \tag{23}$$

where K_{bc} = stiffness of the beam-column combination

m_1 = a distributed torque applied along the axis of the beam

θ_f = total rotation of the end of the column due to bending in the column

θ_t = average rotation, due to twisting, of the beam with respect to the column

Thus the stiffness of an exterior column can be evaluated by Equation 23 if m_1, θ_f, and θ_t are known.

The value of θ_f can be found on the basis of the same assumptions used to obtain the stiffness of interior columns. Its value is independent of the distribution of the torque along the beam and the torsional stiffness of the beam. No further explanation of this quantity is necessary.

The computation of θ_t requires several simplifying assumptions: (1) The twisting moment (moment applied by the slab) is assumed to be linearly distributed along the axis of the beam. Although this assumption is considerably in error in a corner panel where beams frame into the column from two directions, this situation can be considered by modifying the resulting rotation as described later. In other panels, the assumption appears to give good results. (2) When no edge beams are present, it appears reasonable to consider the portion of the slab equal to the width of the column capital as offering torsional resistance. If edge beams are provided, an L-shaped section including this same portion of the slab in combination with

the beam should be considered. (3) For slabs supported on circular capitals the torsional resistance of capital is infinite. This is consistent with the assumptions for the flexural stiffness of the column at this point. For square column capitals, the infinitely stiff portion can be considered to extend from the centerline of the capital to the intersection of the centerline of the edge beam with a 45-degree line extended outward from the corner of the capital. This accounts for the increased torsional resistance of the beam caused by the stiffening effect of square capitals. (4) The restraint against warping at the midspan of the beam does not affect significantly the torsional rotation of the beam. In Reference 36, Timoshenko and Goodier have shown that this is true so long as the beam is shallow with respect to its length. This approximation is sufficiently accurate for nearly all flat slabs.

The method for obtaining the value of θ_t is illustrated in Fig. 55. Figure 55a shows the combined beam-column member for which the stiffness is to be obtained. The length, L, is taken as the distance between column centerlines. It is assumed the unit torque shown in Fig. 55b is applied uniformly along the centerline of the beam. This results in a twisting moment diagram (Fig. 55c) with the ordinates as shown. Once the twisting moment at each section is known, the unit rotation diagram (Fig. 55d) can be obtained by the ordinary procedures for non-circular cross sections (37). The expression for the curvature at any point is given by the following expression:

$$\Phi = \frac{1}{\sum \beta \, b_1 \, h_1^3} \frac{T}{G} \qquad (24)$$

where Φ = angle of twist per unit of length

T = twisting moment

β = a constant which is a function of the cross section

b_1 = the length (the larger dimension) of each rectangular cross section of the beam

h_1 = the height (the smaller dimension) of each rectangular cross section of the beam

$\sum$ = summation of all rectangular sections

For the system shown in Fig. 55, the average angle of rotation is one-half the area of one of the triangles shown in Fig. 55d. This angle can be obtained from the following expression:

$$\theta_t = \frac{L(1 - c/L)^2}{16\, G \sum \beta\, b_1\, h_1^3} \tag{25}$$

where G = shearing modulus of elasticity

The problem now remains of evaluating the shearing modulus of elasticity, G, and the section constant, $\sum \beta\, b_1\, h_1^3$. For an ideal elastic material, the shearing modulus is given by the expression:

$$G = \frac{E}{2(1 + \mu)} \tag{26}$$

This expression may be used for reinforced concrete with satisfactory accuracy. In view of the variation that may be expected in the modulus of elasticity of concrete in a real structure, it is permissible to let $\mu = 0$ in Equation 26. Thus, the shearing modulus becomes equal to one-half of the "elastic" modulus.

For an L-shaped cross section, the section constant $\sum \beta\, b_1\, h_1^3$, may be obtained by dividing the cross section into two rectangular parts, evaluating $\beta\, b_1\, h_1^3$ for each part, and adding the results. Although there is a small amount of error in this procedure, the results will be sufficiently accurate for use in an equivalent two-dimensional frame analysis. The values of β as a function of b_1/h_1 are shown for convenience in Fig. 56.

If a panel contains a beam parallel to the direction in which the moments are being considered, the assumption of uniformly applied twisting moment will lead to stiffnesses which are too low. It would be possible to assume a different distribution of applied torque but this would complicate the problem considerably. A simpler approach to the problem is to reduce the value of θ_t by the ratio of stiffness of the slab without the beam to that of the slab including the beam. This can be expressed by the following equation:

$$\theta_t' = \theta_t \frac{I_s}{I_{sb}} \tag{26}$$

where θ_t' = the reduced average angle of rotation of a beam

I_s = moment of inertia of the slab without the edge beam

I_{sb} = moment of inertia of the slab including the edge beam

Once the values of θ_f and θ_t have been determined, the stiffnesses of the edge beam-columns can be calculated. This completes the determination of all distribution constants and fixed-end moments. The moments of the column centerlines can now be determined by moment distribution. Moments at the panel centerlines and shears at the columns can be then determined by ordinary methods.

At this stage of the analysis it becomes necessary to reduce the negative moments to the value at the design sections. It is first necessary to make an assumption with regard to the distribution of shear along the design sections. For interior columns, the assumption that the shear is uniformly distributed about the perimeter of the column capital appears to be both simple and, in most cases, conservative. For exterior columns, this assumption may be extended to a uniform distribution across the entire design section.

Once this assumption has been made, the negative moments can be reduced by the moment of the shear taken about the column centerline.

The method of obtaining the negative moment reduction for a square column is illustrated in Fig. 57. The quantities $M_{\text{℄}}$ and M_n represent the moments at the column centerline and the design section respectively. The symbol, V, represents the total shear at the column centerline (as determined from the equivalent frame analysis), v_s represents the uniform shear around the perimenter of the half column, and all other terms are as defined previously. Taking moments about the axis AA, the following expression is obtained for the particular case shown:

$$M_n = M_{\text{℄}} - \left[\frac{3Vc}{8} - \frac{c^3 w}{16}\right] \qquad (27)$$

Similar expressions can be obtained for interior circular capitals, exterior capitals with and without edge beams, or any other support condition.

The moment M_n is the total moment at the negative moment design section. The distribution of the positive and negative moments along the design section can be made according to the coefficients in the ACI Code.

6.2 Comparison with Test Results of Elastic Models

In Reference 38 Huggins and Lin reported the results of tests on an aluminum model of a flat slab. The model contained six 17-in. square panels supported on 4-in. diameter circular column capitals. The columns had an over-all height of 10 in. as measured from the base of the column to the surface of the slab. The columns were bolted to a 1/2-in. aluminum plate at their bases. Loads were applied by means of pneumatic pressure applied through a specially constructed load cell.

Strains were measured on both the top and the bottom of the plate by means of SR-4 electrical resistance strain gages. At each point, strains

were measured in directions both parallel and perpendicular to the three-bay direction of the structure. The strain gages were placed along the column centerlines, panel centerlines, and lines midway between these. A maximum of seven gages was used on each line with several lines having only five gages. As a result of using the limited number of gages, it was necessary in some cases to extrapolate the test results in order to obtain moments at the design sections.

Table 11 gives a comparison of measured moments with those obtained by the proposed frame analysis and by the ACI frame analysis. The values given in the table are the average moments across the entire structure. It can be seen that the total moment measured in each span is in good agreement with the total moment obtained by the proposed frame analysis and is considerably higher than that obtained by the ACI analysis. The positive moments obtained by the proposed analysis, although low, are in better agreement with the measured moments than are those obtained by the ACI frame analysis. At the interior column design sections, the proposed method gives coefficients which are higher than the measured values while the ACI analysis gives moments which are higher than measured in the exterior span and about the same as measured in the interior span. At the exterior row of columns, the ACI analysis predicts only about half of the measured moment. Although still low, the proposed method gives a coefficient which is much closer to the measured value.

In Reference 39, Chinn pointed out that Poisson's ratio will cause an aluminum slab to have considerably different distribution of moment than that in a reinforced concrete slab. Since the test model had a $\mu = 0.33$ while a reinforced concrete slab has a μ of between 0 and 0.15, the aluminum slab should exhibit higher positive moments and lower negative moments.

This correction would make the measured moments agree even more closely with those obtained by the proposed method. Since the total moment in each span would be unchanged, the moments obtained by the ACI Code frame analysis would still not agree with the measured moments.

Bowen and Shaffer have reported the results of a test on a flat plate model made of Lucite (40). The model was constructed to simulate a typical panel of an infinite array of uniformly loaded square panels. In order to approximate this condition, a nine-panel structure was constructed with an overhang beyond the exterior columns which extended approximately to the theoretical point of contraflexure of the adjacent panels. During load tests, a load was applied to this overhang in order to reproduce the shear at this section of an interior panel. Each panel was 5.568 in. square and was supported on 0.348-in. diameter circular columns with no column capitals. The slab was 0.157 in. thick and had no drop panels.

Curvatures of the loaded model were determined by means of a photographic process. Shears and moments were then obtained from the curvatures by means of relations developed from the theory of flexure for plates.

Table 12 gives a comparison of measured moments with those computed by both the proposed frame analysis and the ACI frame analysis. This table shows that the total moment measured in the panel is in good agreement with that computed by the proposed frame analysis but, as expected, is considerably higher than that computed by the Code frame analysis. At both the positive and negative design sections, the proposed method again gives good agreement with the measured moment while the ACI analysis is low.

The measured moments are based on a value of Poisson's ratio of 0.18. Since this is approximately the same value as that normally assumed for concrete, it would be expected that the measured moments would be very nearly the same as might be expected at the design sections of a reinforced

concrete flat plate before cracking. As previously mentioned, the total moment in a panel is unaffected by the value of μ.

Tests of a 25-panel Plexiglass (μ = 0.37) model of a flat slab were reported in Reference 41. The model was unusual in that no columns were provided at the edge of the exterior row of panels. This resulted in a structure consisting of nine panels supported on columns with the remaining panels acting as a continuous cantilever around the edge. The panels were 26 cm square, 0.8 cm thick, and were supported on circular column capitals 10.4 cm in diameter giving a c/L ratio of 0.4. The columns were 1.73 cm in diameter and had a length, from base of the column to the mid-depth of the slab, of 15.6 cm.

During the tests, the columns were supported on a rigid base. Loads were obtained by applying hydrostatic pressure to specially constructed load cells which reacted against a rigid frame. Several types of loading arrangements were investigated and, for each type of loading, measured moments were reported for the center panel, an edge panel, and a corner panel. No moments were reported for the first interior panel.

Table 13 shows a comparison of measured moments (for μ = 1/6) with those computed by both the proposed frame analysis and the ACI frame analysis. Both uniform loading over the entire structure and strip loading for maximum positive moment in the center panel are considered.

For uniform loading over the entire structure, measured moments are in good agreement with those computed by the proposed frame analysis. The agreement is good at both the positive and negative design sections. As in the model tests cited previously, the total measured moment is in good agreement with the static moment in the span. As expected moments based on

the ACI frame analysis are considerably lower than the measured moments.*

For the case of strip loading, the total moment measured in the center panel is again in good agreement with that computed by the proposed frame analysis. Measured and computed moments at the design sections do not agree as well as in the case of uniform load. Again the ACI frame analysis gives moments which are considerably less than those measured. At the positive design section, the maximum moment computed by the ACI frame analysis is even less than that measured under uniform load.

In general, the proposed method gives good results for this model. Where differences exist, they can be attributed to the unusual layout of the model and to the effects of Poisson's ratio as discussed previously.

6.3 Comparison with Test Results of Reinforced Concrete Models

Several tests on quarter-scale models of reinforced concrete slabs have been carried out at the University of Illinois. The properties and dimensions of two of these models (a flat plate and a flat slab) and the test setup are described in References 42 and 43. A portion of the test results for these two models is reported in Reference 26.

The quarter-scale flat plate model was a nine-panel structure supported on square columns which were hinged at the base. The structure had neither column capitals nor drop panels. The nominal c/L ratio was 0.1 and the panels were 5 ft square. Deep edge beams were provided along two adjacent sides and shallow edge beams were provided along the other two. The structure was designed in such a way that the torsional and flexural resistances provided by the edge beams were nearly the same as in the slab analyzed by finite

---

* The measured and computed moments are given for capitals with a c/L of 0.4. Since the capitals used in the model have curved rather than straight sides, the c/L ratio would be about 0.3 according to the ACI Code definition. Since moments at this section of the capital were not reported, all comparisons were based on the larger capitals.

difference methods and reported in Table 6 (UI94). For convenience, the layout and dimensions of the test slab are shown in Fig. 58.

The structure was loaded by means of nine hydraulic jacks. One jack was provided for each panel of the structure. Loads were transmitted to the panels through a system of statically determinate H-frames. Moments at the design sections of each panel were determined by measuring strains in the reinforcing steel and converting these strains to moments on the basis of relations determined on separate tests on beams (44). In addition, column reactions were measured and moments across the entire structure were computed from these.

In Table 14 measured moments across the entire structure and in the center row of panels are compared with computed moments. The measured moments are those obtained with the full design load on the structure.

Comparing the moments across the entire structure shows that the moments obtained by finite difference solutions (UI94) compare favorably with measured moments in the center bay of panels. The difference at the negative moment section can be ascribed to the slight difference in the stiffness of the columns assumed in the analysis and that in the test structure. In the exterior bays, the finite difference solution gives moments at the exterior columns which are larger than measured. At the positive and interior negative moment sections, the computed moments are less than measured. These differences are due to the fact that, in the analysis the edge columns were assumed to have infinite flexural rigidity while in the test model, the edge columns were flexible. Moments computed by the proposed frame analysis are generally in agreement with the measured moments. Although differences exist at individual sections, the over-all agreement is the best of any of the computed moments. Moments obtained by the two methods permitted by the ACI

Code are lower than the measured moments at all sections except the exterior columns. The differences at these sections are due to the fact that these methods do not recognize the reduction in relative stiffness of the edge columns caused by torsional rotation of the edge beams. Although the ACI empirical moment coefficients do not appear to be extremely low, it should be pointed out that a large portion of this moment is assigned to the edge beams. A more realistic comparison for the empirical method can be obtained in an interior strip which does not contain edge beams.

For the interior row of panels, the finite difference solution gives moments which again agree with the measured moments in the center bay. In the exterior panels, the differences in computed and measured moments are slightly greater than they were when the entire structure was considered. Again, these discrepancies are caused by assuming the edge columns to be infinitely stiff in flexure. In this row of panels, the proposed frame analysis gives negative moments which are slightly higher than those measured. This is due to a difference between the assumed distribution of shear around the columns and that which actually existed in the structure. In all cases, these differences are on the safe side. As expected, the ACI empirical moments for the interior row of panels are considerably lower than the measured moments at all sections except the exterior columns. In the center panel, the difference is more than 20 percent. The reasons for these differences were discussed previously.

Table 15 compares measured and computed moments for the exterior strips of columns. These comparisons indicate that moments computed by finite differences and by the proposed frame analysis are in about the same relation to the measured moments as they were in the comparisons of Table 14. Moments determined by the ACI empirical method are generally higher than the moments

measured in the exterior strips. This is due to the fact that, in the empirical method, the edge beams are considered separately and are designed to carry a certain fraction of the panel load. This results in an unduly large amount of the moment being assigned to the edge beams. As would be expected, the moments measured in the edge beams were much lower than would be determined by the empirical method.

The quarter-scale flat slab model contained nine 5-ft square panels. Both drop panels and column capitals were provided. The nominal c/L ratio was 0.2. All columns were 1 ft 10-1/4 in. long and were hinged at their bases. Deep edge beams were provided along two adjacent sides and shallow edge beams were provided along the other two. The layout and dimensions of the slab model are shown in Fig. 59.

Loads were applied by means of the same system used to load the nine-panel flat plate. Moments for the individual panels were again determined from measured steel strains. In addition, reactions were measured and moments across the entire structure were computed from these.

Measured moments across the entire structure and in the center row of panels are compared with computed moments in Table 16. All measured moment coefficients are those obtained with the full design load on the structure.

Over the entire structure, moments obtained by the proposed frame analysis compare well with the measured moments. In the center bay, the positive computed moment is lower than that measured. This gives a total moment in the center bay which is somewhat smaller than measured. The difference is not large, however. The ACI Code frame analysis predicts moments which are smaller than the measured moments at all sections. In this model, the effect of the torsional resistance of the edge beams is not large.

Since the columns are already relatively flexible, the reduction in stiffness caused by the rotation of the edge beams has little influence on the over-all stiffness. Although the empirical moment coefficients again appear to be in agreement with the measured values, the comparison is not valid because a large portion of this moment is assigned to the beams.

In the interior strip of panels, the proposed frame analysis again gives moments which compare well with the measured values. As expected, moments computed by the ACI frame analysis fall below those measured. The empirical moments for the center strip are considerably less than measured moments at all sections except the exterior columns. Since the empirical method does not consider the stiffness of the exterior columns, it provides for moments which are higher than those developed at the section.

Table 17 shows a comparison of measured and computed moments in the exterior rows of panels. In this comparison, the proposed frame analysis gives moments which are lower than those measured. This difference is due in part to the stiffening effect of the edge beams. Since the edge rows of panels are stiffer than the interior, some shear is transferred across the column lines thus increasing the moments in the exterior panels. Further evidence of this can be seen in the fact that measured moments in the center row of panels were slightly lower than those computed. The ACI empirical moments for the exterior rows of panels are nearly as large as the measured moments. Again, this is due to designing the beams as separate structural elements. If only the moment assigned to the slab were considered, the comparison for the exterior panels would be about the same as it was for the interior row of panels.

The above comparisons show that the ACI Code frame analysis and empirical method predict moments in the slab which are lower than those

measured. In the exterior panels, the empirical method increases the moments by considering the beams separately and designing them for a certain percentage of the panel load. At working loads, the moments in the beams are much lower than the empirical moments would indicate while the moments in the slab are correspondingly higher. In general, the proposed frame analysis predicts moments which are in good agreement with those measured. The comparisons show that, in all cases, the proposed method is in better agreement with the test results than are the other methods of computation. At the exterior row of panels, the proposed method consistently predicts moments which agree with the tests while the ACI methods predict values which agree with the tests in only a few cases.

7. NUMERICAL EXAMPLE

7.1 Description of Structure

This chapter presents a numerical example of the proposed frame analysis described in Section 6.1. The method is used to determine the moments in the interior row of panels of the nine-panel flat slab model illustrated in Fig. 59.

In order to analyze the center row of panels, it is assumed that the structure is divided into three rows of panels. The boundaries of the center strip are assumed to be the centerlines of the interior rows of columns. This strip is dimensionally identical to a strip containing an interior row of columns and bounded by the panel centerlines. For simplicity, the illustrations show the entire column at the center of the panel rather than half of it at each side.

Figure 60 shows the layout of the row of panels considered. The cross sections give the dimensions of the structure at the places necessary for the determination of the stiffnesses of the equivalent two-dimensional frame. For purposes of illustration, the Cross moment distribution procedure (35) is considered in this example. However, other methods can be used to determine the final moments in the equivalent two-dimensional frame using the stiffnesses of the individual members determined as shown here.

7.2 Determination of Distribution Constants for the Slab

The center panel of the slab is symmetrical about its centerline and has the cross-sectional dimensions shown by sections AA, BB, and CC in Fig. 60. Section AA gives the dimensions of the slab between drop the panels, Section BB gives the dimensions within the drop panels, and Section CC gives the dimensions over the column capital.

Since the exterior column capitals are not identical to those of the interior columns, the exterior panels are not symmetrical. The dimensions over the exterior column capitals are shown in Section DD. The dimensions at other sections are identical to those of the center panel.

The stiffnesses of the panels are determined from the moments of inertia of the gross cross-sectional areas. For the center row of panels, the numerical values of the moments of inertia for the sections shown in Fig. 60 are:

$$I_{AA}^{*} = 26.80 \text{ in.}^4$$
$$I_{BB} = 48.00 \text{ in.}^4$$
$$I_{CC} = 91.29 \text{ in.}^4$$
$$I_{DD} = 66.78 \text{ in.}^4$$

After these moments of inertia have been determined, the 1/EI diagrams can be constructed for the equivalent two-dimensional beams. Figure 61a shows the 1/EI diagram for the exterior spans and Fig. 61b for the center span. For simplicity, the diagrams are shown in terms of the moment of inertia at the center of the panels.

Once the 1/EI diagrams have been determined, the stiffnesses, carry-over factors, and fixed-end moments can be determined by ordinary methods. The constants for the equivalent two-dimensional beams are given in Table 18. The fixed-end moments are given in terms of M/WL and stiffnesses in terms of the ratio of the stiffness, K, to the modulus of elasticity, E.

7.3 Determination of Distribution Constants of the Columns

The cross-sectional dimensions of the exterior and interior columns are represented by sections EE and FF respectively in Fig. 60. The numerical

---

* Subscripts refer to the corresponding cross section in Fig. 60.

values of the moments of inertia of these cross sections are:

$$I_{EE} = 17.86 \text{ in.}^4$$

$$I_{FF} = 16.48 \text{ in.}^4$$

In this example, it is assumed that the moment of inertia of the columns varies linearly from that of the column at the base of the capital to infinity at the point where the column reaches its full width. The 1/EI diagrams for the interior and exterior columns are shown in Figs. 61c and 61d respectively.

The stiffness of the interior columns can be computed on the basis of the 1/EI diagram by ordinary methods. Table 18 gives the numerical value of the stiffness of the interior columns.

For the exterior columns, it is necessary to compute the stiffnesses of the beam-column combinations at each end of the row of panels. From the 1/EI diagram in Fig. 61d, the numerical value of the rotation of the end of the column, θ_f, due to a unit moment applied at the top of the column is:

$$\theta_f = \frac{0.220}{E}$$

In order to find the total rotation of the beam column combinations at each edge column, it is necessary to add the average rotation, θ_t, of the beams to θ_f. The cross-sectional dimensions of the deep and shallow beams are shown in Fig. 62. On the basis of these cross sections, the rotation for each beam can be obtained by means of Equation 25.

For the deep beam (Fig. 62a) it is convenient to consider the two parts labeled I and II. The quantities necessary for Equation 25 are as follows:

$$G = E/2 \qquad L = 60 \qquad c/L = 0.283$$

Part	b/h	β	$\beta b_1 h_1^3$
I	3.00	0.264	12.67
II	3.28	0.270	8.32
			20.99

Substituting these values into Equation 25, the average rotation of the beam becomes:

$$\theta_t = \frac{0.184}{E}$$

Substituting the quantities θ_f and θ_t into Equation 23, the stiffness for the combined deep beam and edge column becomes:

$$K_{bc} = 2.48E$$

The shallow beam can also be divided into two parts (Fig. 62b). The quantities necessary to find the rotation of the shallow beam are:

$$G = E/2 \qquad L = 60 \qquad c/L = 0.283$$

Part	b/h	β	$\beta b_1 h_1^3$
I	1.80	0.218	15.33
II	1.86	0.221	3.85
			19.18

Substituting into Equation 25, the average rotation of the beam becomes:

$$\theta_t = \frac{0.200}{E}$$

The stiffness of the combined shallow beam and edge column is then found to be:

$$K_{bc} = 2.38E$$

This completes the computation of the distribution constants necessary for the moment distribution procedure. From the constants shown in

Table 18, the moments at the column centerlines and panel centerlines are found to be:

M/WL

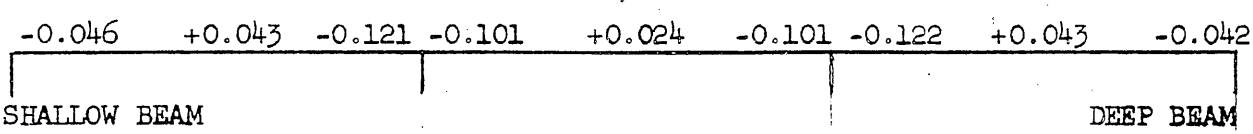

It is now necessary to reduce the negative moments to the values at the design sections.

7.4 Determination of Moments at Design Sections

The first step in determining the negative moment reductions is to find the reactions at the ends of the spans. For the center row of panels, the reactions are found to be:

W

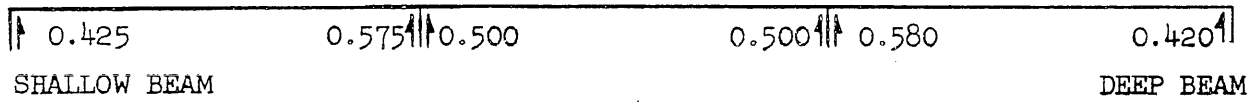

The reduced negative moments at the interior design sections can be found by means of Equation 27. At each edge column, the moment reduction may be found by assuming the reaction linearly distributed along the face of the beam and the column and then summing up the moments about the design section. This is done in the same way as illustrated in Fig. 57 for an interior column. After these reductions have been made, the moments at the design sections of the center row of columns are:

W/WL

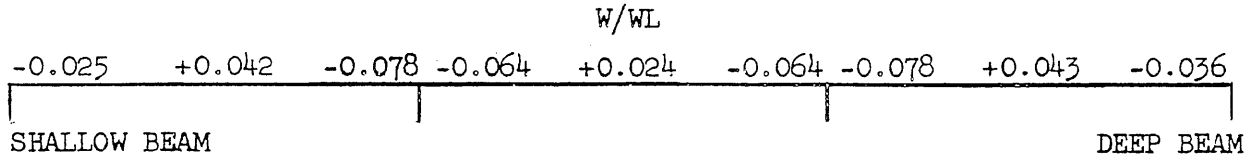

This completes the determination of the moments at the design sections of the center strip of columns.

8. SUMMARY

This study involves the quantitative comparison of moments in reinforced concrete slabs as determined by the analysis of equivalent two-dimensional elastic frames, by analysis based on the theory of flexure for plates, and by tests on both elastic and reinforced concrete models. In the first portion of the investigation, moments determined from the analysis of equivalent frames are compared with the moments based on plate theory. Moments determined from plate theory included solutions by the use of finite difference methods and by the use of a double-infinite Fourier Series. These solutions included the following conditions:

1. A typical panel of an infinite array of uniformly loaded square panels supported on circular column capitals.

2. A typical panel of an infinite array of uniformly loaded square panels supported on square column capitals.

3. A typical panel of an infinite array of uniformly loaded rectangular panels supported on square column capitals.

4. A loaded panel of an infinite array of square panels with strip loading for maximum positive moments and supported on square column capitals.

5. A nine-panel structure supported on infinitely rigid square columns and having no edge beams.

6. A nine-panel structure supported on infinitely rigid square supports and having deep edge beams on two adjacent sides and shallow edge beams on the other two sides.

These studies indicated that the ACI equivalent frame analysis* predicted moments which were lower than those obtained by plate theory. However, the comparisons showed that the frame analysis predicted the correct trend of the changes in the moments with the critical variables. On the basis of these comparisons, the properties of the hypothetical equivalent frame used

---

* ACI 318-56, Section 1003, "Design by Elastic Analysis," Reference 31.

in the two-dimensional analysis were modified to yield moments in good agreement with those obtained by plate theory.

In Chapter 6, moments obtained by the proposed frame analysis are compared with those measured in tests on elastic and reinforced concrete models of slabs. These tests include:

1. A six-panel aluminum flat slab.
2. A nine-panel Lucite flat plate loaded to simulate an infinite array of panels.
3. A twenty-five-panel Plexiglass flat slab.
4. A nine-panel reinforced concrete flat plate.
5. A nine-panel reinforced concrete flat slab.

Although a two-dimensional frame analysis should not be expected to give the exact moments in slabs, it does give values which are sufficiently accurate for design purposes. The comparisons show that even though the moments obtained by the proposed frame analysis differ from measured moments at some sections, the agreement is generally good. In nearly every case, moments obtained by the proposed frame analysis are in better agreement with the measured moments than are those computed by the methods of the 1956 ACI Code.

On the basis of this investigation, the following general conclusions are reached:

1. The present ACI Code frame analysis gives moments which are lower than either those obtained on the basis of plate theory or those measured in tests on models.
2. In the present frame analysis, the assumptions for stiffness over the supports are unrealistic.
3. An equivalent frame analysis can be used to calculate the moments at the design sections of a reinforced concrete slab with rectilinear panels.
4. The equivalent two-dimensional frame proposed in this report gives moments which compare well with the moments measured in tests on models.

In Chapter 7, a numerical example is given in which the interior strip of the reinforced concrete flat slab model is analyzed. This example illustrates how the proposed frame analysis can be applied to a typical strip of panels.

REFERENCES

1. Westergaard, H. M. and W. A. Slater, "Moments and Stresses in Slabs," Journal ACI, V. 17, 1926, pp. 415-538.

2. Euler, L., "De sono campanarum, Novi Commentarii Academiae Petropolitanae," V. 10, 1766.

3. Bernouilli, J., "Esaai Théorétique sur les vibrations des plaques élastiques rectangulaires et libres," Nova Acta Academiae Scientarum Petropolitanae, V. 5, 1787.

4. Todhunter, I. and K. Pearson, "A History of the Theory of Elasticity," Cambridge, 1886.

5. Poisson, S. D., "Mémoire sur l'équilibre et le mouvement des corps élastique," Memoirs of the Paris Academy, V. 8, 1829, pp. 357-570.

6. Kirchhoff, G. R., "Ueber das Gleichgewicht und die Bewegung einer elastischen Scheibe," Crelles Journal, 1850, V. 40, pp. 51-58.

7. Timoshenko, S. P., "History of Strength of Materials," McGraw-Hill, New York, 1953, p. 452.

8. Boussinesq, J., "Étude nouvelle sur l'équilibre et le mouvement des corps solides élastiques dont certaines dimensions, sont très-petites par rapport a d'autres," Journal de Mathématiques, 1871, pp. 125-274, and 1879, pp. 329-344.

9. Lavoinne, E., "Sur la résistance des parois planes des chaudières a vapeur," Annales des Ponts et Chaussées, V. 3, 1872, pp. 276-303.

10. Levy, M., "Sur l'équilibre élastique d'une plaque rectangulaire," Comptes Rendus, V. 129, 1899, pp. 535-539.

11. Bach, C., "Versuche über die Winderstandsfähigkeit eberner Platten," Zeitschr. d. Ver. deutscher Ingenieure, V. 34, 1890, pp. 1041-1048, 1080-1086, 1103-1111, 1139-1144.

12. Bach, C., "Die Berechnung flacher, durch Anker oder Stehbolzen unterstützer Kesselwandunger und die Ergebnisse der nauesten hierauf bezüglichen Versuche," Zeitschr. d. Ver. deutscher Ingenieure, 1894, pp. 341-349.

13. Ritz, W., "Ueber eine neue Methodé zur Lössung gewisser Variations-probleme der mathematischen Physik," Crelles Journal, V. 135, 1909, pp. 1-61.

14. Nielsen, N. J., "Bestemmelse af Spaendinger i Plader ved Anvendelse af Differensligninger," Copenhagen, 1920

15. Marcus, H., "Die Theorie elastischer Gewebe und ihre Anwendung auf die Berechnung biegsamer Platten," Julius Springer, Berlin, 1924.

16. Casillas, G. De L., J., N. Khachaturian, and C. P. Siess, "Studies of Reinforced Concrete Beams and Slabs Reinforced with Steel Plates," Civil Engineering Studies, Structural Research Series No. 134, University of Illinois, Urbana, Illinois, April 1957.

17. Ang, A., "The Development of a Distribution Procedure for the Analysis of Continuous Rectangular Plates," Civil Engineering Studies, Structural Research Series No. 176, University of Illinois, Urbana, Illinois, May 1959.

18. Nichols, J. R., "Statical Limitations Upon the Steel Requirement in Reinforced Concrete Flat Slab Floors," Trans. ASCE, V. 77, 1914, pp. 1670-1681.

19. Siess, C. P., "Re-Examination of Nichols' Expression for the Static Moment in a Flat Slab Floor," ACI Journal, V. 30, No. 7, Jan. 1959, (Proceedings V. 55), pp. 811-813.

20. Cassie, W. F., "Early Reinforced Concrete in Newcastle-upon-Tyne," The Structural Journal, April 1955, pp. 134-137.

21. Eddy, H. T. and C. A. P. Turner, "Concrete Steel Construction," 2nd Edition, 1919.

22. Turner, C. A. P., Discussion of: "Reinforced Concrete Warehouse for Northwest Knitting Co., Minneapolis, Minnesota," Engineering News, V. 54, No. 15, Oct. 12, 1905, p. 383.

23. Bill, M., "Robert Maillart," Zurich, 1947, 180 p.

24. Lord, A. R., "A Test of a Flat Slab Floor in a Reinforced Concrete Building," Proceedings of National Association of Cement Users (ACI), V. 7, 1911, pp. 156-179.

25. Eddy, H. T., "Steel Stresses in Flat Slabs," Transactions ASCE, V. 77, 1914, pp. 1338-1454.

26. Hatcher, D. S., M. A. Sozen, and C. P. Siess, "A Study of Tests on a Flat Plate and a Flat Slab," Civil Engineering Studies, Structural Research Series No. 217, University of Illinois, Urbana, Illinois.

27. Taylor, F. W., S. E. Thompson, and E. Smulski, "Concrete, Plain and Reinforced," 4th Edition, John Wiley and Sons, 1925.

28. Dewell, H. D. and H. B. Hammill, "Flat Slabs and Supporting Columns and Walls Designed as Indeterminate Structural Frames," Journal ACI, Jan.-Feb. 1938, (Proceedings V. 34), pp. 321-344.

29. Di Stasio, J. and M. P. Van Buren, "Background of Chapter 10, 1956 ACI Regulations for Flat Slabs," Private Communication, Di Stassio and Van Buren, Consulting Engineers, New York City.

30. Peabody, D., "Continuous Frame Analysis of Flat Slabs," Journal Boston Society of Civil Engineers, V. 26, No. 3, July 1939, pp. 183-207.

31. "Building Code Requirements for Reinforced Concrete," (ACI 318-56).

32. Zweig, A., Discussion of: "Proposed Revision of Building Code Requirements for Reinforced Concrete (ACI 318-51)," Journal ACI, V. 28, No. 6, Part II, Dec. 1956, (Proceedings V. 52) pp. 1287-1296.

33. Lewe, V., "Pilzdecken," Wilhelm Ernst and Son, Berlin, 1926, 182 p.

34. Newmark, N. M., "Numerical Methods of Analysis of Bars, Plates, and Elastic Bodies," An Article from "Numerical Methods of Analysis in Engineering," Edited by L E. Grinter, MacMillan Co., New York, 1949.

35. Shedd, T. C., and J. Vawter, "Theory of Simple Structures," 2nd Edition, John Wiley and Sons, Inc., New York, 1941, p. 397.

36. Timoshenko, S. P., and J. N. Goodier, "Theory of Elasticity," McGraw-Hill, New York, 1951, p. 302.

37. Seely, F. B., and J. O. Smith, "Advanced Mechanics of Materials," 2nd Edition, John Wiley and Sons, New York, 1959.

38. Huggins, M. W., and W. L. Lin, "Moments in Flat Slabs," Trans. ASCE, V. 123, 1958, pp. 824-841.

39. Chinn, J., Discussion of: "Moments in Flat Slabs," Trans. ASCE, V. 123, 1958, pp. 842-845.

40. Bowen, G. and R. W. Shaffer, "Flat Slab Solved by Model Analysis," ACI Journal, V. 26, No. 6, Feb. 1955, (Proceedings V. 51), pp. 553-570.

41. Bergvall, B., "Rapport Över Modellförsök Med Pelardäck," Stockholm 1959.

42. Mayes, G. T., M. A. Sozen, and C. P. Siess, "Tests on a Quarter-Scale Model of a Multiple-Panel Reinforced Concrete Flat Plate Floor," Civil Engineering Studies, Structural Research Series No. 181, University of Illinois, Urbana, Illinois, September 1959.

43. Hatcher, D. S., M. A. Sozen, and C. P. Siess, "An Experimental Study of a Quarter-Scale Reinforced Concrete Flat Slab Floor," Civil Engineering Studies, Structural Research Series No. 200, University of Illinois, Urbana, Illinois, June 1960.

44. Mila, F. J., "Relationship Between Reinforcement Strain and Bending Moment in Reinforced Concrete," A report on the research project, "Investigation of Multiple-Panel Reinforced Concrete Floor Slabs," Civil Engineering Department, University of Illinois, July, 1960.

TABLE 1

EARLY LOAD TESTS ON FLAT SLABS, DIMENSIONS AND LOADING ARRANGEMENTS*

	Shredded Wheat Factory	Jersey City Dairy Co. Bldg.	Purdue Test Slabs "S"	Purdue Test Slabs "J"	Sanitary Can Factory	Shonk Bldg.	Larkin Bldg.	Franks Bldg.	Shulze Baking Co. Bldg.	Western Newspaper Union Bldg.	Northwestern Glass Co. Bldg.	Bell Street Warehouse	Channon Bldg.	International Hall
Panel Dimensions (L_a and L_b)**	20'-0" by 22'-0"	17'-11" by 10'-8$\frac{1}{4}$"	16'-0" by 16'-0"	16'-0" by 16'-0"	22'-0' by 22'-0"	22'-0" by 22'-0"	20'-0" by 24'-2"	20'-3" by 11'-4"	20'-0" by 17'-6"	17'-4$\frac{1}{2}$" by 19'-4$\frac{1}{2}$"	16'-0" by 17'-0"	20'-0" by 20'-9"	20'-0$\frac{1}{2}$" by 20'-0$\frac{1}{2}$"	18'-0" by 18'-0"
Column Head Diameter, c, in.	42	62	45	45	60	60	60	44	54	54	56	57	54	40
c/L_a**	0.175	0.288	0.234	0.234	0.227	0.227	0.250	0.181	0.225	0.259	0.292	0.238	0.225	0.185
c/L_b**	0.159	0.262	0.234	0.234	0.227	0.227	0.208	0.190	0.257	0.232	0.275	0.229	0.225	0.185
Slab Thickness, in.	7.29	8	5.77	5.47	10.57	10.8	9	9.25	8.87	8.5	8.08	10.86	8	7.1
Drop Panel Thickness, in.	9.13	10	7.74	7.61	14.07	13.8	15.75	13.25	14.28	None	None	None	12$\frac{1}{2}$	None
No. of Panels Loaded	9	1	4	4	4	4	5	4	4	4	4	4	4	4
Maximum Test Load, psf	282	508	522	872	532	535	730	428	722	1019	349	834	750	483

* For further details see Reference 1.

** L_a is span length in direction of short span

L_b is span length in direction of long span

TABLE 2. DIMENSIONS, PROPERTIES, AND AVERAGE MOMENTS FOR PANELS ANALYZED BY LEWE

Designation	Ratio of Span Lengths L_b/L_a*	Size of Capital c/L_1**	Distribution of Reaction	Distribution of Load	Computed Moment at Design Section M/WL_1**		
					Positive	Negative	Sum
LS1	1	0	Point	Uniform	0.0412	0.0838	0.1250
LS2	1	0.125	Uniform	Uniform	0.0407	0.0612	0.1019
LS3	1	0.250	Uniform	Uniform	0.0391	0.0437	0.0828
LS4	1	0.333	Uniform	Uniform	0.0376	0.0337	0.0713
LS5	1	0.500	Uniform	Uniform	0.0308	0.0123	0.0431
LR1							
Long Span	2	0	Point	Uniform	0.0400	0.0836	0.1236
Short Span	2	0	Point	Uniform	0.0410	0.0840	0.1250
LR2							
Long Span	2	0.125	Uniform	Uniform	0.0364	0.0428	0.0792
Short Span	2	0.250	Uniform	Uniform	0.0406	0.0606	0.1012
LS2S	1	0.125	Uniform	Alternate Strips	0.0831+		
LS3S	1	0.250	Uniform	Alternate Strips	0.0812+		
LS4S	1	0.333	Uniform	Alternate Strips	0.0811+		

* L_a is span length in direction of short span
L_b is span length in direction of long span

** L_1 is in terms of length of span in direction considered

\+ Only maximum positive moment is given for strip loading

TABLE 3. DIMENSIONS, PROPERTIES, AND AVERAGE MOMENTS FOR PANELS ANALYZED BY NIELSEN

Designation	L_b/L_a *	c/L_1 **	Distribution of Reaction	Stiffness in Capital/Stiffness at Centerline of Slab		Moment at Design Section M/WL_1 **		
				Edge	Center	Positive	Negative	Sum
NS1	1	0	Point	--	1	0.0425	0.0825	0.1250
NS2	1	0	Point	4+	4+	0.0294	0.0956	0.1250
NS3	1	0.20	Uniform	1	1	0.0401	0.0517	0.0918
NS4	1	0.20	Line	1	∞	0.0358	0.0539	0.0897
NS5	1	0.40	Uniform	1	9	0.0326	0.0283	0.0609
NR6								
Long Span	1.50	0	Point	1	1	0.0464	0.0787	0.1250
Short Span	1.50	0	Point	1	1	0.0437	0.0813	0.1250

* L_a is span length in direction of short span
L_b is span length in direction of long span

** L_1 is in terms of length of span in the direction considered

\+ Slab NS2 has square drop panels of 0.40 of the span length

TABLE 4. DIMENSIONS, PROPERTIES, AND AVERAGE MOMENTS FOR PANELS ANALYZED BY MARCUS

Designation	L_b/L_a *	c/L_1 **	Distribution of Reaction	Stiffness in Capital/Stiffness at Centerline of Slab		Moment at Design Section M/WL_1 **		
				Edge	Center	Positive	Negative	Sum
MS1	1	0	Point	-	1	0.0436	0.0814	0.1250
MS2	1	0.25	Line	1	1	0.0356	0.0439	0.0795
MR3								
Long Span	1.33	0.125	Line	1	1	0.0404	0.0636	0.1040
Short Span	1.33	0.166	Line	1	1	0.0412	0.0564	0.0976

* L_a is span length in direction of short span
L_b is span length in direction of long span
** L_1 is in terms of length of span in the direction considered

TABLE 5. DIMENSIONS, LOADING, AND AVERAGE MOMENTS FOR UNIVERSITY OF ILLINOIS INVESTIGATIONS OF SQUARE INTERIOR PANELS

Designation	c/L	Distribution of Reaction	Distribution of Load	Moment at Design Section M/WL		
				Positive	Negative	Sum
UI1	0.100	Concentrated at Corners of Capital	Uniform	0.0386	0.0632	0.1018
UI2	0.125	Concentrated at Corners of Capital	Uniform	0.0361	0.0611	0.0962
UI3	0.200	Concentrated at Corners of Capital	Uniform	0.0316	0.0464	0.0780
UI4	0.250	Concentrated at Corners of Capital	Uniform	0.0284	0.0401	0.0685
UI5	0.200	Concentrated at Corners of Capital	Alternate Strips	0.0350*	0.0411*	0.0761*

* Moments are those in a direction perpendicular to the loaded strips; thus, the positive moment is the maximum possible under any loading conditions. Negative moment is given for information only.

TABLE 6. DIMENSIONS, PROPERTIES, AND LOADING FOR UNIVERSITY OF ILLINOIS INVESTIGATION OF 9-PANEL STRUCTURES

Designation	c/L	Marginal Beams				Panels Loaded
		Deep Beams		Shallow Beams		
		H_f	J	H_f	J	
UI91	0.1	0	0	0	0	1, 4, 7
UI92	0.1	0	0	0	0	2, 5, 8
UI93	0.1	0	0	0	0	All
UI94	0.1	1.00	0.25	0.25	0.25	All

TABLE 7. DIMENSIONS, PROPERTIES, AND AVERAGE MOMENTS FOR PANELS ANALYZED BY WESTERGAARD

Designation	L_b/L_a^*	c/L_1	Distribution of Reaction	Moment at Design Section M/WL_1		
				Positive	Negative	Sum
WS1	1	0.15	Line	0.0361	0.0653	0.1014
WS2	1	0.20	Line	0.0334	0.0594	0.0928
WS3	1	0.25	Line	0.0319	0.0522	0.0841
WS4	1	0.30	Line	0.0283	0.0456	0.0739

* L_a is span length in direction of short span

L_b is span length in direction of long span

** L_1 is in terms of length of span in the direction considered

TABLE 8. COMPARISON OF MOMENTS IN 9-PANEL STRUCTURE WITHOUT EDGE BEAMS

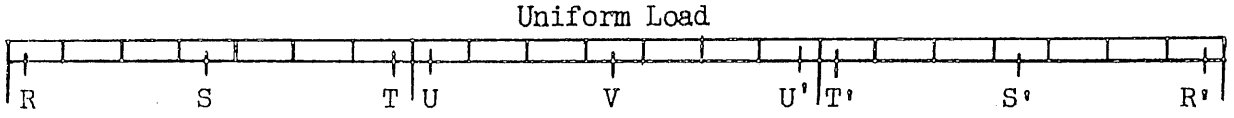

Moment Coefficients of WL

Section	R	S	T	Sum	U	V	Sum
Exterior Row of Panels							
Computed Moments (U of I)*	0.029	0.044	0.069	0.093	0.062	0.037	0.099
ACI Code Frame Analysis**	0.061	0.034	0.061	0.095	0.061	0.034	0.095
ACI Code Empirical	0.041	0.040	0.056	0.089	0.056	0.031	0.087
Interior Row of Panels							
Computed Moments (U of I)*	0.032	0.044	0.065	0.093	0.062	0.038	0.100
ACI Code Frame Analysis**	0.061	0.034	0.061	0.095	0.061	0.034	0.095
ACI Code Empirical	0.041	0.040	0.056	0.089	0.056	0.031	0.087
Entire Structure							
Computed Moments (U of I)*	0.030	0.044	0.068	0.093	0.062	0.037	0.099
ACI Code Frame Analysis**	0.061	0.034	0.061	0.095	0.061	0.034	0.095
ACI Code Empirical	0.041	0.040	0.056	0.089	0.056	0.031	0.087

* Twisting moments around columns are not included

** Moments obtained by frame analysis are not reduced to M_o

TABLE 9. COMPARISON OF MOMENTS IN 9-PANEL STRUCTURE WITHOUT EDGE BEAMS

Strip Loads

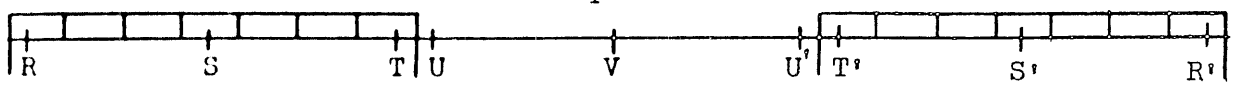

Moment Coefficients of WL

Section	R	S	T	Sum	U	V	Sum
			Entire Structure				
Computed Moments (U of I)*	0.032	0.048	0.053	0.098	0.015	0.009	--
ACI Code Frame Analysis**	0.061	0.034	0.061	0.095	0	0	--

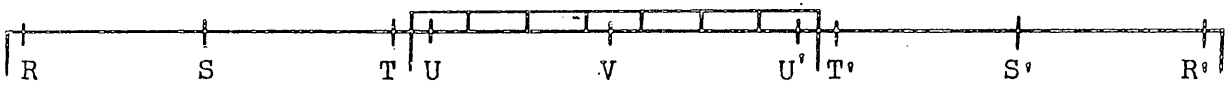

Section	R	S	T	Sum	U	V	Sum
			Entire Structure				
Computed Moments (U of I)*	0.002	0.004	0.012	--	0.047	0.046	0.093
ACI Code Frame Analysis**	0	0	0	--	0.061	0.034	0.095

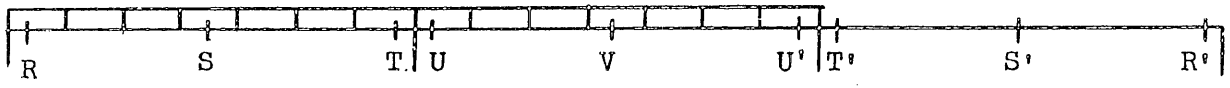

Section	R	S	T	Sum	U	V	U'	Sum	T'	S'	R'	Sum
					Entire Structure							
Computed Moments (U of I)*	0.030	0.044	0.065	0.092	0.064	0.051	0.044	0.105	0.011	0.004	0.002	--
ACI Code Frame Analysis**	0.061	0.034	0.061	0.095	0.061	0.034	0.061	0.095	0	0	0	--

* Twisting moments around columns are not included

** Moments obtained by frame analysis are not reduced to M_o

TABLE 10. COMPARISON OF MOMENTS IN 9-PANEL STRUCTURE WITH EDGE BEAMS

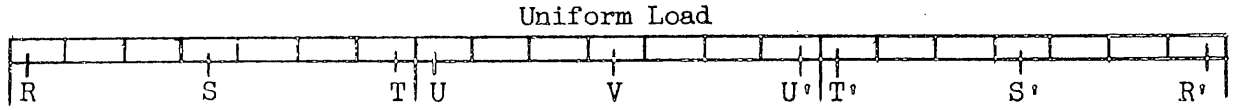

Moment Coefficients of WL

Section	R	S	T	Sum	U	V	U'	Sum	T'	S'	R'	Sum
Exterior Row of Panels (Deep Beam)												
Computed Moments (U of I)*	0.051	0.041	0.064	0.099	0.062	0.038	0.052	0.100	0.063	0.042	0.052	0.100
ACI Code Frame Analysis**	0.061	0.034	0.061	0.095	0.061	0.034	0.061	0.095	0.061	0.034	0.061	0.095
ACI Code Empirical	0.067	0.051	0.080	0.125	0.080	0.044	0.080	0.124	0.080	0.051	0.070	0.126
Exterior Row of Panels (Shallow Beam)												
Computed Moments (U of I)*	0.049	0.042	0.063	0.098	0.062	0.038	0.062	0.100	0.063	0.042	0.049	0.098
ACI Code Frame Analysis**	0.061	0.084	0.061	0.095	0.061	0.034	0.061	0.095	0.061	0.034	0.061	0.095
ACI Code Empirical	0.054	0.045	0.068	0.106	0.068	0.039	0.068	0.107	0.068	0.045	0.057	0.108
Interior Row of Panels												
Computed Moments (U of I)*	0.045	0.043	0.062	0.097	0.061	0.039	0.061	0.100	0.062	0.043	0.046	0.097
ACI Code Frame Analysis**	0.061	0.034	0.061	0.095	0.061	0.034	0.061	0.095	0.061	0.034	0.061	0.095
ACI Code Empirical	0.041	0.040	0.056	0.089	0.054	0.031	0.054	0.085	0.056	0.040	0.043	0.090
Entire Structure												
Computed Moments (U of I)*	0.048	0.042	0.063	0.098	0.062	0.038	0.061	0.100	0.063	0.043	0.049	0.099
ACI Code Frame Analysis**	0.061	0.034	0.061	0.095	0.061	0.034	0.061	0.095	0.061	0.034	0.061	0.095
ACI Code Empirical	0.054	0.045	0.068	0.106	0.067	0.038	0.067	0.105	0.068	0.045	0.057	0.108

* Twisting moments around columns are not included

** Moments obtained by frame analysis are not reduced to M_o

TABLE 11. COMPARISON OF MEASURED MOMENTS WITH MOMENTS COMPUTED FOR 6-PANEL ALUMINUM FLAT SLAB MODEL

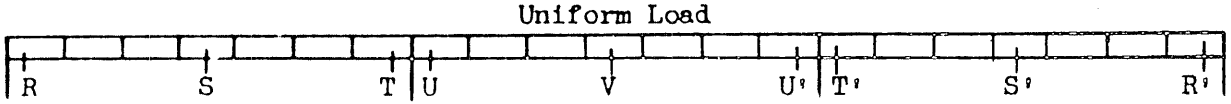

Moment Coefficients of WL

Section	R	S	T	Sum	U	V	Sum
			Entire Structure				
Measured Moments	0.027	0.047	0.051	0.086	0.049	0.039	0.088
Proposed Frame Analysis	0.021	0.043	0.069	0.088	0.057	0.031	0.088
ACI Code Frame Analysis*	0.015	0.033	0.057	0.069	0.048	0.021	0.069

* Moments obtained by ACI Code frame analysis are not reduced to M_o

TABLE 12. COMPARISON OF MEASURED MOMENTS WITH MOMENTS COMPUTED FOR LUCITE FLAT PLATE MODEL

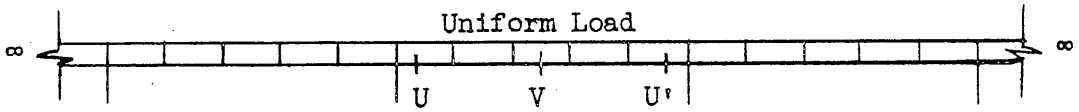

Moment Coefficients of WL

Section	U	V	Sum
Measured Moments	0.0724	0.0426	0.1150
Proposed Frame Analysis	0.0741	0.0410	0.1151
ACI Code Frame Analysis*	0.0667	0.0366	0.1033

* Moments obtained by ACI Code frame analysis are not reduced to M_o

TABLE 13. COMPARISON OF MEASURED MOMENTS WITH MOMENTS COMPUTED FOR CENTER PANEL OF 25-PANEL PLEXIGLASS FLAT SLAB MODEL

Uniform Load

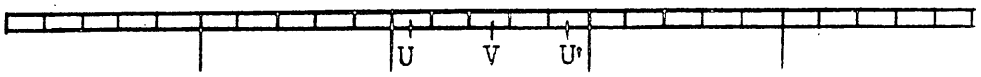

Moment Coefficients of WL

Section	U	V	Sum
Measured Moments	0.033	0.030	0.063
Proposed Frame Analysis	0.031	0.033	0.064
ACI Code Frame Analysis*	0.023	0.018	0.041

Strip Loading

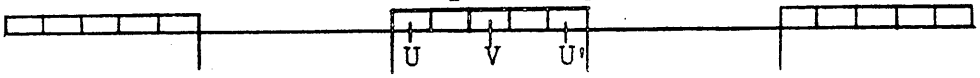

Section	U	V	Sum
Measured Moments	0.012	0.051	0.063
Proposed Frame Analysis	0.021	0.043	0.064
ACI Code Frame Analysis*	0.018	0.023	0.041

* Moments obtained by ACI Code frame analysis are not reduced to M_o

TABLE 14. COMPARISON OF MEASURED MOMENTS WITH MOMENTS COMPUTED FOR 9-PANEL REINFORCED CONCRETE FLAT PLATE MODEL

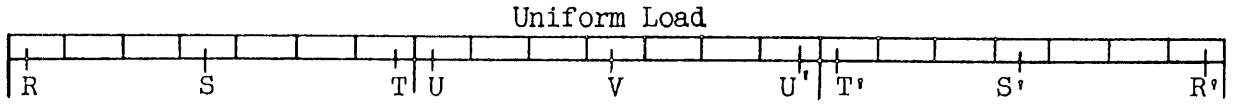

Moment Coefficients of WL

Section	R	S	T	Sum	U	V	U'	Sum	T'	S'	R'	Sum
					Entire Structure							
Moments Measured from Strains+	0.029	0.052	0.069	0.101	0.063	0.038	0.062	0.101	0.064	0.048	0.035	0.098
Moments Measured from Reactions+	0.030	0.053	0.078	0.107	0.071	0.037	0.070	0.108	0.078	0.052	0.041	0.112
Difference Solutions (UI94)*	0.045	0.043	0.062	0.096	0.061	0.039	0.061	0.100	0.062	0.043	0.046	0.097
Proposed Frame Analysis	0.024	0.051	0.090	0.108	0.068	0.038	0.068	0.0106	0.092	0.052	0.031	0.114
ACI Code Frame Analysis**	0.058	0.036	0.066	0.098	0.061	0.034	0.061	0.095	0.066	0.036	0.058	0.098
ACI Code Empirical Moments	0.049	0.031	0.071	0.091	0.063	0.041	0.063	0.104	0.071	0.031	0.052	0.093
					Interior Row of Panels							
Moments Measured from Strains+	0.025	0.049	0.066	0.095	0.063	0.039	0.063	0.103	0.058	0.047	0.032	0.092
Difference Solutions (UI94)*	0.045	0.053	0.062	0.096	0.061	0.039	0.061	0.100	0.062	0.043	0.046	0.097
Proposed Frame Analysis	0.034	0.048	0.088	0.108	0.069	0.037	0.069	0.106	0.090	0.048	0.041	0.113
ACI Code Frame Analysis**	0.058	0.036	0.066	0.098	0.061	0.034	0.061	0.095	0.066	0.036	0.058	0.098
ACI Code Empirical Moments	0.042	0.040	0.058	0.090	0.051	0.031	0.051	0.082	0.058	0.040	0.044	0.051

+ Measured moment coefficients are given for the design load
* Twisting moments around columns are not included
** Moments obtained by ACI Code frame analysis are not reduced to M_o

TABLE 15. COMPARISON OF MEASURED MOMENTS WITH MOMENTS COMPUTED FOR 9-PANEL REINFORCED CONCRETE FLAT PLATE MODEL

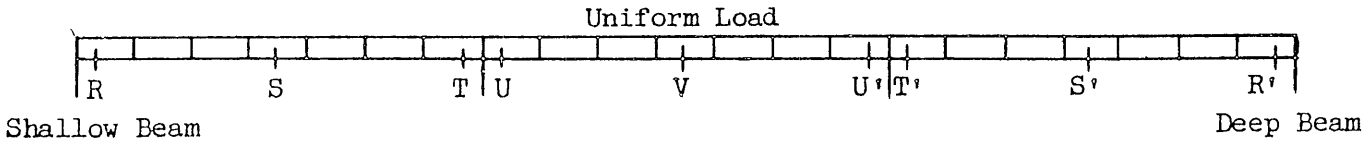

Moment Coefficients of WL

Section	R	S	T	Sum	U	V	U'	Sum	T'	S'	R'	Sum
Exterior Row of Panels (Deep Beam)												
Moments Measured from Strains+	0.030	0.051	0.068	0.100	0.058	0.030	0.058	0.088	0.069	0.044	0.037	0.097
Difference Solutions (UI94)*	0.051	0.041	0.064	0.098	0.062	0.038	0.062	0.100	0.063	0.042	0.052	0.099
Proposed Frame Analysis	0.026	0.053	0.083	0.108	0.067	0.040	0.067	0.106	0.084	0.054	0.036	0.113
ACI Code Empirical Moments	0.055	0.059	0.082	0.128	0.072	0.048	0.072	0.120	0.082	0.059	0.059	0.130
Exterior Row of Panels (Shallow Beam)												
Moments Measured from Strains+	0.032	0.055	0.072	0.107	0.068	0.046	0.068	0.113	0.065	0.052	0.036	0.103
Difference Solutions (UI94)*	0.049	0.042	0.063	0.098	0.062	0.038	0.062	0.099	0.063	0.042	0.049	0.099
Proposed Frame Analysis	0.033	0.048	0.086	0.108	0.069	0.038	0.069	0.106	0.088	0.049	0.041	0.114
ACI Code Empirical Moments	0.051	0.053	0.074	0.115	0.066	0.043	0.066	0.108	0.074	0.053	0.054	0.117

+ Measured moment coefficients are given for the design load

* Twisting Moments around columns are not included

TABLE 16. COMPARISON OF MEASURED MOMENTS WITH MOMENTS COMPUTED FOR 9-PANEL REINFORCED CONCRETE FLAT SLAB MODEL

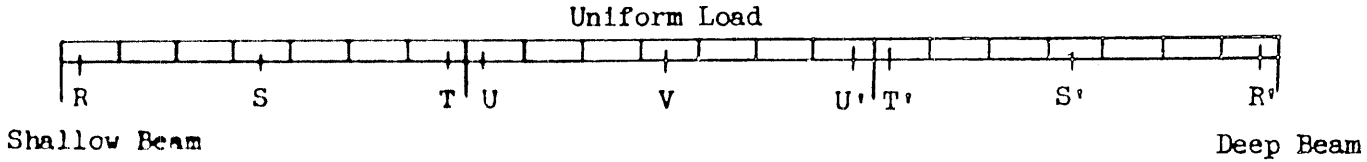

Moment Coefficients of WL

Section	R	S	T	Sum	U	V	U'	Sum	T'	S'	R'	Sum
Entire Structure												
Moments Measured from Strains+	0.025	0.050	0.083	0.104	0.077	0.035	0.073	0.110	0.081	0.048	0.040	0.108
Moments Measured from Reactions+	0.023	0.049	0.069	0.095	0.059	0.035	0.058	0.093	0.070	0.049	0.040	0.104
Proposed Frame Analysis	0.019	0.046	0.088	0.100	0.061	0.027	0.061	0.088	0.098	0.046	0.036	0.113
ACI Code Frame Analysis*	0.022	0.031	0.058	0.071	0.050	0.021	0.050	0.071	0.058	0.031	0.022	0.071
ACI Code Empirical Moments	0.044	0.041	0.063	0.095	0.058	0.032	0.058	0.090	0.063	0.041	0.047	0.096
Interior Row of Panels												
Moments Measured from Strains+	0.022	0.041	0.067	0.084	0.059	0.028	0.059	0.087	0.060	0.036	0.033	0.082
Proposed Frame Analysis	0.025	0.042	0.078	0.093	0.064	0.024	0.064	0.088	0.079	0.043	0.036	0.096
ACI Code Frame Analysis*	0.022	0.031	0.058	0.071	0.050	0.021	0.050	0.071	0.058	0.031	0.022	0.071
ACI Code Empirical Moments	0.036	0.029	0.048	0.071	0.043	0.023	0.043	0.066	0.048	0.029	0.037	0.071

+ Measured moment coefficients are given for the design load
* Moments obtained by ACI Code frame analysis are not reduced to M_o

TABLE 17. COMPARISON OF MEASURED MOMENTS WITH MOMENTS COMPUTED FOR 9-PANEL REINFORCED CONCRETE FLAT SLAB MODEL

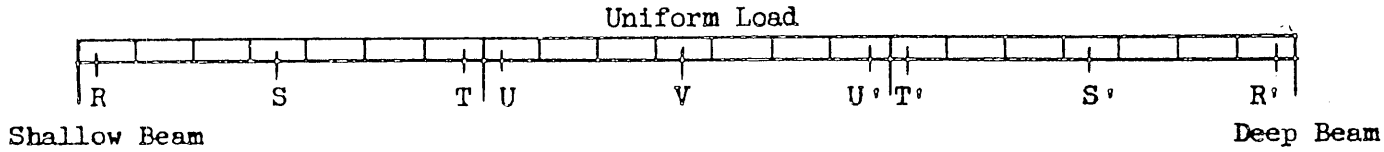

Moment Coefficients of WL

Section	R	S	T	Sum	U	V	U'	Sum	T'	S'	R'	Sum
Exterior Row of Panels (Deep Beam)												
Moments Measured from Strains+	0.026	0.052	0.099	0.114	0.094	0.038	0.094	0.132	0.101	0.059	0.042	0.130
Proposed Frame Analysis	0.014	0.051	0.084	0.100	0.071	0.029	0.071	0.099	0.084	0.051	0.031	0.109
ACI Code Empirical Moments	0.050	0.050	0.074	0.112	0.070	0.037	0.070	0.107	0.074	0.050	0.052	0.114
Exterior Row of Panels (Shallow Beam)												
Moments Measured from Strains+	0.027	0.057	0.083	0.112	0.075	0.038	0.075	0.112	0.080	0.049	0.044	0.111
Proposed Frame Analysis	0.023	0.042	0.093	0.100	0.076	0.024	0.076	0.099	0.092	0.042	0.041	0.110
ACI Code Empirical Moments	0.046	0.043	0.067	0.100	0.062	0.035	0.062	0.096	0.067	0.043	0.051	0.102

+ Measured moment coefficients are given for the design load

TABLE 18. DISTRIBUTION CONSTANTS FOR CENTER STRIP OF PANELS

Equivalent Beams

Fixed-End Moment, M/WL		-0.0914	-0.0992	-0.0967	-0.0967	-0.0992	-0.0914
Carry-Over Factor	Left to Right	-0.643		-0.620		-0.581	
	Right to Left	-0.581		-0.620		-0.643	
Stiffness, K/E		2.79	2.89	2.94	2.94	2.89	2.79

Equivalent Columns

Column No.	I	II and III	IV
Stiffness, K/E	2.38	4.19	2.48

PANELS 4, 5, AND 6 UNIFORMLY LOADED

c/L = 1/10

MOMENT COEFFICIENTS OF WL

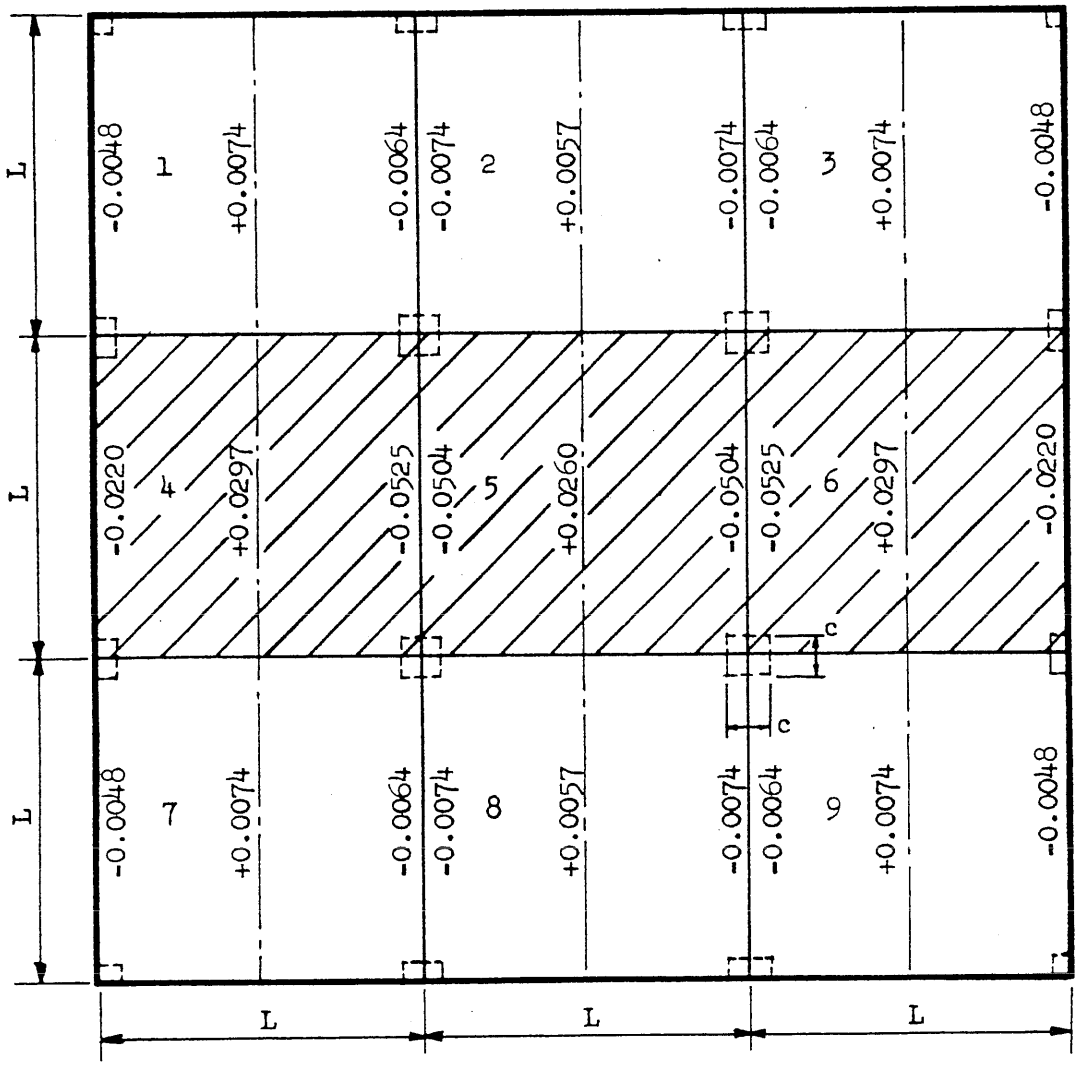

AVERAGE MOMENT ACROSS ENTIRE STRUCTURE

FIG. 1 MOMENTS IN NINE-PANEL STRUCTURE WITH CENTER STRIP LOADED

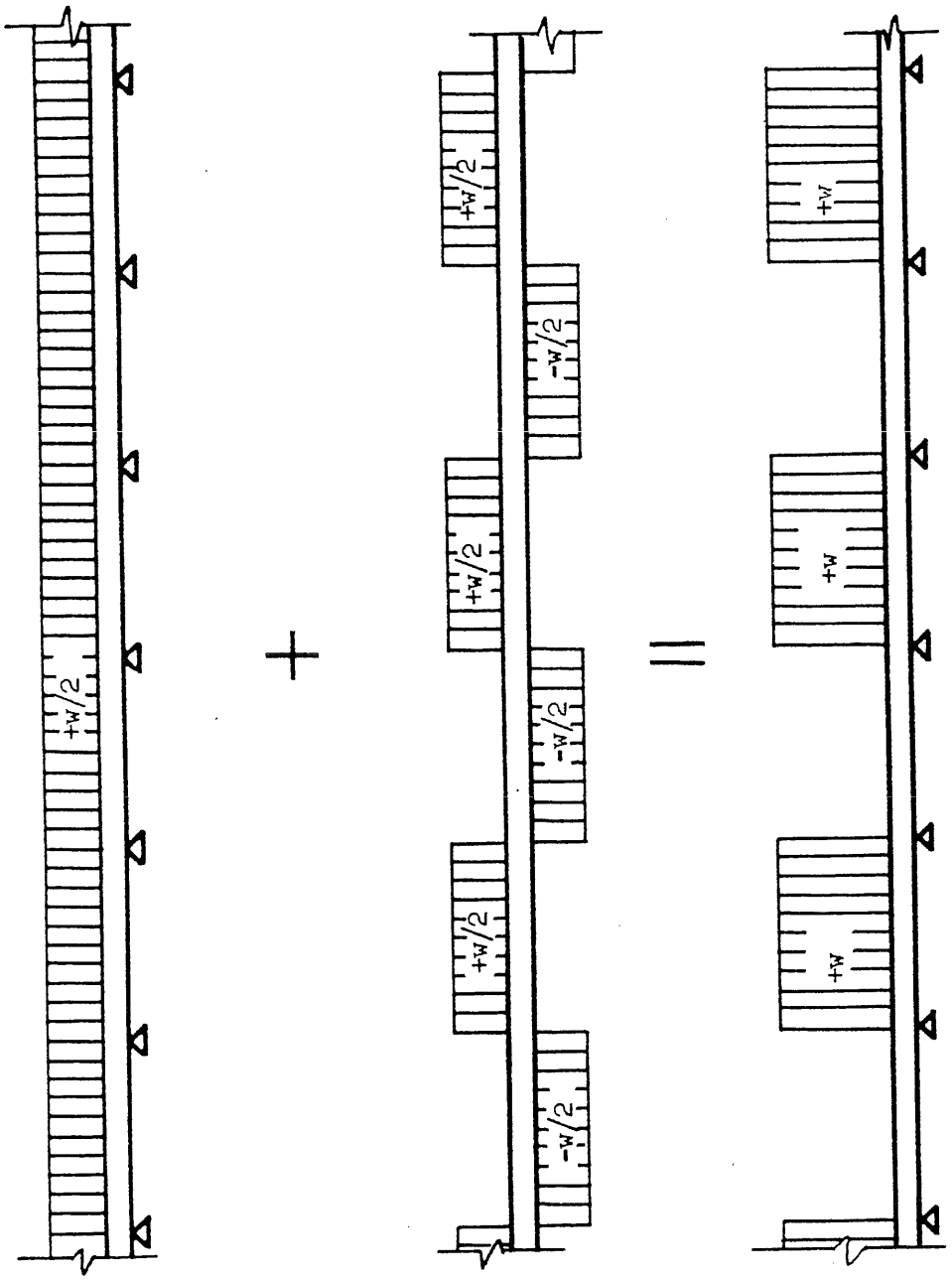

FIG. 2 SUPERPOSITION OF LOADS TO OBTAIN ALTERNATE STRIP LOADING

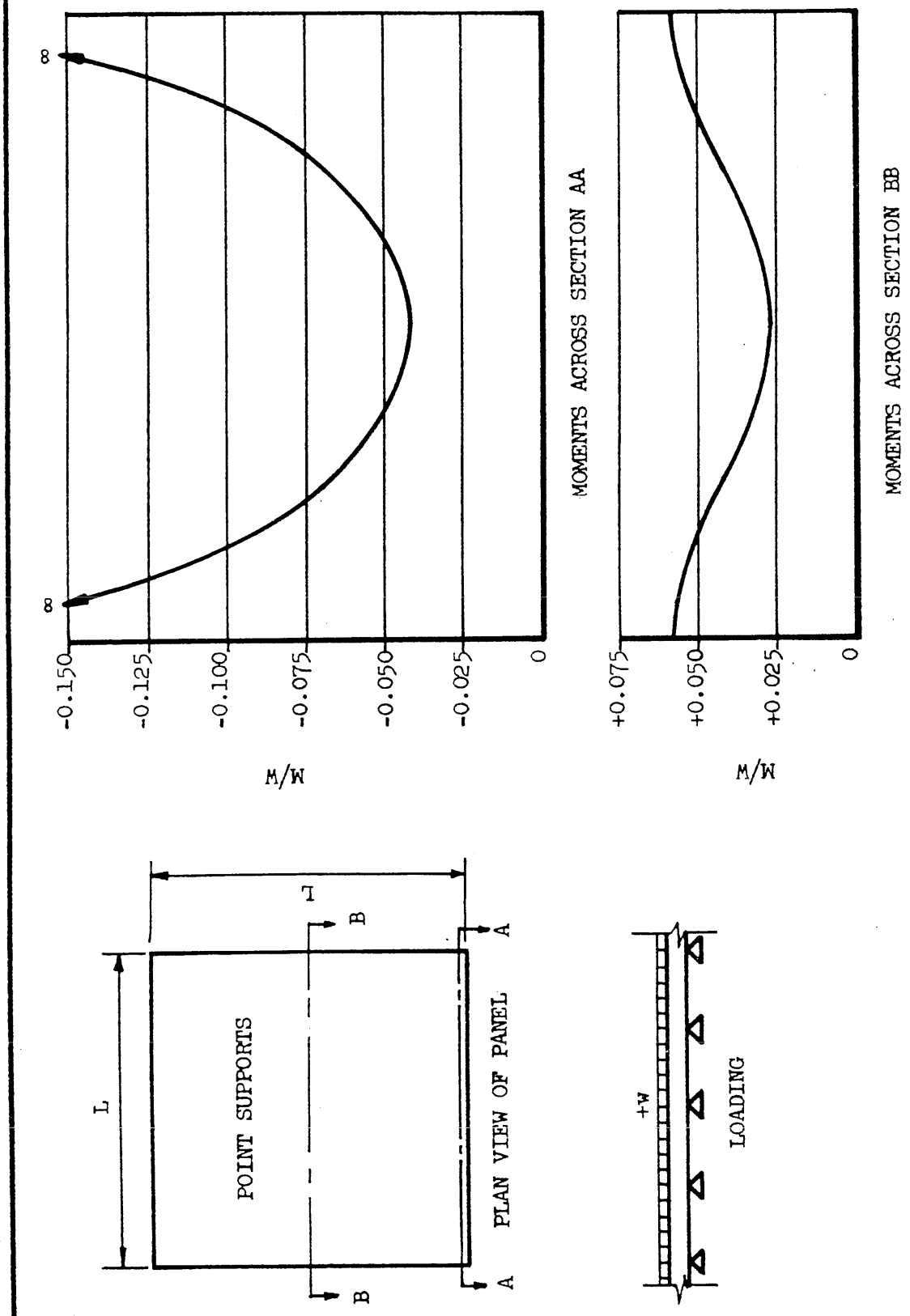

FIG. 3 MOMENTS COMPUTED BY LEWE FOR SQUARE PANELS WITH POINT SUPPORTS

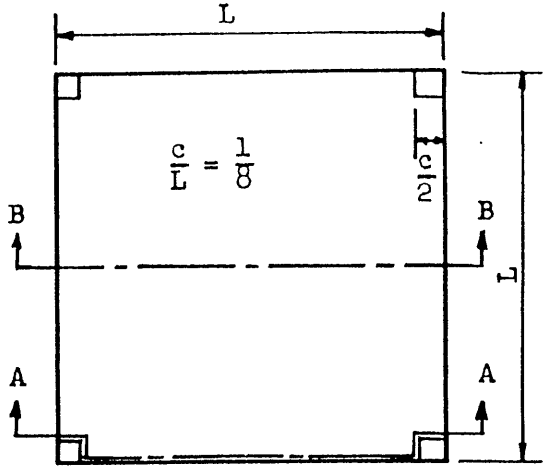

PLAN VIEW OF PANEL

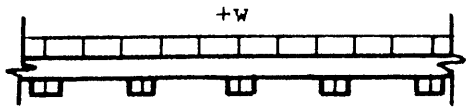

LOADING

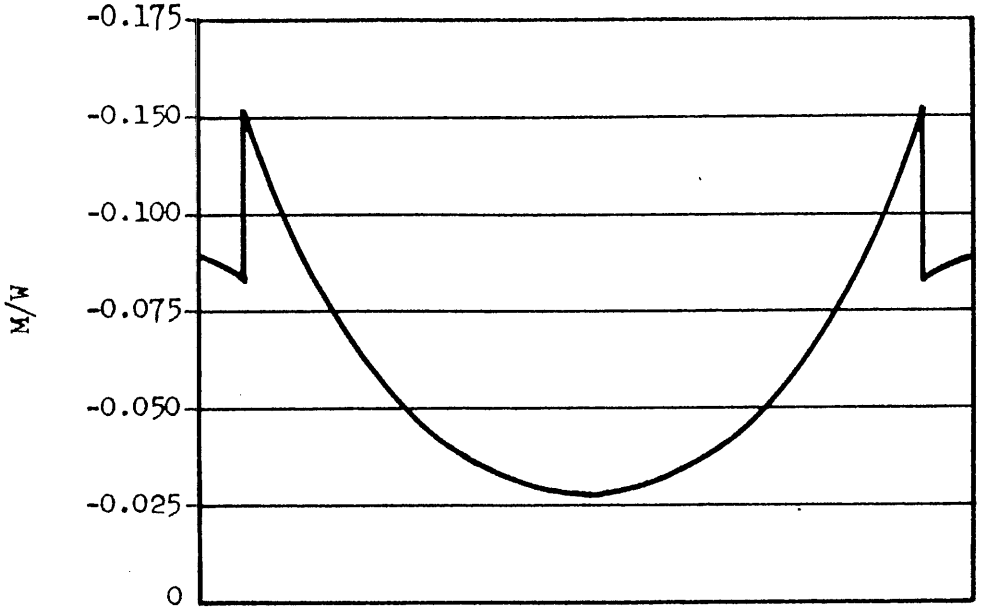

MOMENT ACROSS SECTION AA

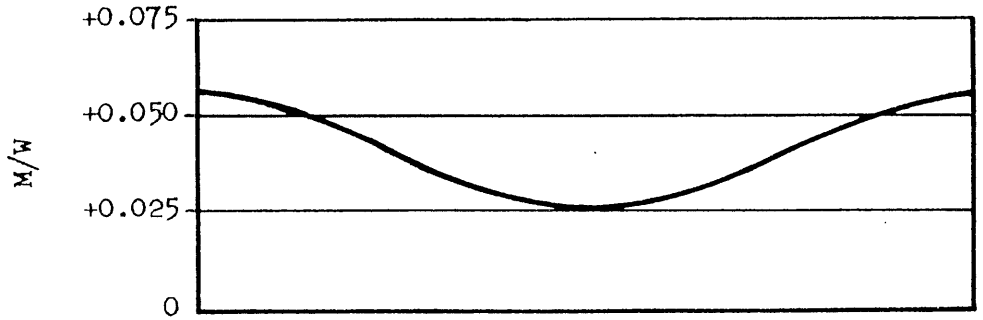

MOMENT ACROSS SECTION BB

FIG. 4 MOMENTS COMPUTED BY LEWE FOR SQUARE PANELS WITH c/L = 1/8

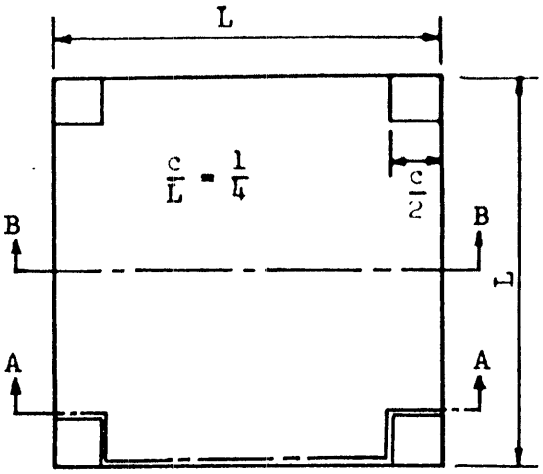

PLAN VIEW OF PANEL

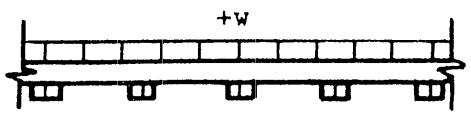

LOADING

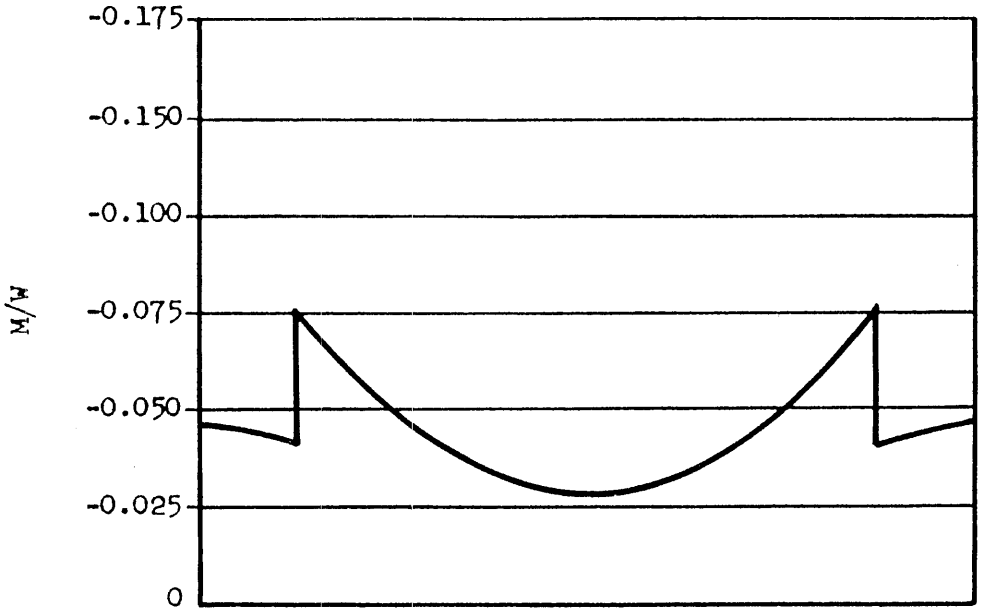

MOMENT ACROSS SECTION AA

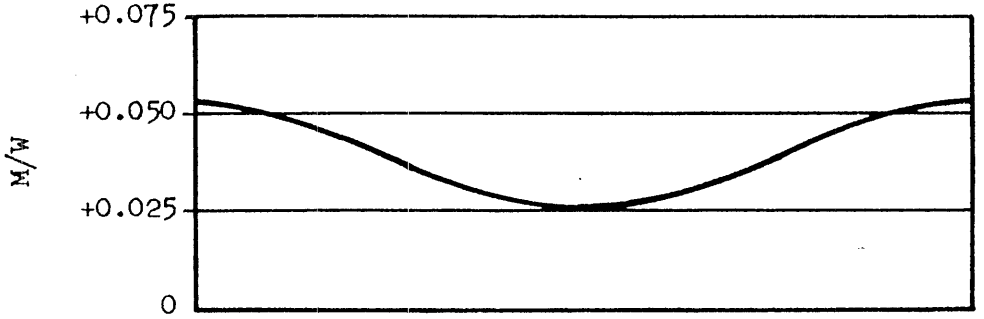

MOMENT ACROSS SECTION BB

FIG. 5 MOMENTS COMPUTED BY LEWE FOR SQUARE PANELS WITH c/L = 1/4

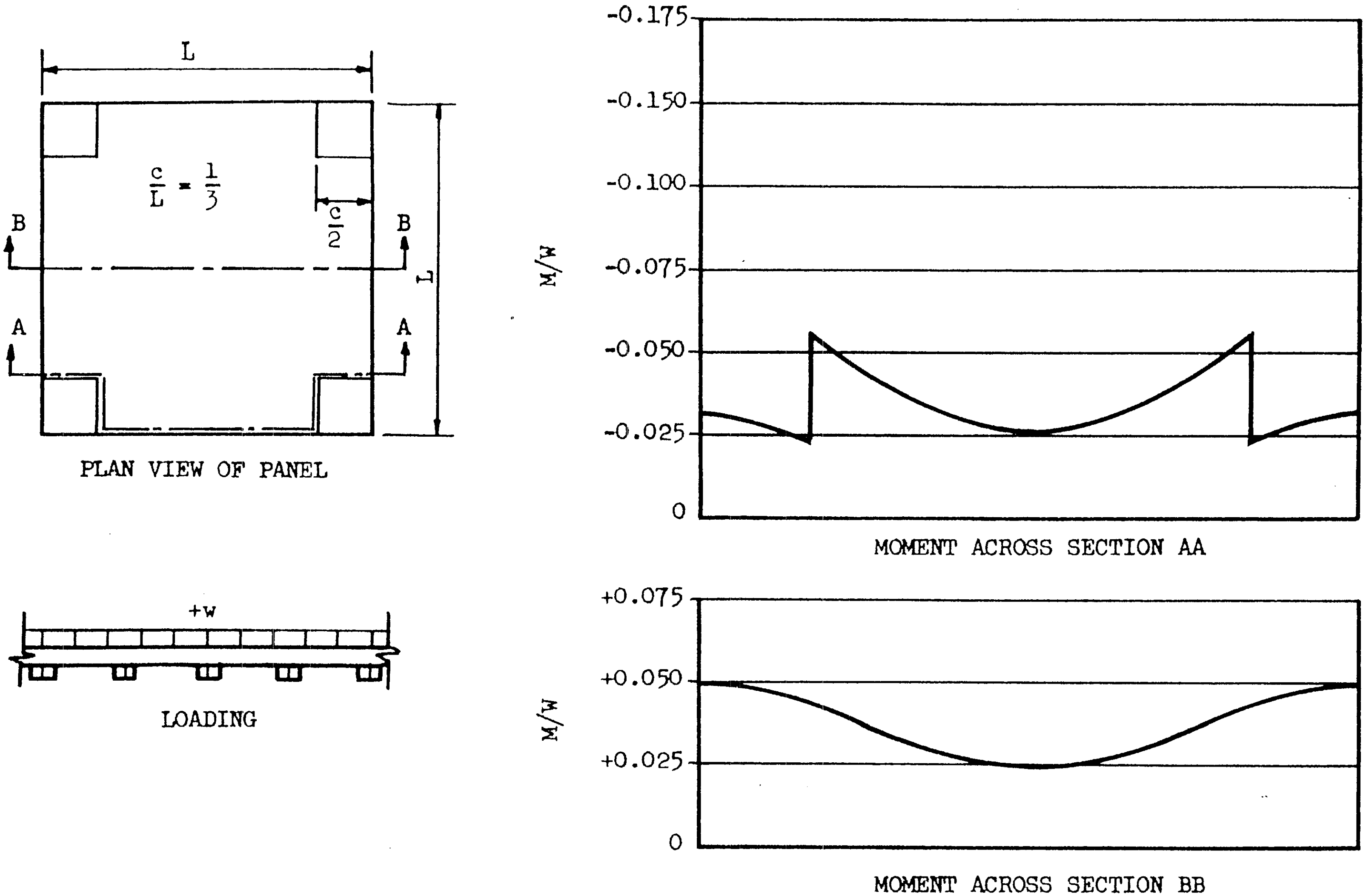

FIG. 6 MOMENTS COMPUTED BY LEWE FOR SQUARE PANELS WITH c/L = 1/3

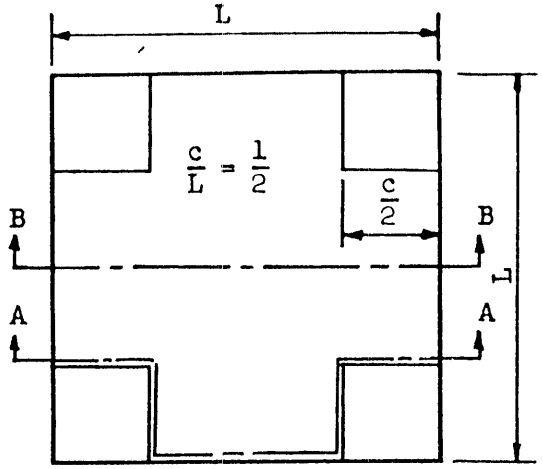

PLAN VIEW OF PANEL

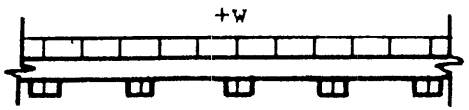

LOADING

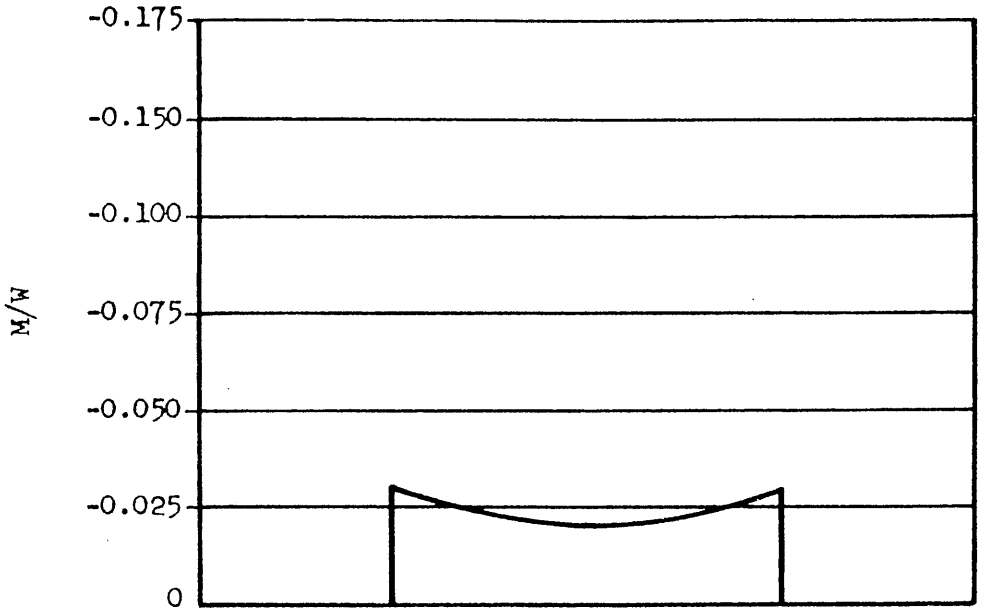

MOMENT ACROSS SECTION AA

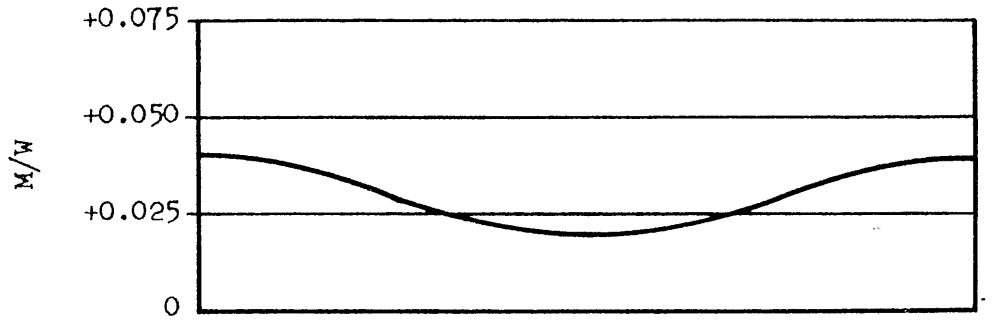

MOMENT ACROSS SECTION BB

FIG. 7 MOMENTS COMPUTED BY LEWE FOR SQUARE PANELS WITH c/L = 1/2

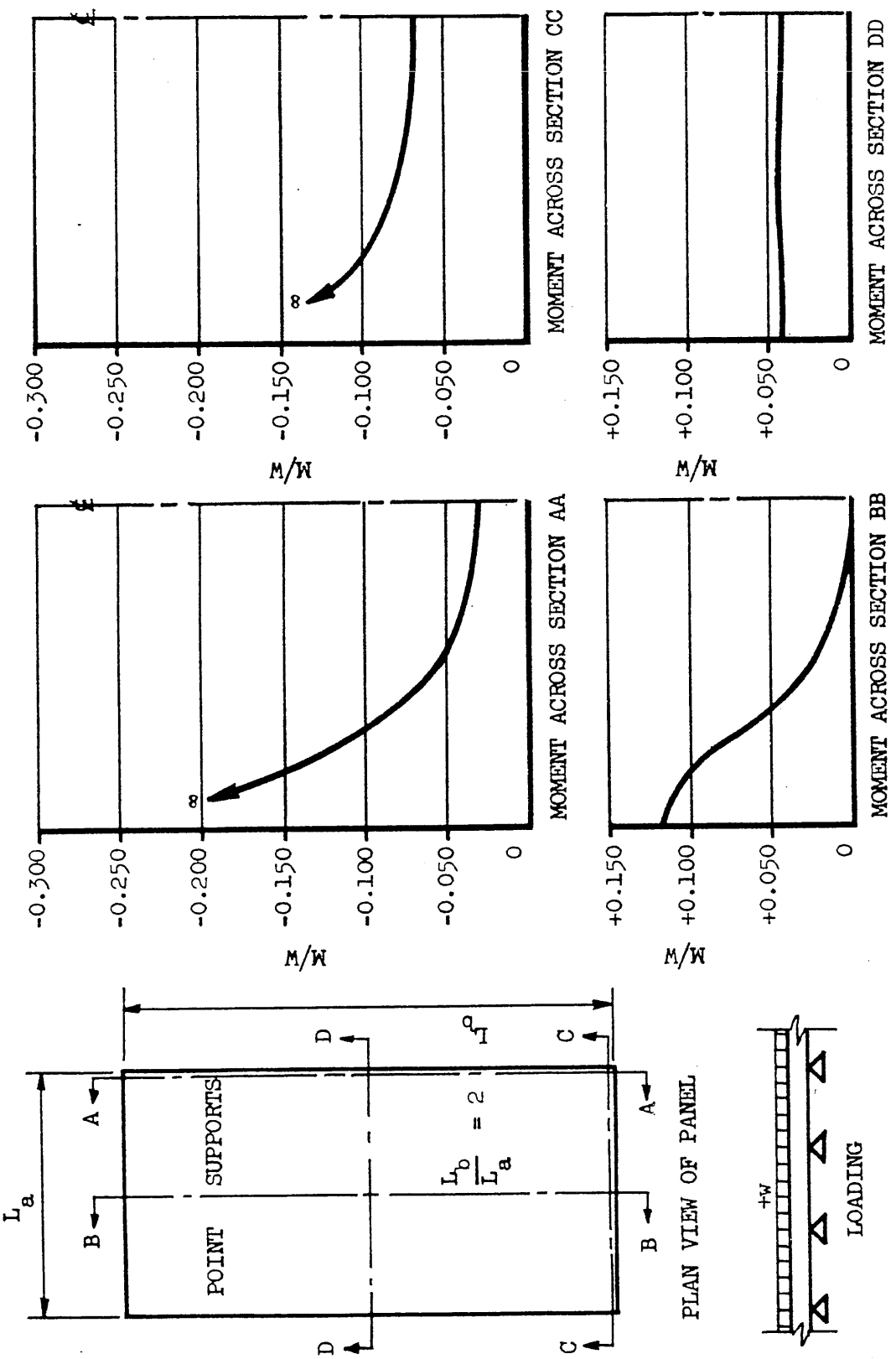

FIG. 8 MOMENTS COMPUTED BY LEWE FOR RECTANGULAR PANELS WITH POINT SUPPORTS

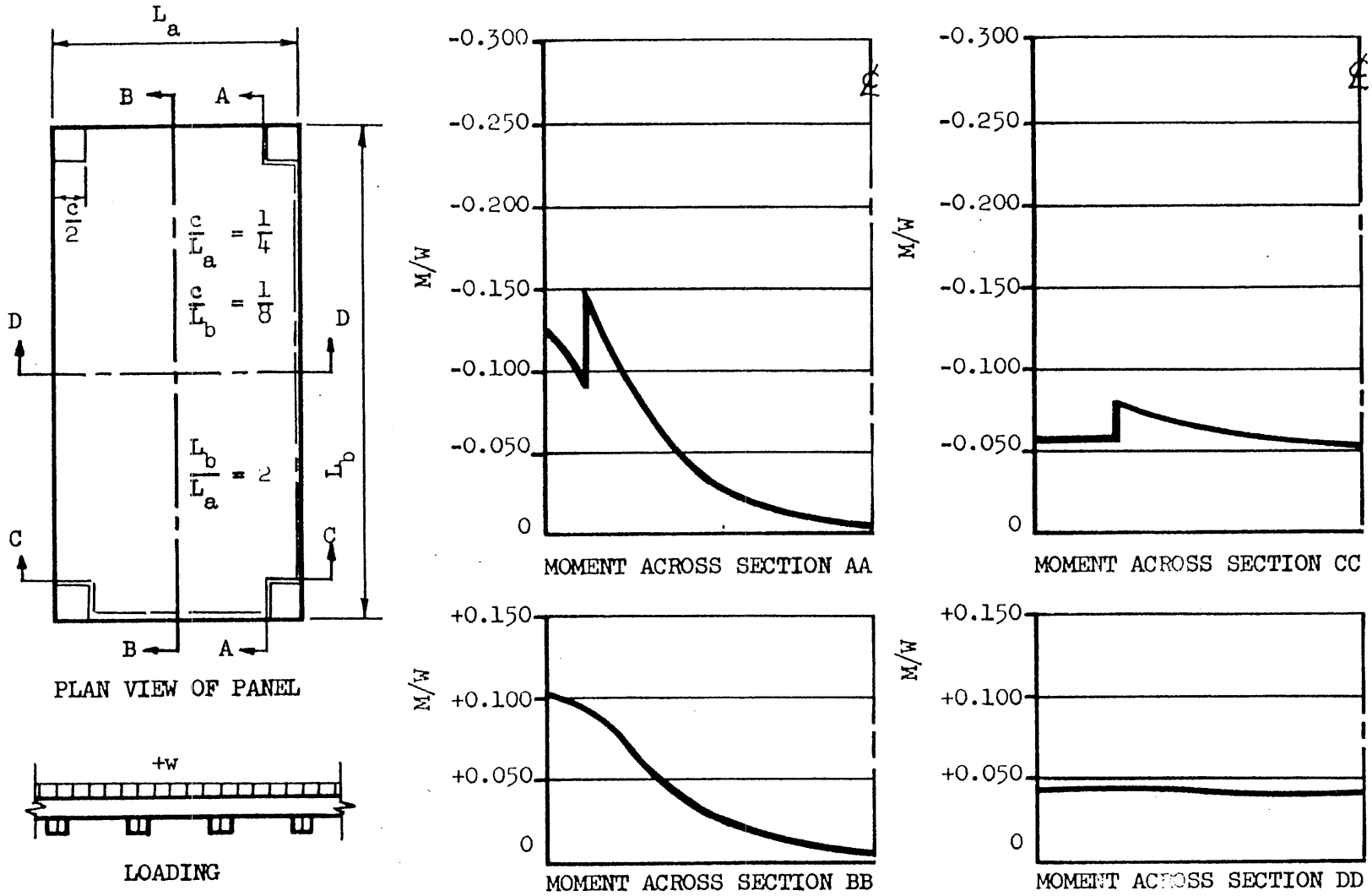

FIG. 9 MOMENTS COMPUTED BY LEWE FOR RECTANGULAR PANELS WITH $c/L_a = 1/4$ AND $c/L_b = 1/8$

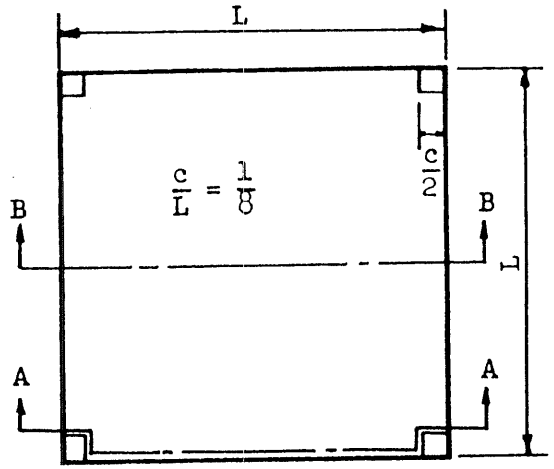

$\frac{c}{L} = \frac{1}{8}$

PLAN VIEW OF PANEL

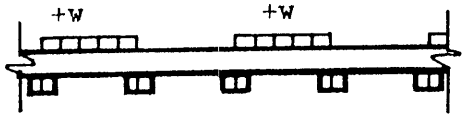

LOADING

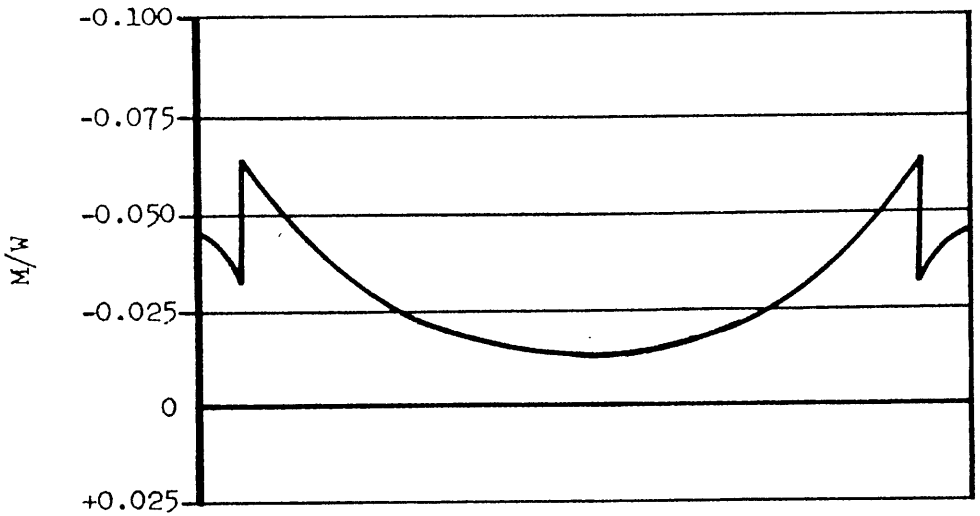

MOMENT ACROSS SECTION AA

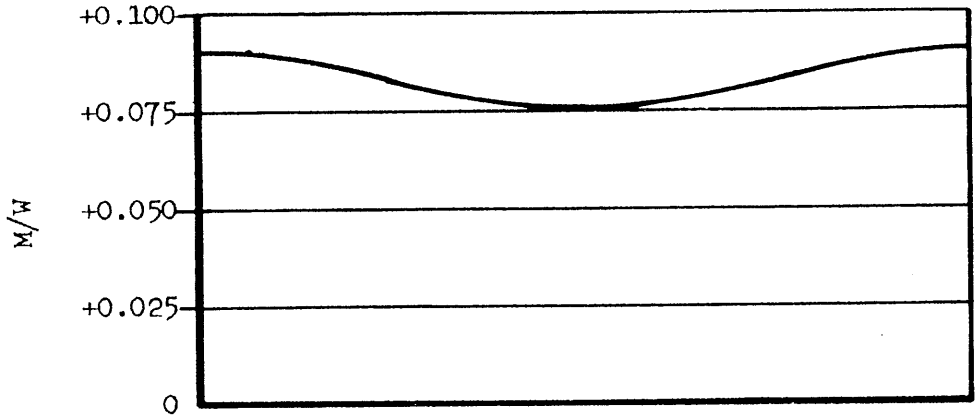

MOMENT ACROSS SECTION BB

FIG. 10 MOMENTS COMPUTED BY LEWE FOR SQUARE PANELS WITH STRIP LOADING AND c/L = 1/8

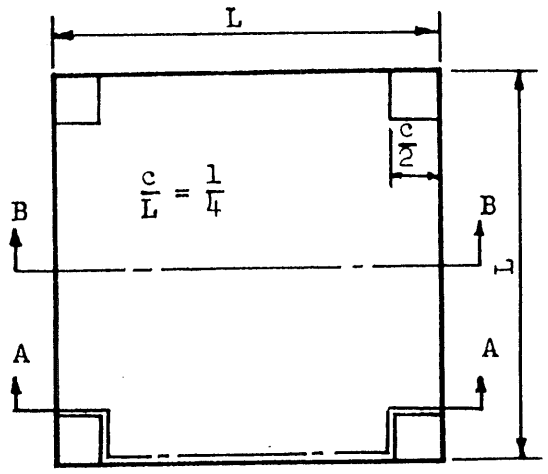

PLAN VIEW OF PANEL

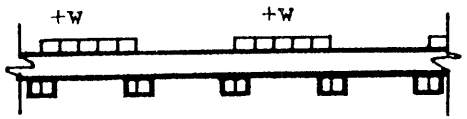

LOADING

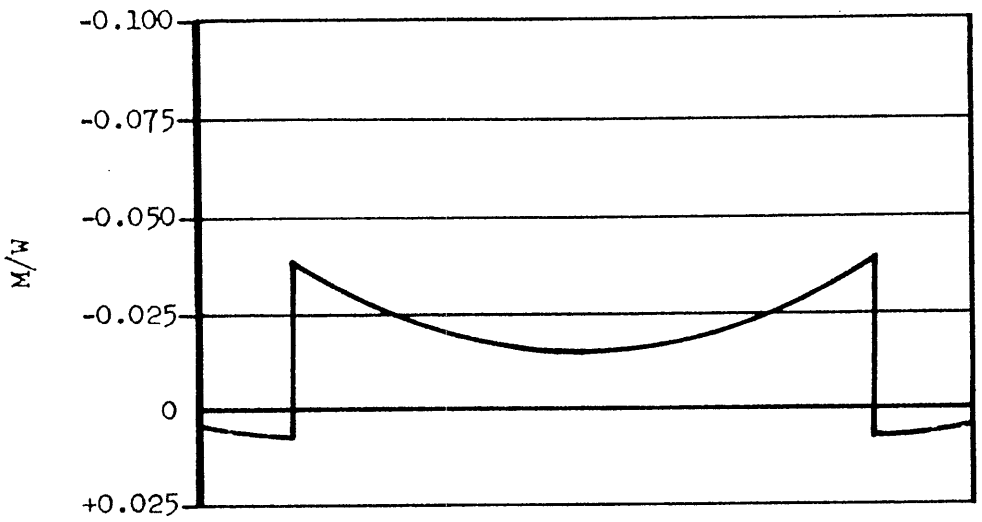

MOMENT ACROSS SECTION AA

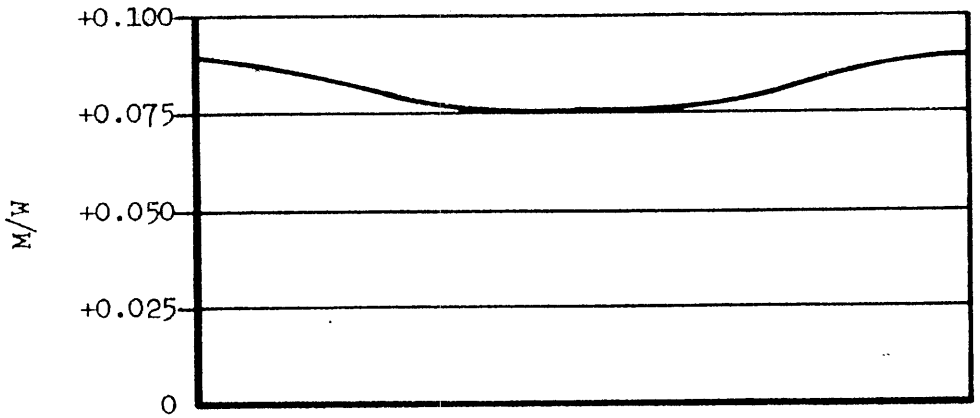

MOMENT ACROSS SECTION BB

FIG. 11 MOMENTS COMPUTED BY LEWE FOR SQUARE PANELS WITH STRIP LOADING AND c/L = 1/4

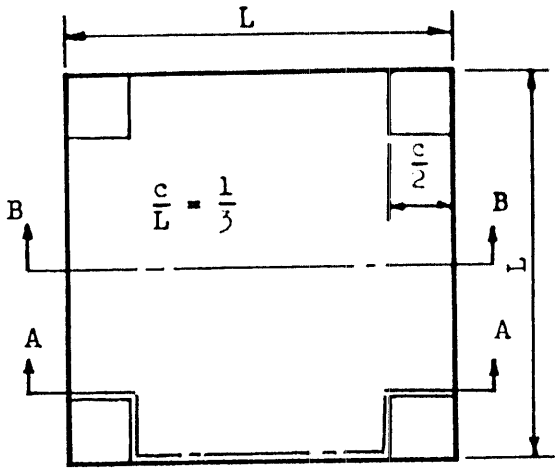

PLAN VIEW OF PANEL

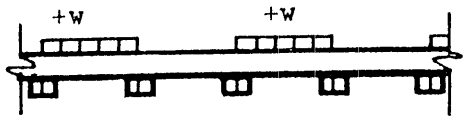

LOADING

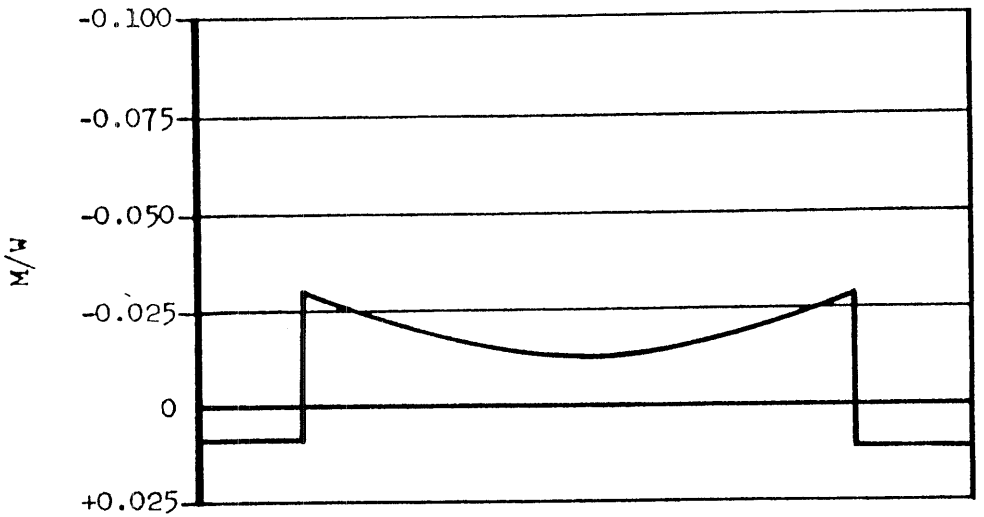

MOMENT ACROSS SECTION AA

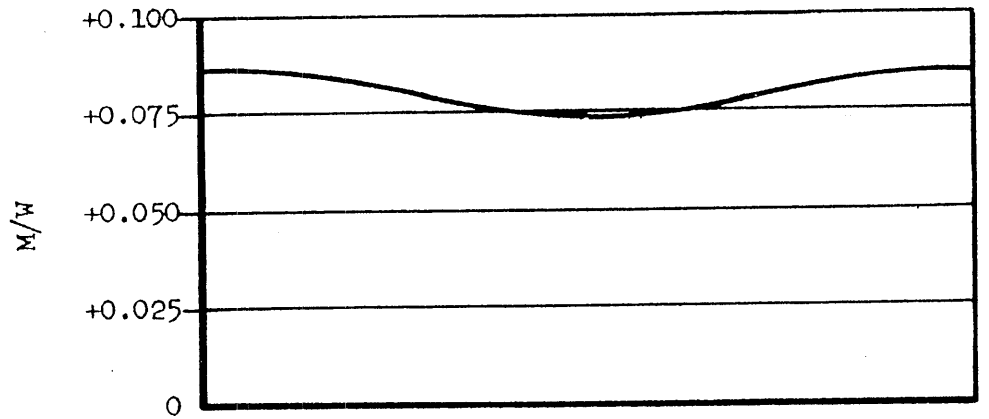

MOMENT ACROSS SECTION BB

FIG. 12 MOMENTS COMPUTED BY LEWE FOR SQUARE PANELS WITH STRIP LOADING AND c/L = 1/3

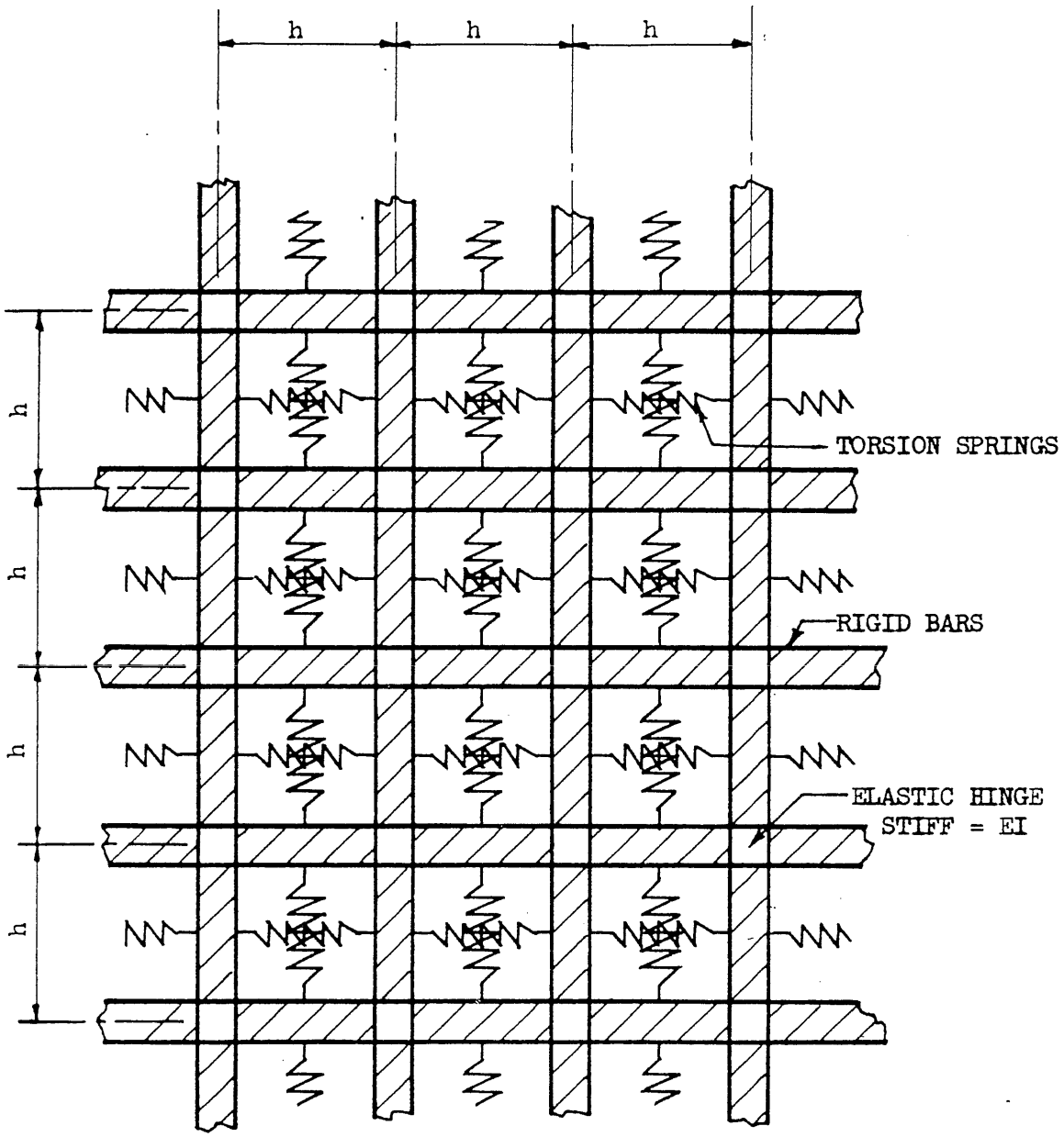

FIG. 13 PLATE ANALOG AT GENERAL INTERIOR POINT

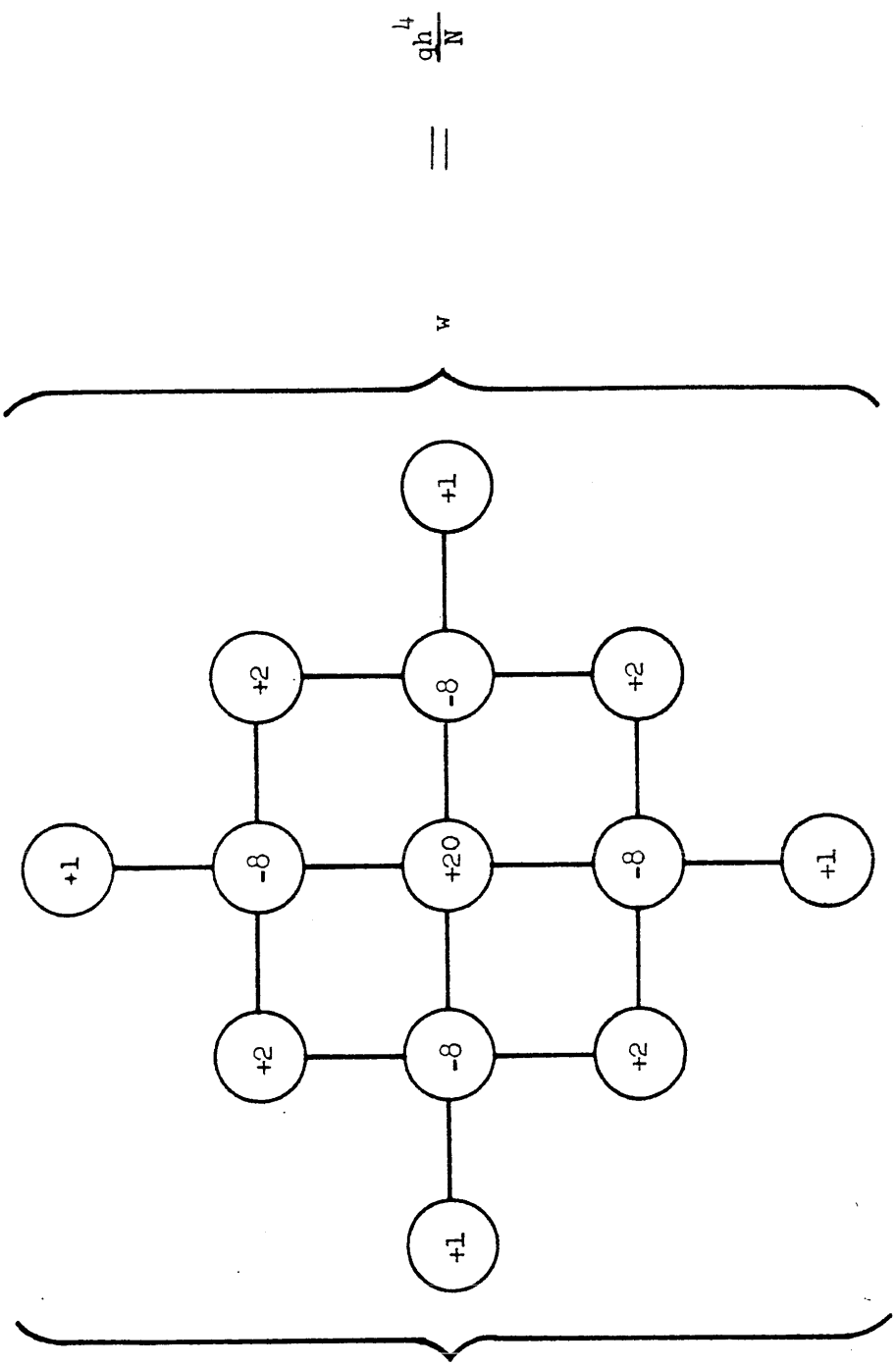

FIG. 14 FINITE DIFFERENCE OPERATOR FOR TYPICAL INTERIOR POINT

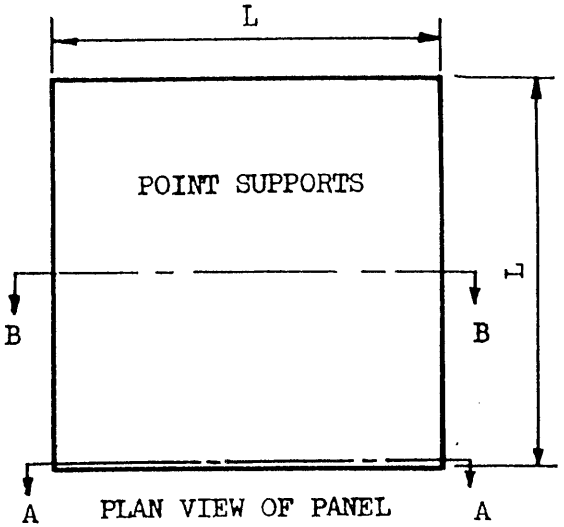

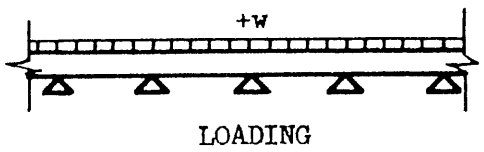

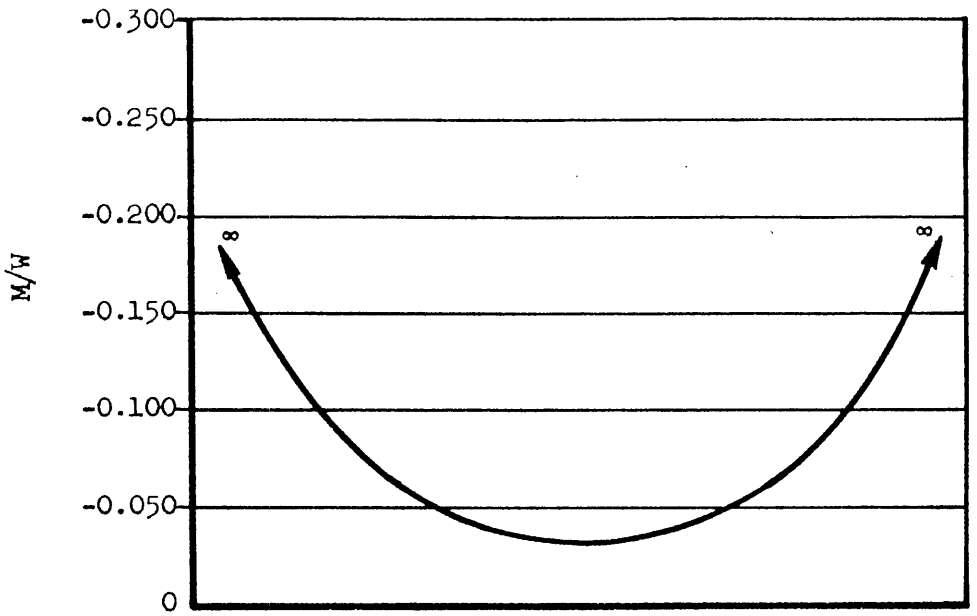

MOMENTS ACROSS SECTION AA

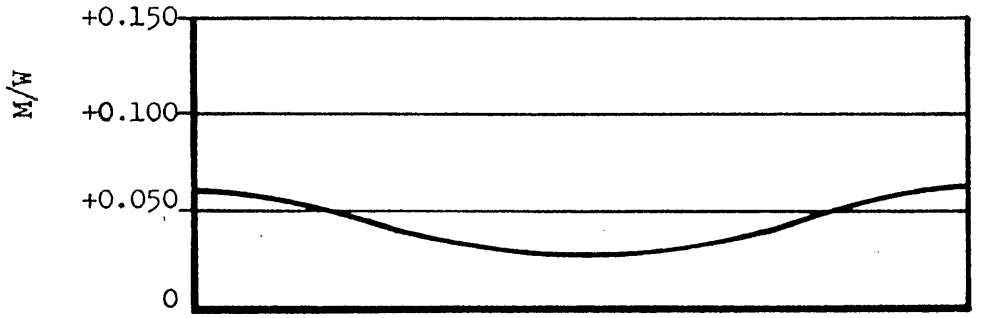

MOMENTS ACROSS SECTION BB

FIG. 15 MOMENTS COMPUTED BY NIELSEN FOR SQUARE PANELS WITH POINT SUPPORTS

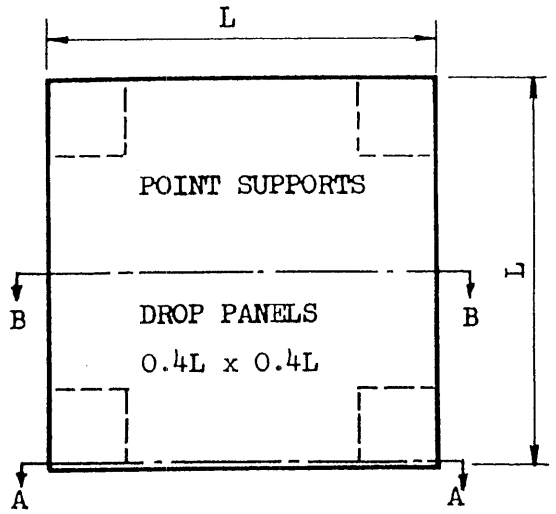

PLAN VIEW OF PANEL

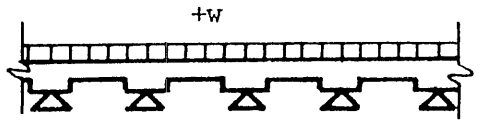

LOADING

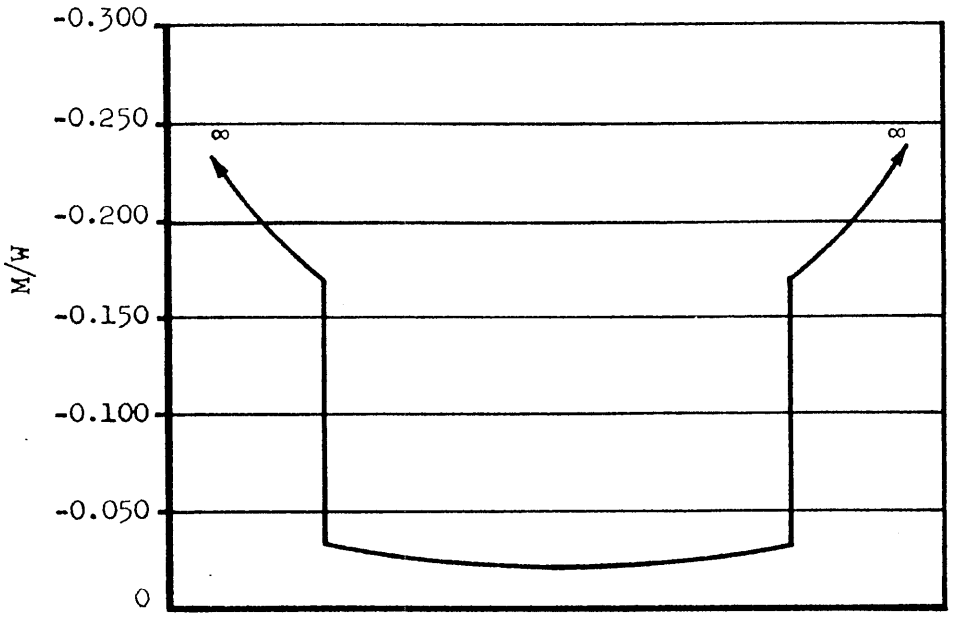

MOMENT ACROSS SECTION AA

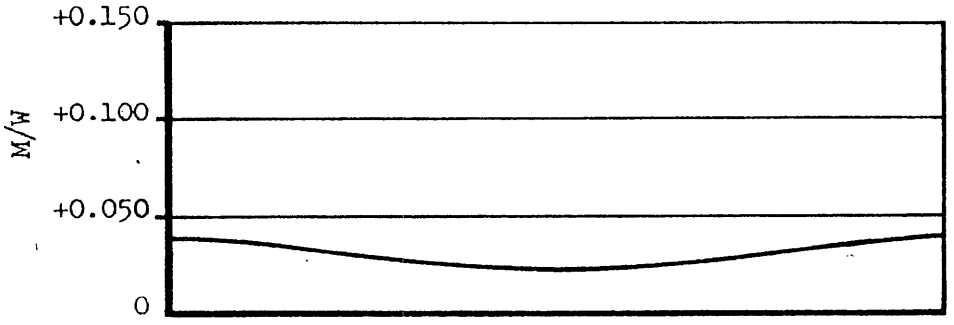

MOMENTS ACROSS SECTION BB

FIG. 16 MOMENTS COMPUTED BY NIELSEN FOR SQUARE PANELS WITH DROP PANELS AND POINT SUPPORTS

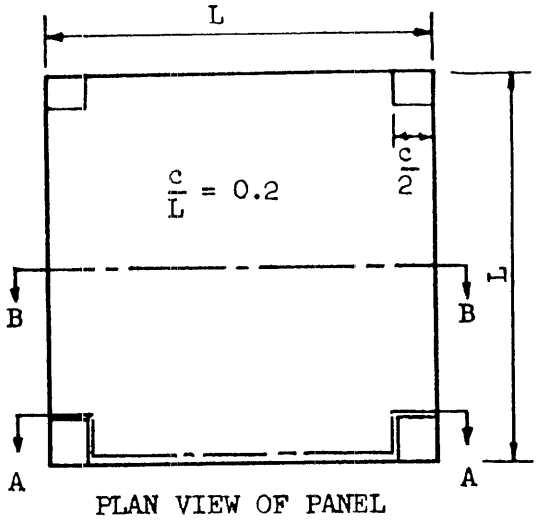

PLAN VIEW OF PANEL

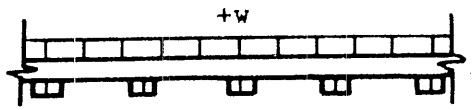

LOADING

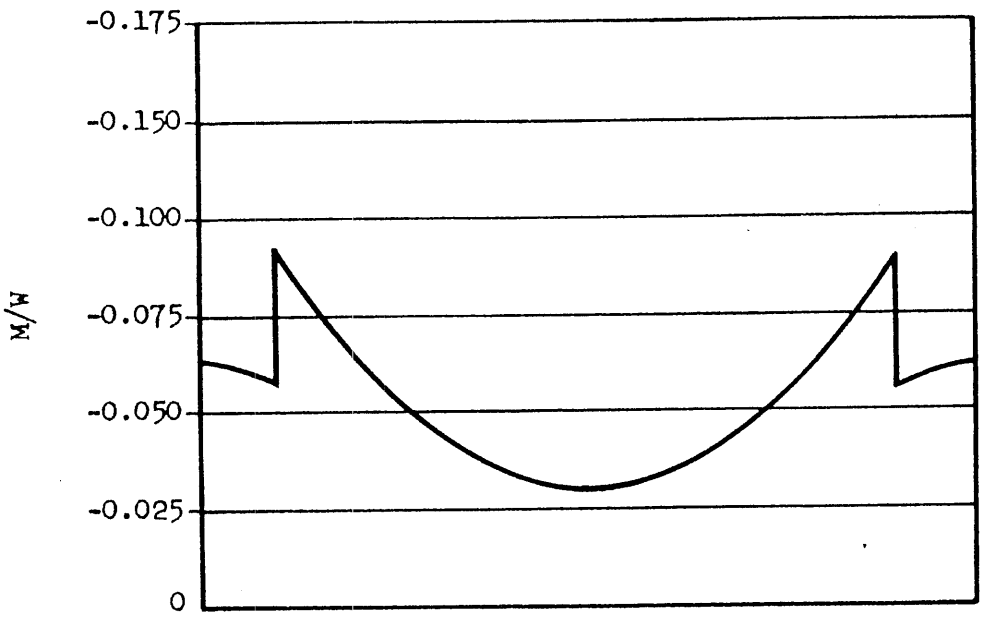

MOMENT ACROSS SECTION AA

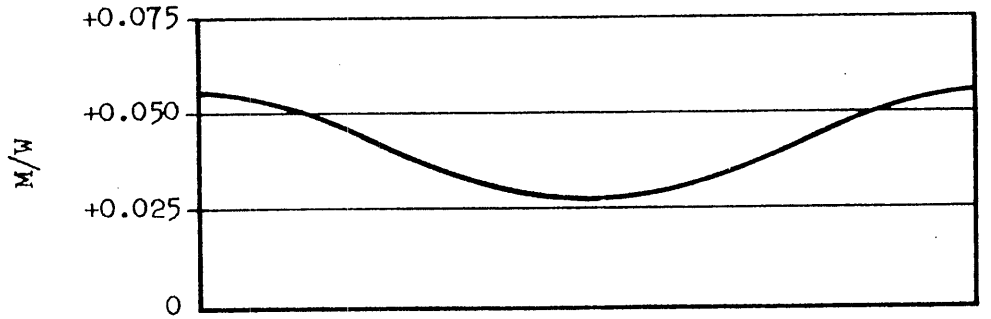

MOMENT ACROSS SECTION BB

FIG. 17 MOMENTS COMPUTED BY NIELSEN FOR SQUARE PANELS WITH c/L = 0.2

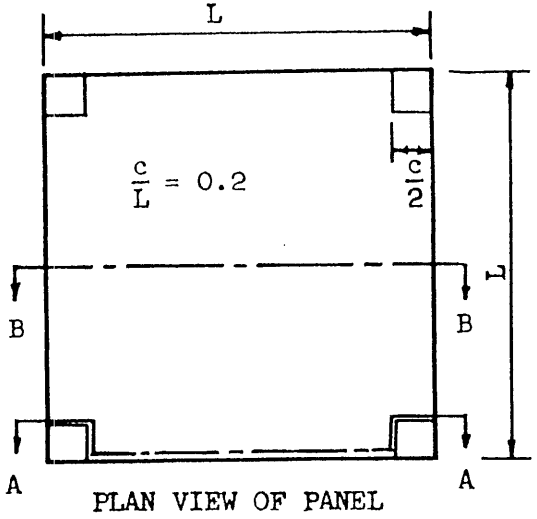

PLAN VIEW OF PANEL

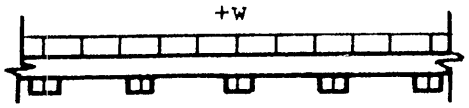

LOADING

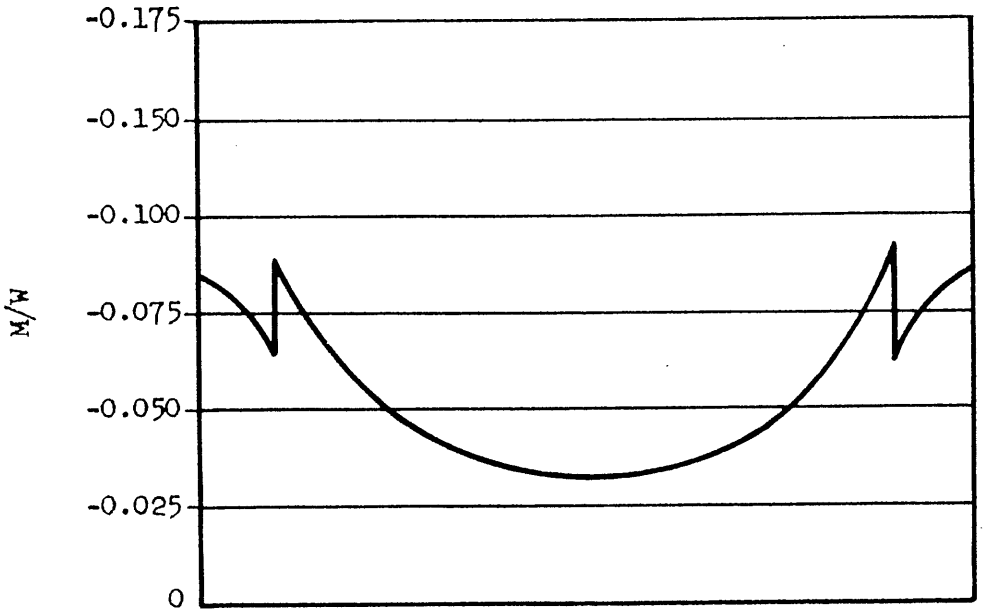

MOMENT ACROSS SECTION AA

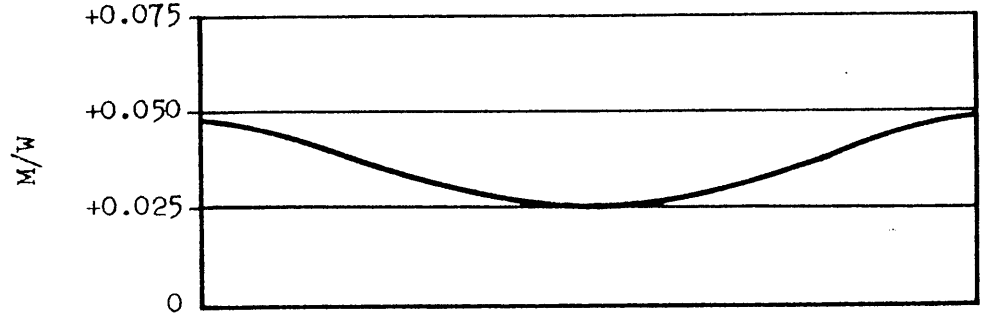

MOMENT ACROSS SECTION BB

FIG. 18 MOMENTS COMPUTED BY NIELSEN FOR SQUARE PANELS AND c/L = 0.2

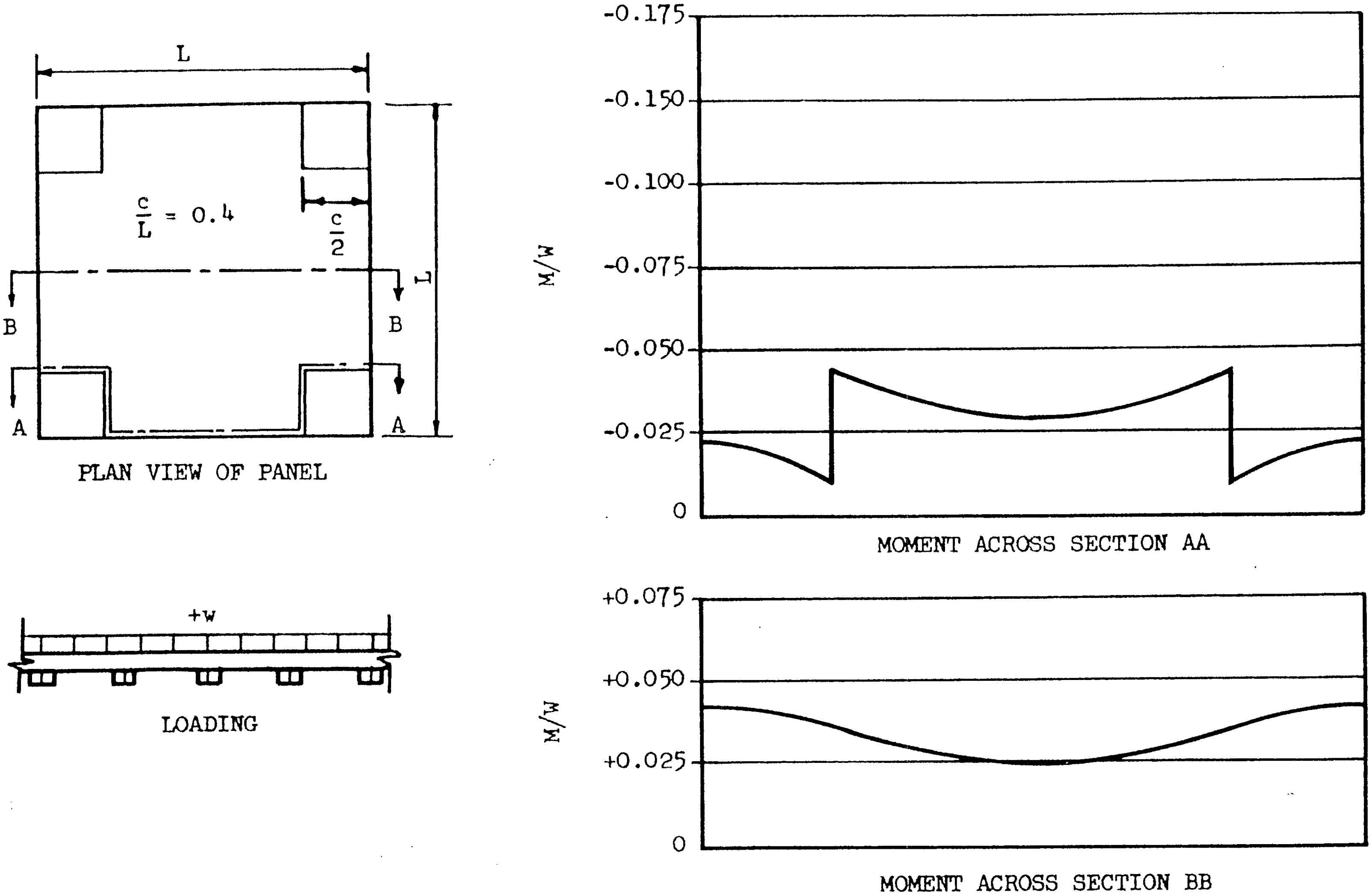

FIG. 19 **MOMENTS** COMPUTED BY NIELSEN FOR SQUARE PANELS WITH c/L = 0.4

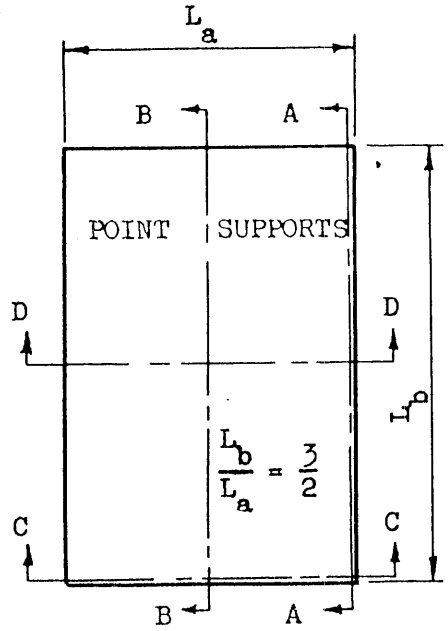

PLAN VIEW OF PANEL

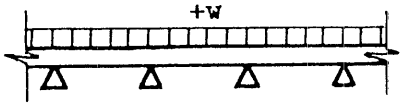

LOADING

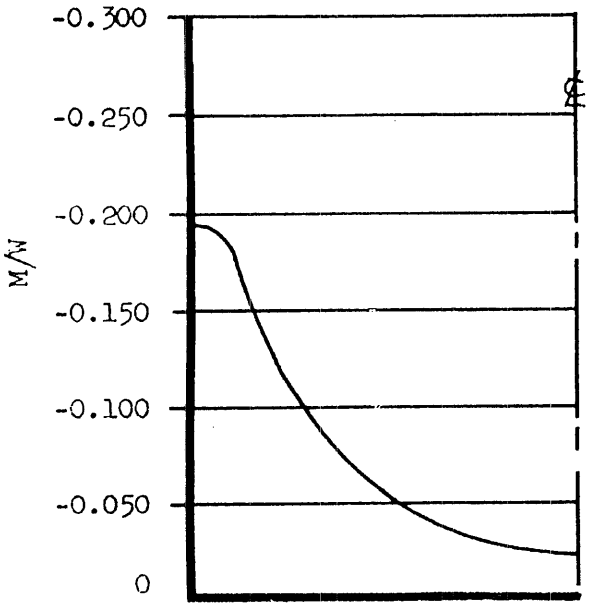

MOMENTS ACROSS SECTION AA

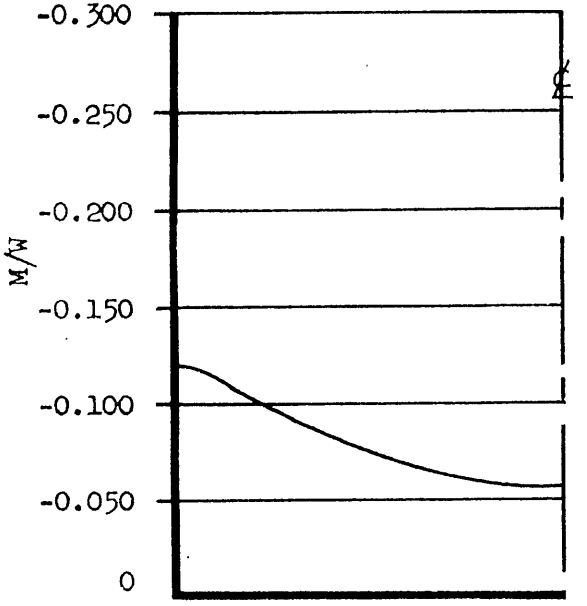

MOMENTS ACROSS SECTION CC

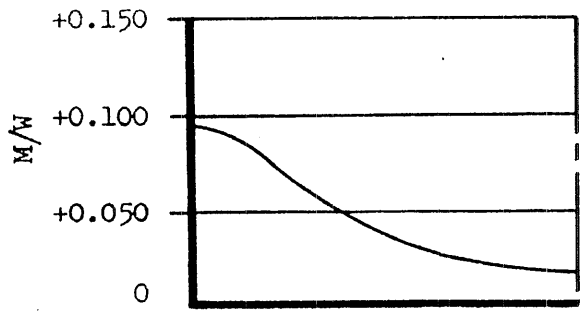

MOMENTS ACROSS SECTION BB

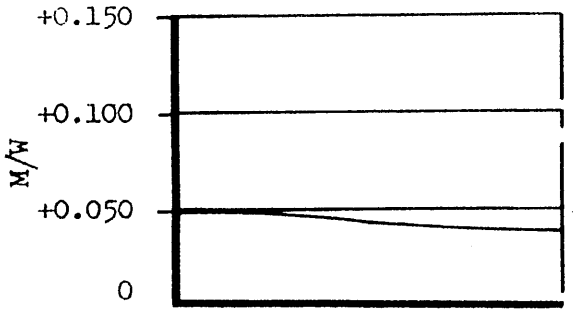

MOMENTS ACROSS SECTION DD

FIG. 20 MOMENTS COMPUTED BY NIELSEN FOR RECTANGULAR PANELS WITH POINT SUPPORTS

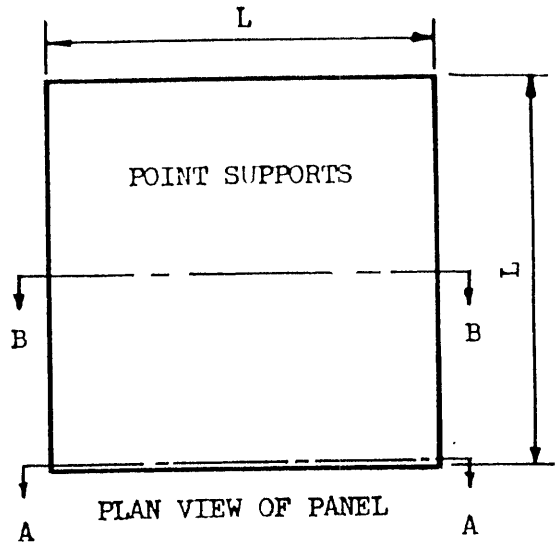

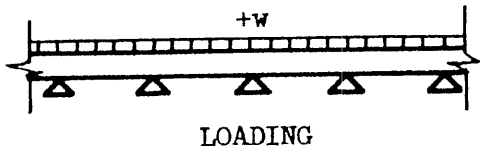

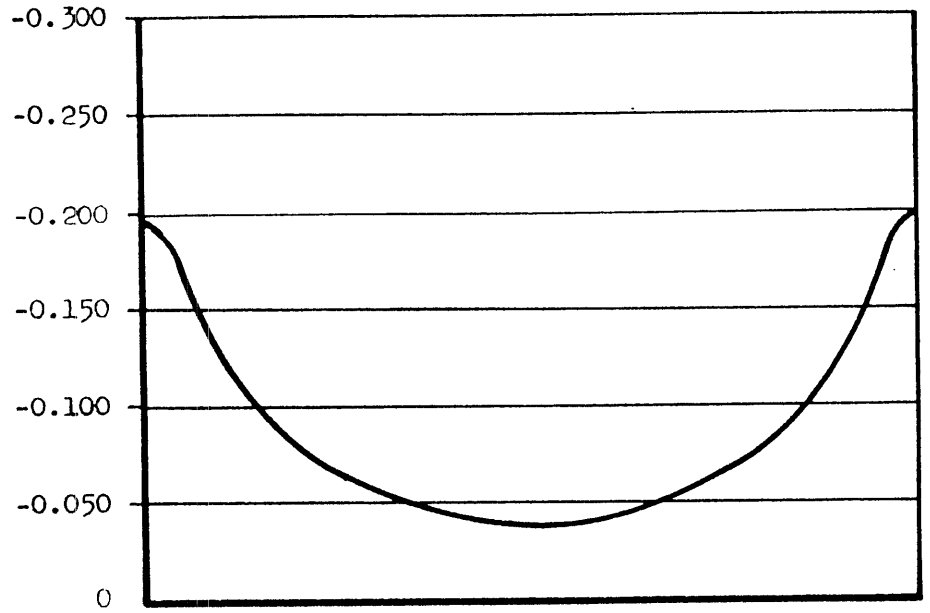

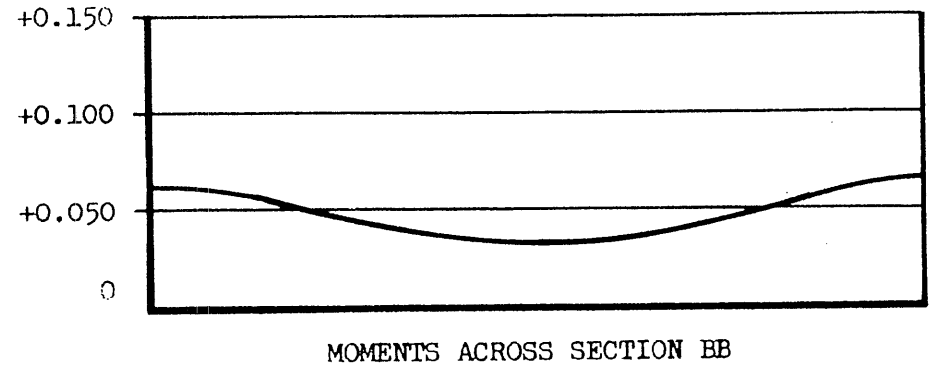

FIG. 21 MOMENTS COMPUTED BY MARCUS FOR SQUARE PANELS WITH POINT SUPPORTS

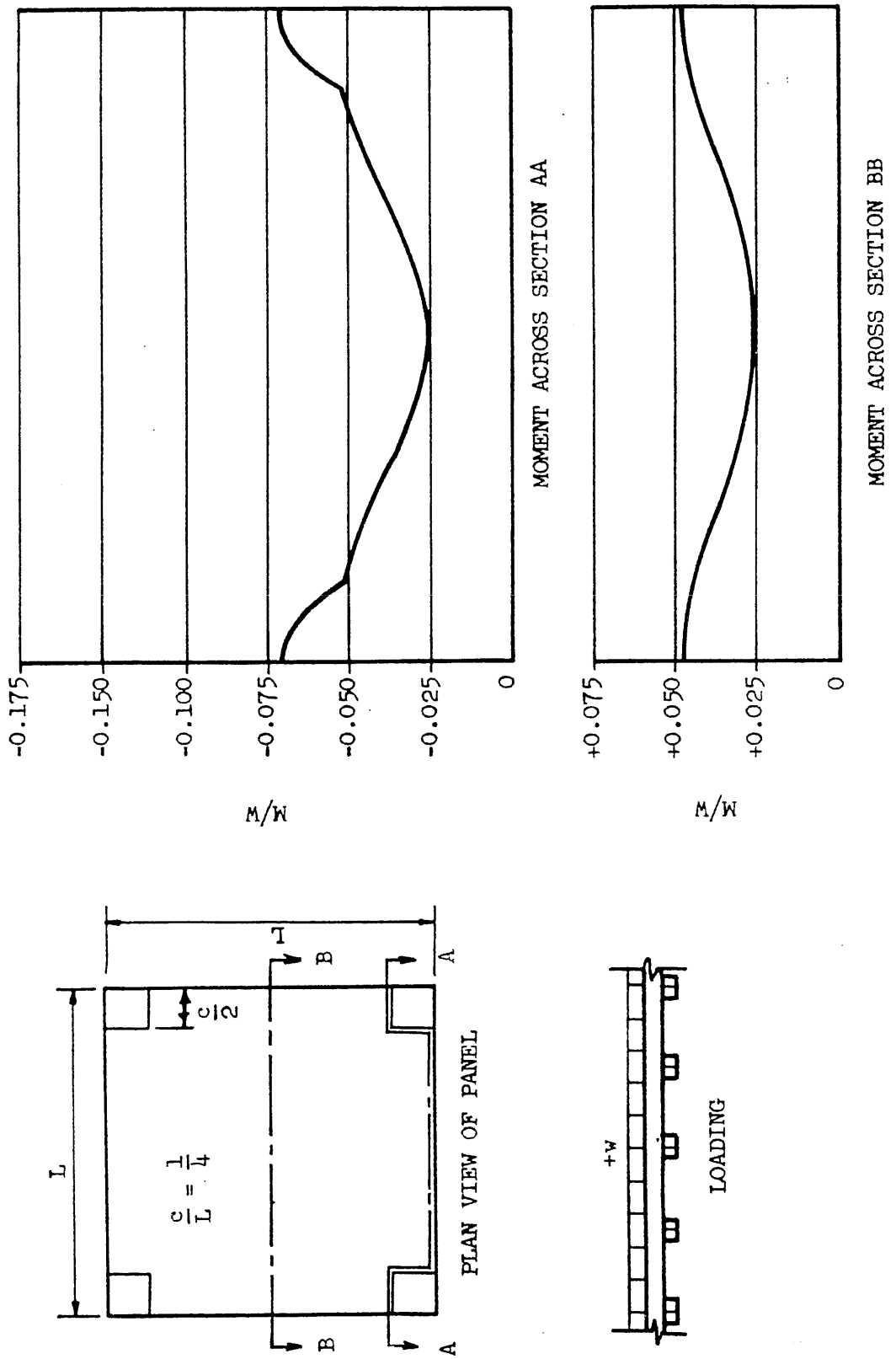

FIG. 22 MOMENTS COMPUTED BY MARCUS FOR SQUARE PANELS WITH c/L = 1/4

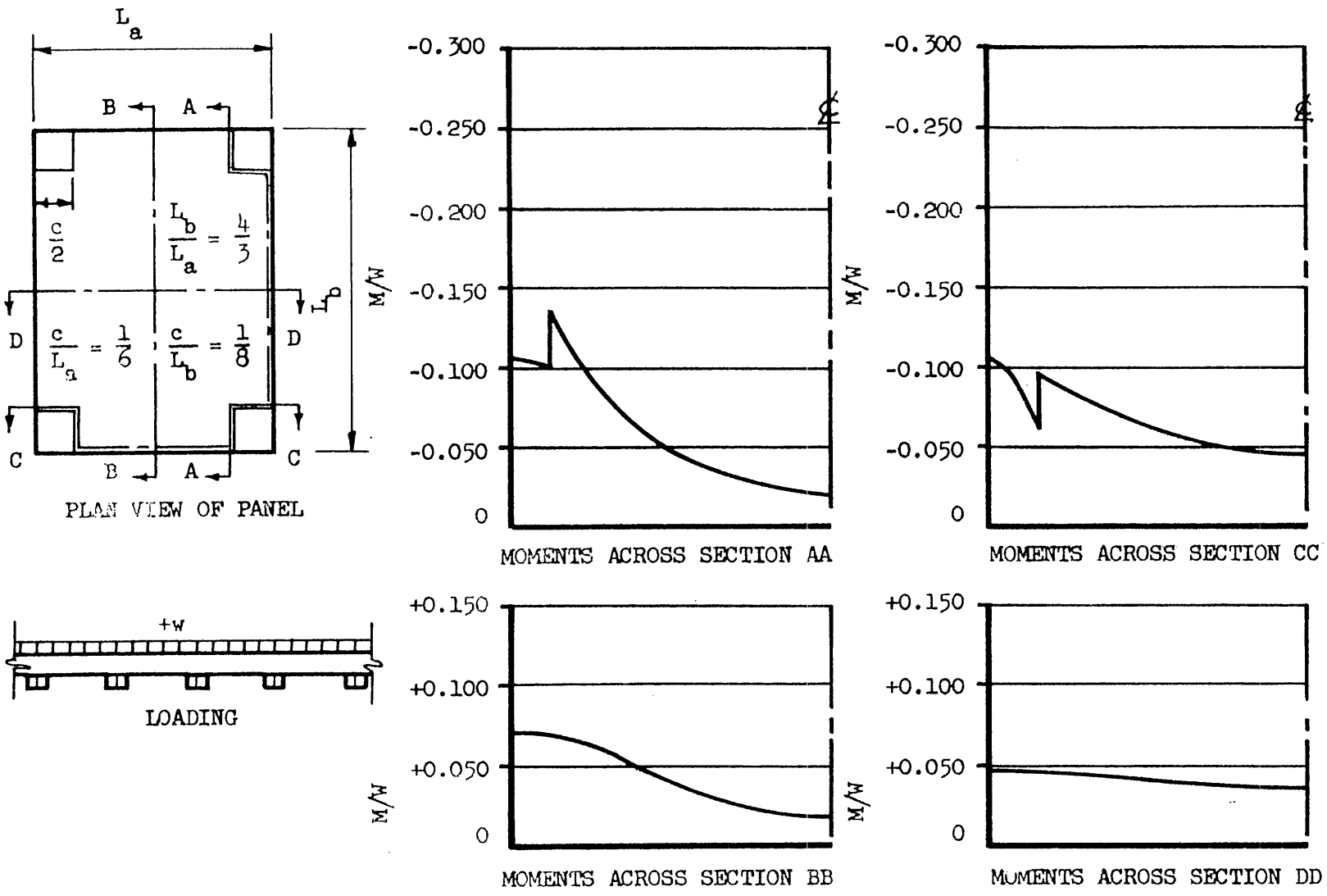

FIG. 23 MOMENTS COMPUTED BY MARCUS FOR RECTANGULAR PANELS WITH $c/L_a = 1/6$ AND $c/L_b = 1/8$

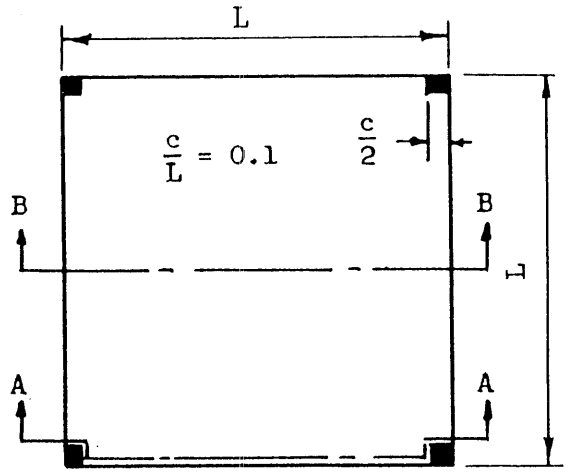

PLAN VIEW OF PANEL

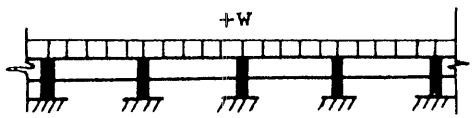

LOADING

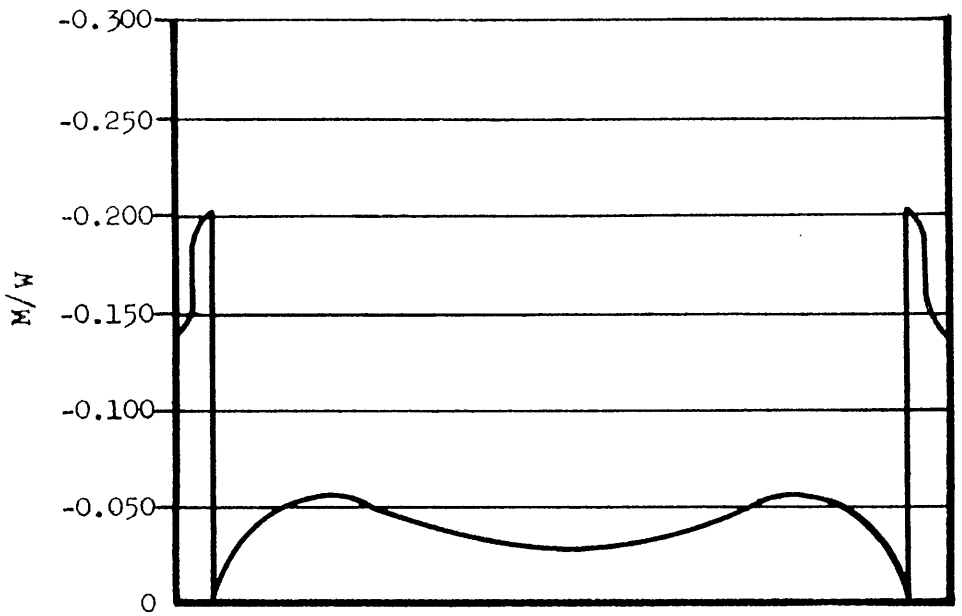

MOMENT ACROSS SECTION AA

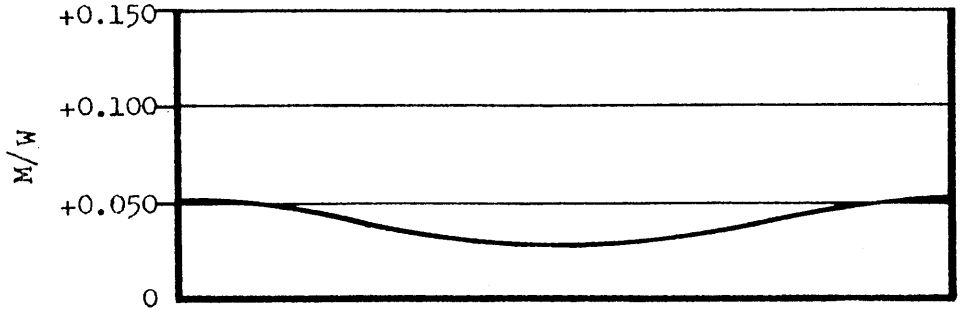

MOMENT ACROSS SECTION BB

FIG. 24 MOMENTS COMPUTED AT THE UNIVERSITY OF ILLINOIS FOR SQUARE PANELS WITH c/L = 0.1

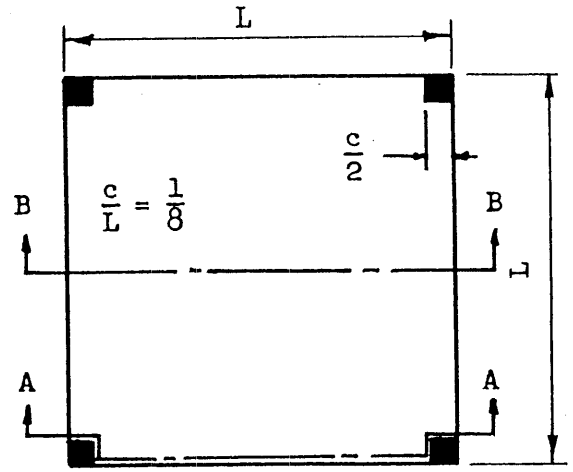

PLAN VIEW OF PANEL

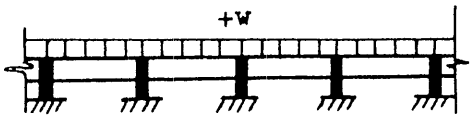

LOADING

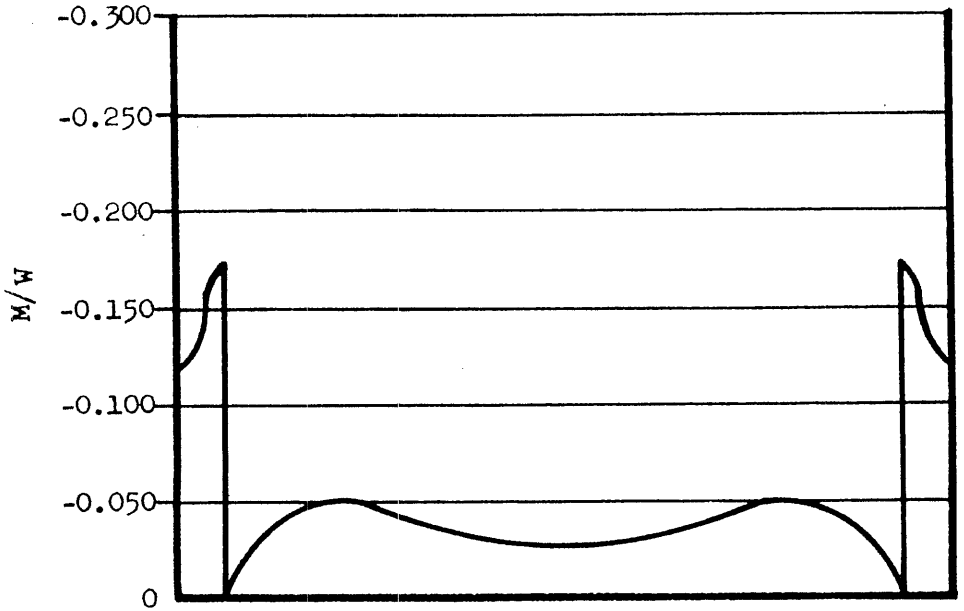

MOMENT ACROSS SECTION AA

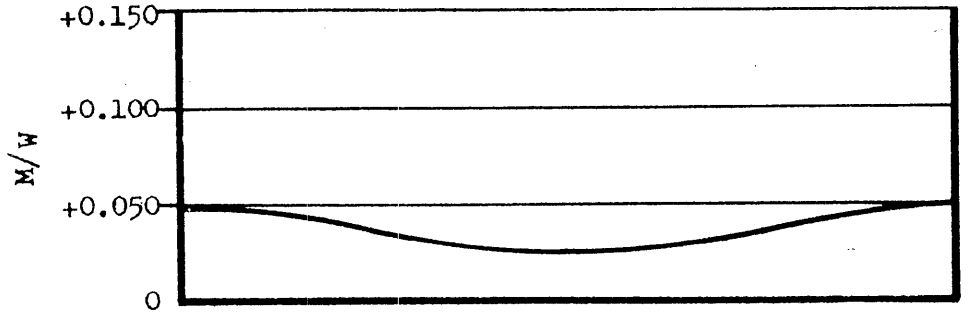

MOMENT ACROSS SECTION BB

FIG. 25 MOMENTS COMPUTED AT THE UNIVERSITY OF ILLINOIS FOR SQUARE PANELS WITH c/L = 1/8

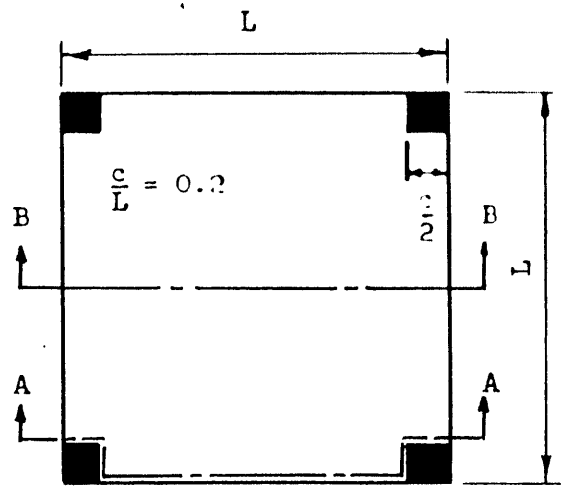

PLAN VIEW OF PANEL

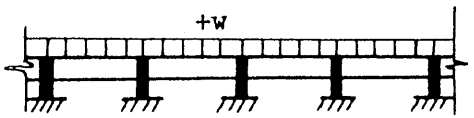

LOADING

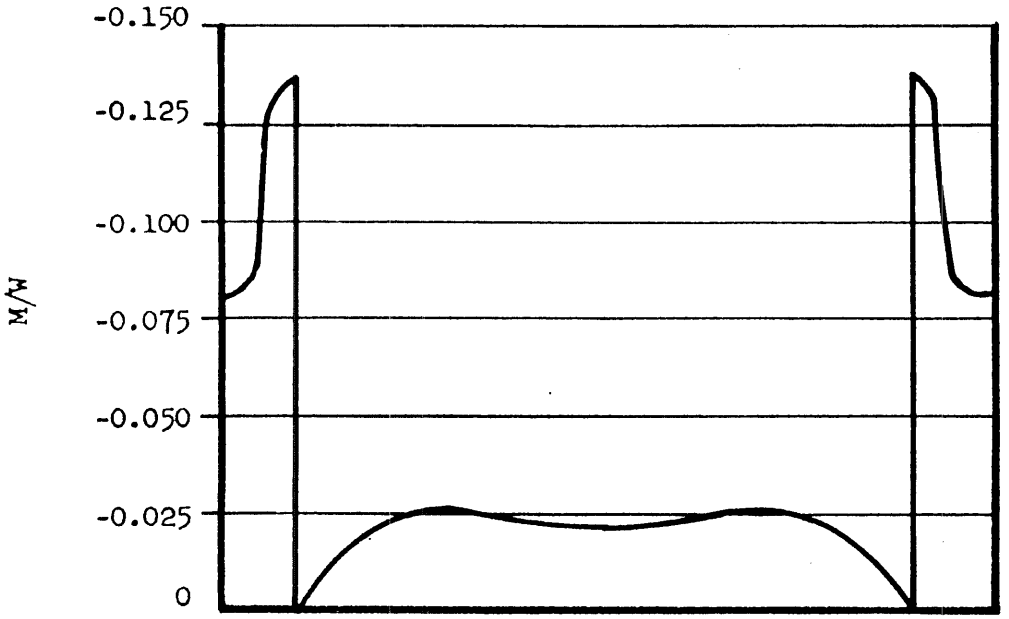

MOMENT ACROSS SECTION AA

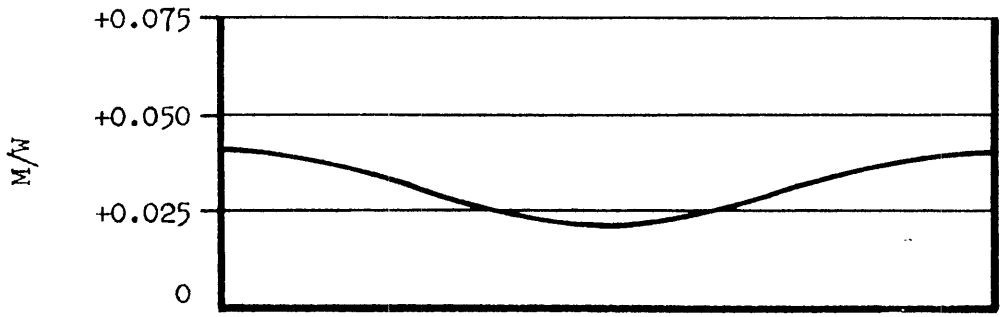

MOMENT ACROSS SECTION BB

FIG. 26 MOMENTS COMPUTED AT THE UNIVERSITY OF ILLINOIS FOR SQUARE PANELS WITH c/L = 0.2

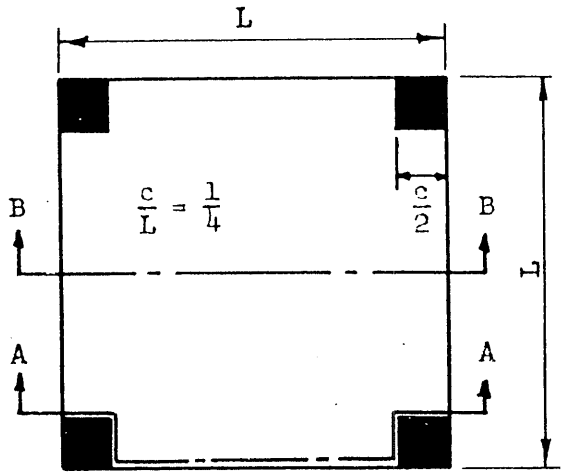

PLANE VIEW OF PANEL

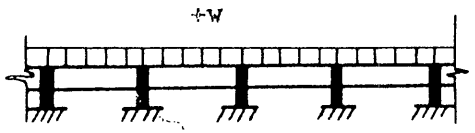

LOADING

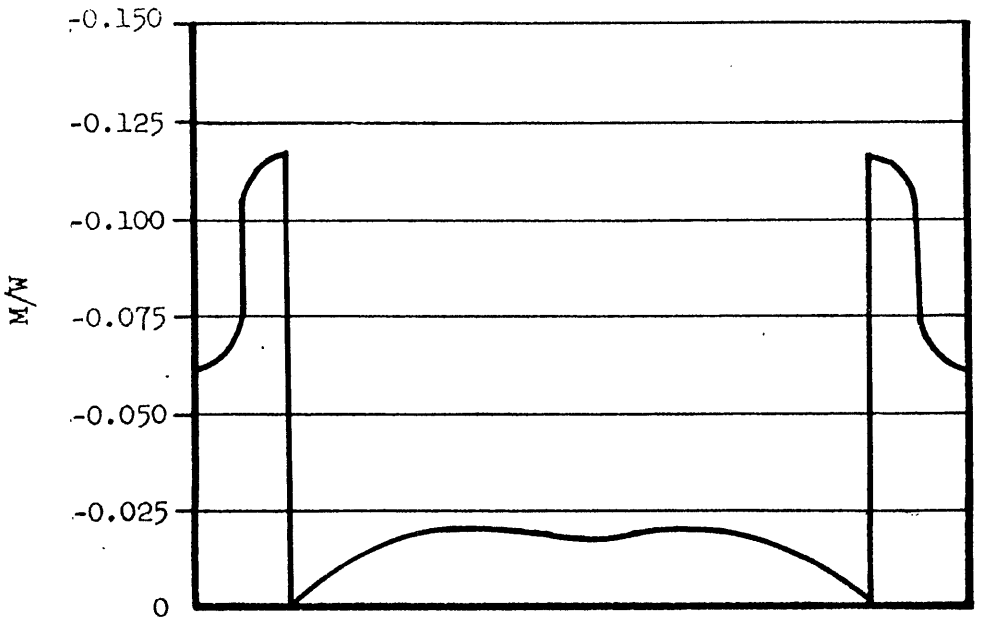

MOMENT ACROSS SECTION AA

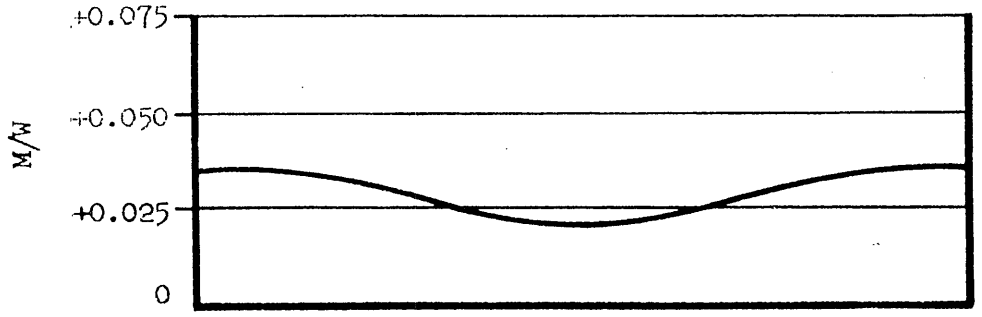

MOMENT ACROSS SECTION BB

FIG. 27 MOMENTS COMPUTED AT THE UNIVERSITY OF ILLINOIS FOR SQUARE PANELS WITH c/L = 1/4

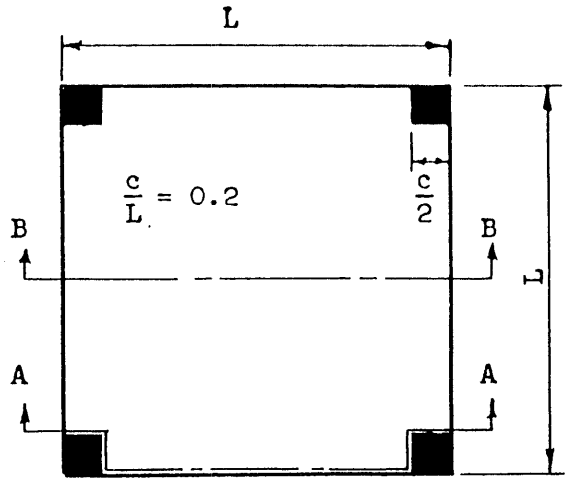

PLAN VIEW OF PANEL

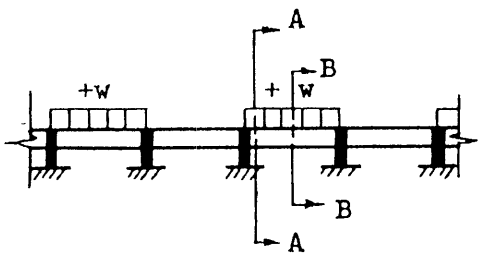

LOADING

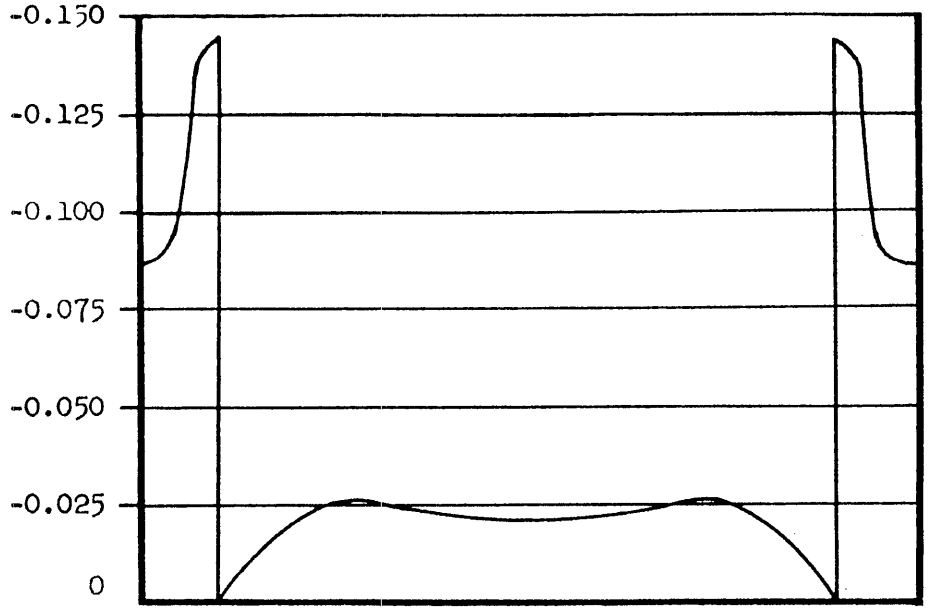

MOMENT ACROSS SECTION AA

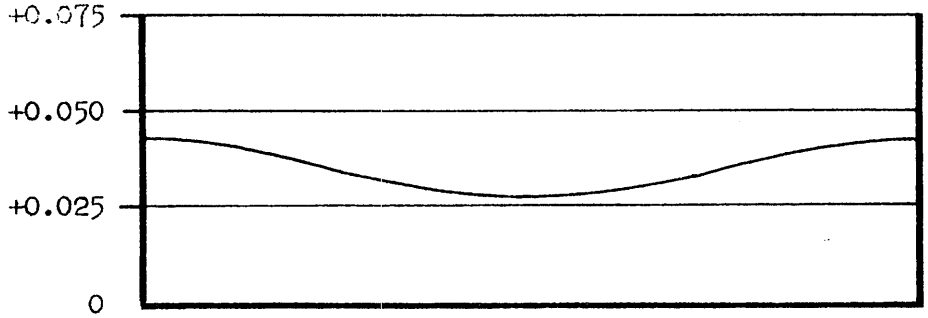

MOMENT ACROSS SECTION BB

FIG. 28 MOMENTS COMPUTED AT THE UNIVERSITY OF ILLINOIS FOR SQUARE PANELS WITH STRIP LOADING AND c/L = 0.2

PANELS 1, 4, AND 7 UNIFORMLY LOADED

c/L = 1/10

MOMENT COEFFICIENTS OF WL

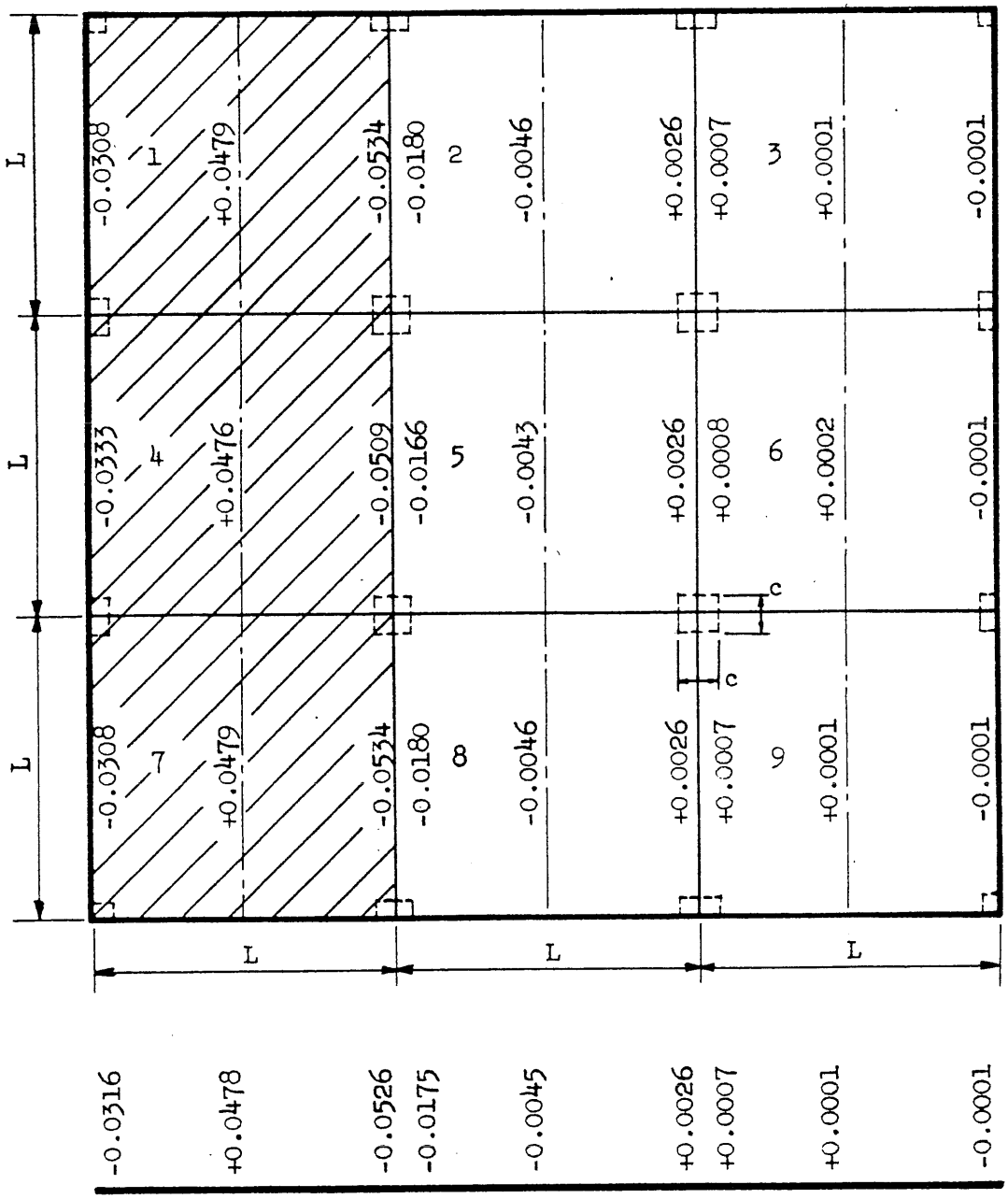

AVERAGE MOMENT ACROSS ENTIRE STRUCTURE

FIG. 29 MOMENTS IN NINE-PANEL STRUCTURE WITHOUT EDGE BEAMS

PANELS 2, 5, AND 8 UNIFORMLY LOADED

c/L = 1/10

MOMENT COEFFICIENTS OF WL

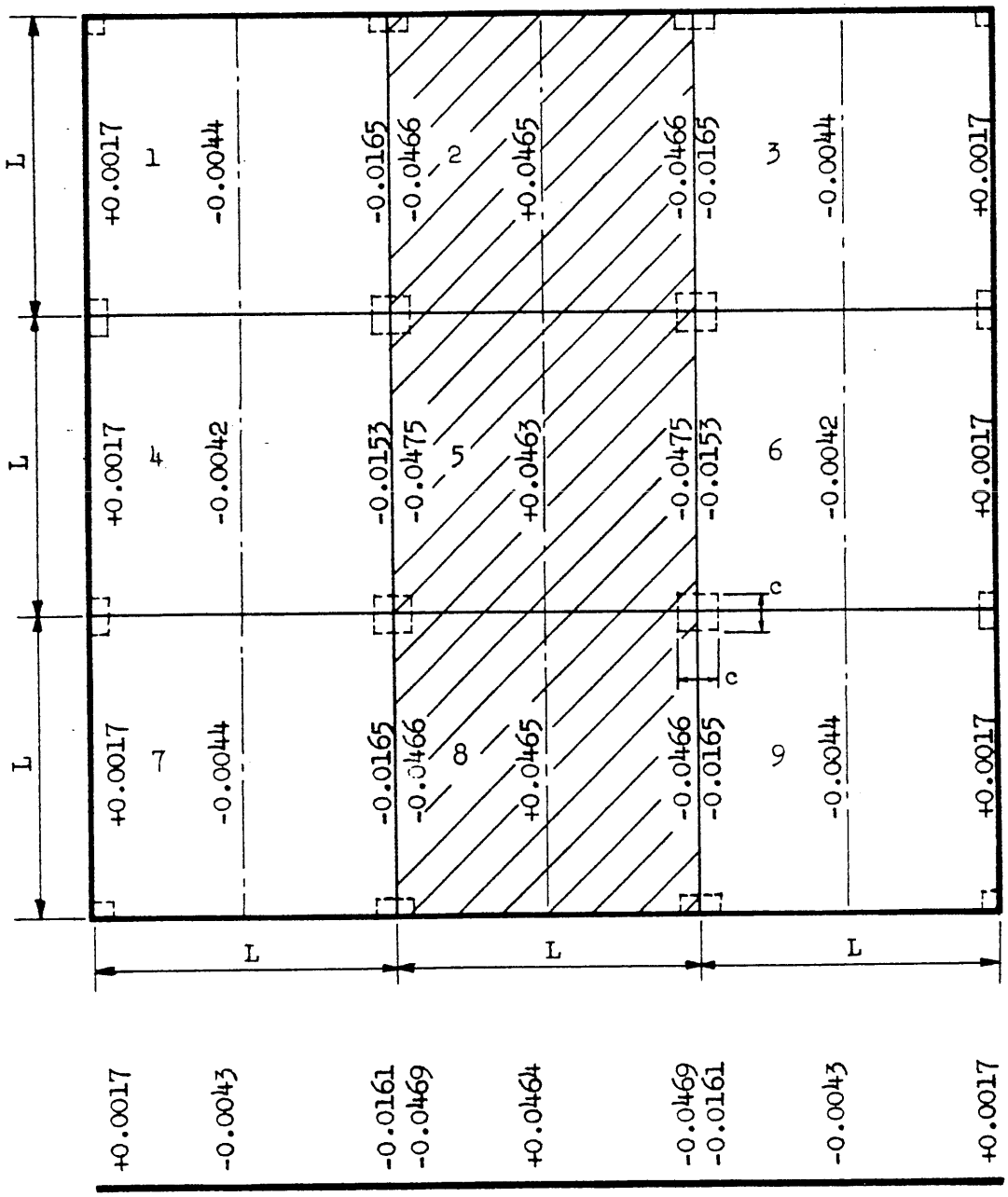

AVERAGE MOMENT ACROSS ENTIRE STRUCTURE

FIG. 30 MOMENTS IN NINE-PANEL STRUCTURE WITHOUT EDGE BEAMS

ALL PANELS UNIFORMLY LOADED

c/L = 1/10

MOMENT COEFFICIENTS OF WL

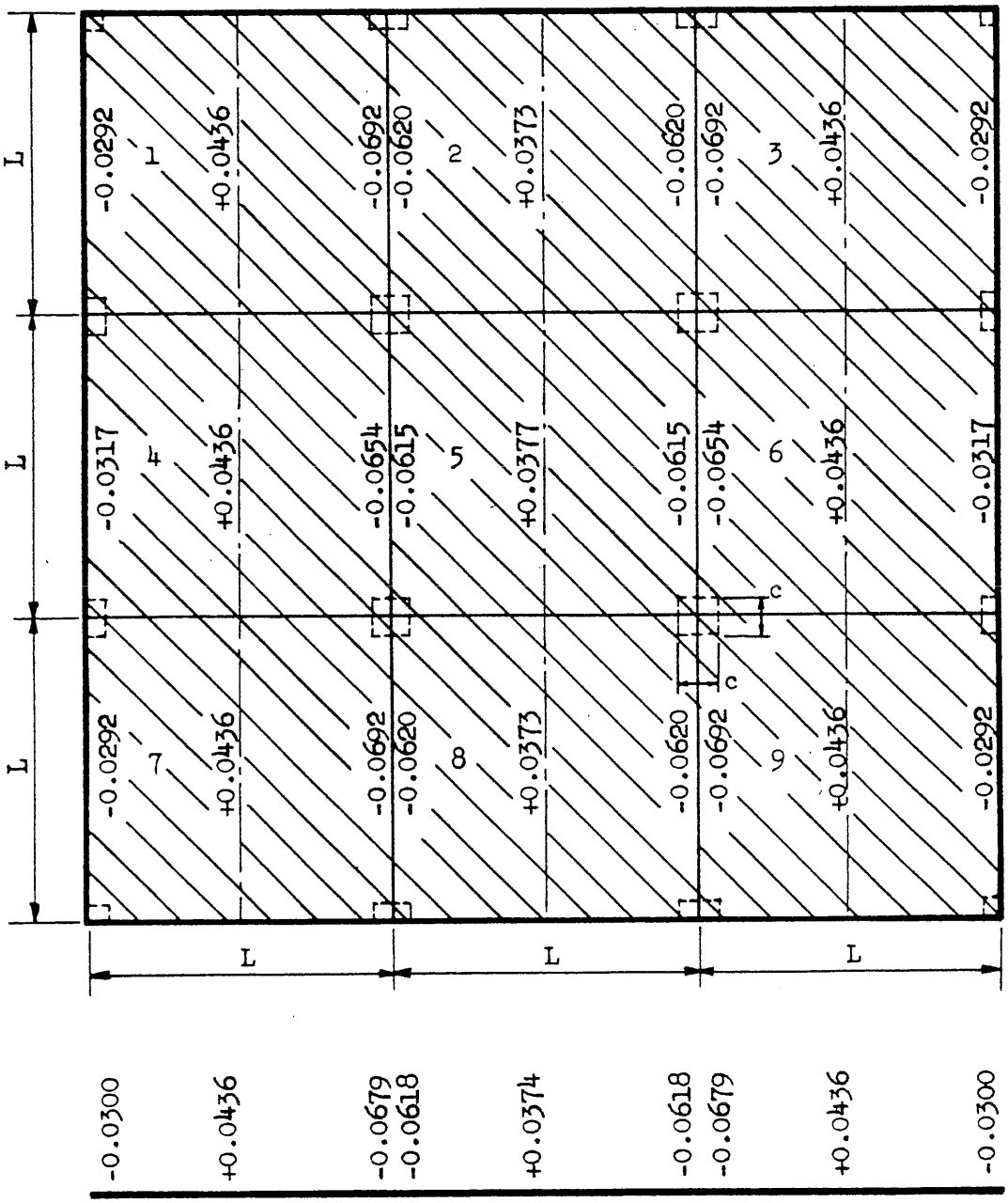

AVERAGE MOMENT ACROSS ENTIRE STRUCTURE

FIG. 31 MOMENTS IN NINE-PANEL STRUCTURE WITHOUT EDGE BEAMS

ALL PANELS UNIFORMLY LOADED

c/L = 1/10

MOMENT COEFFICIENTS OF WL

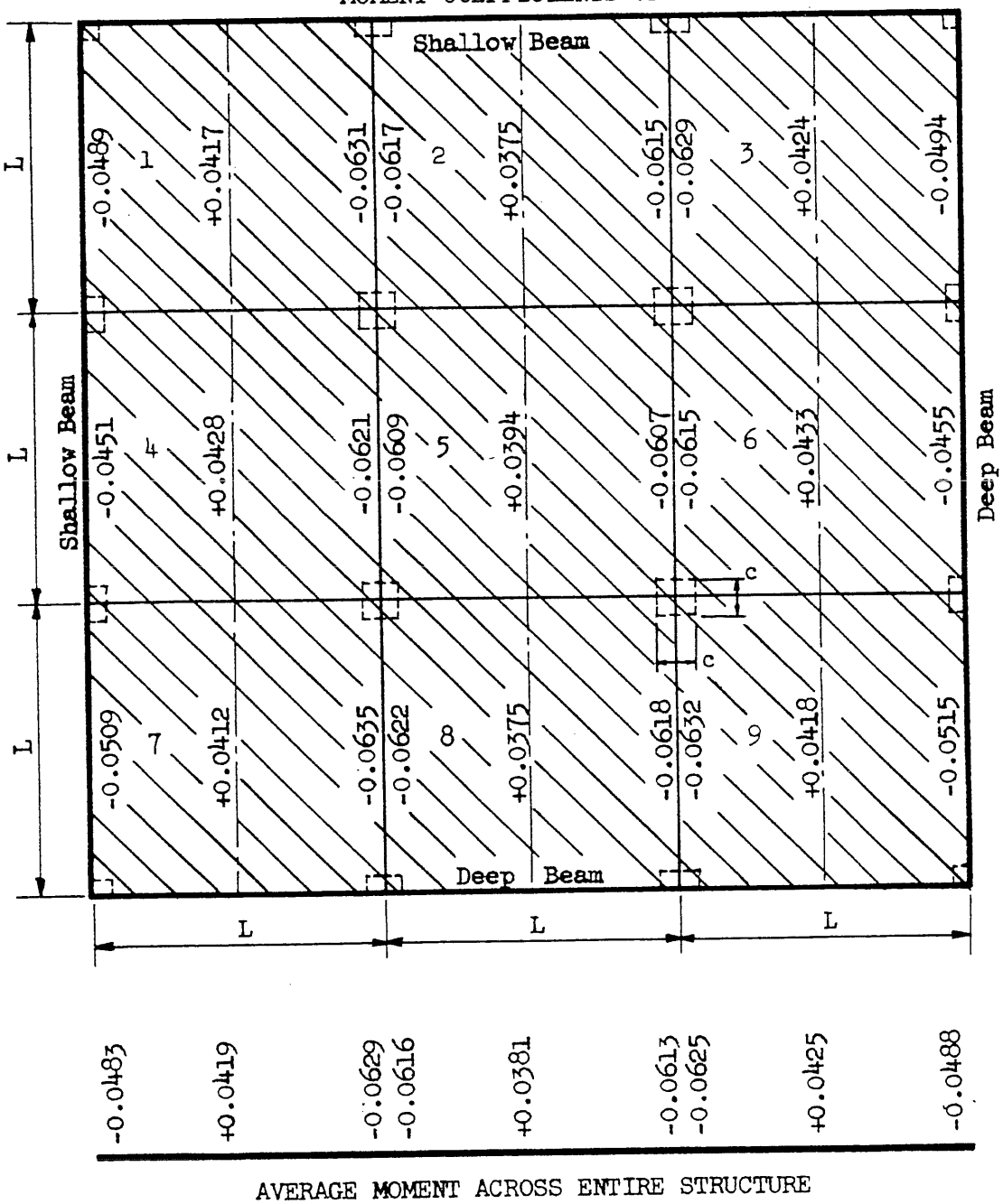

AVERAGE MOMENT ACROSS ENTIRE STRUCTURE

FIG. 32 MOMENTS IN NINE-PANEL STRUCTURE WITH EDGE BEAMS

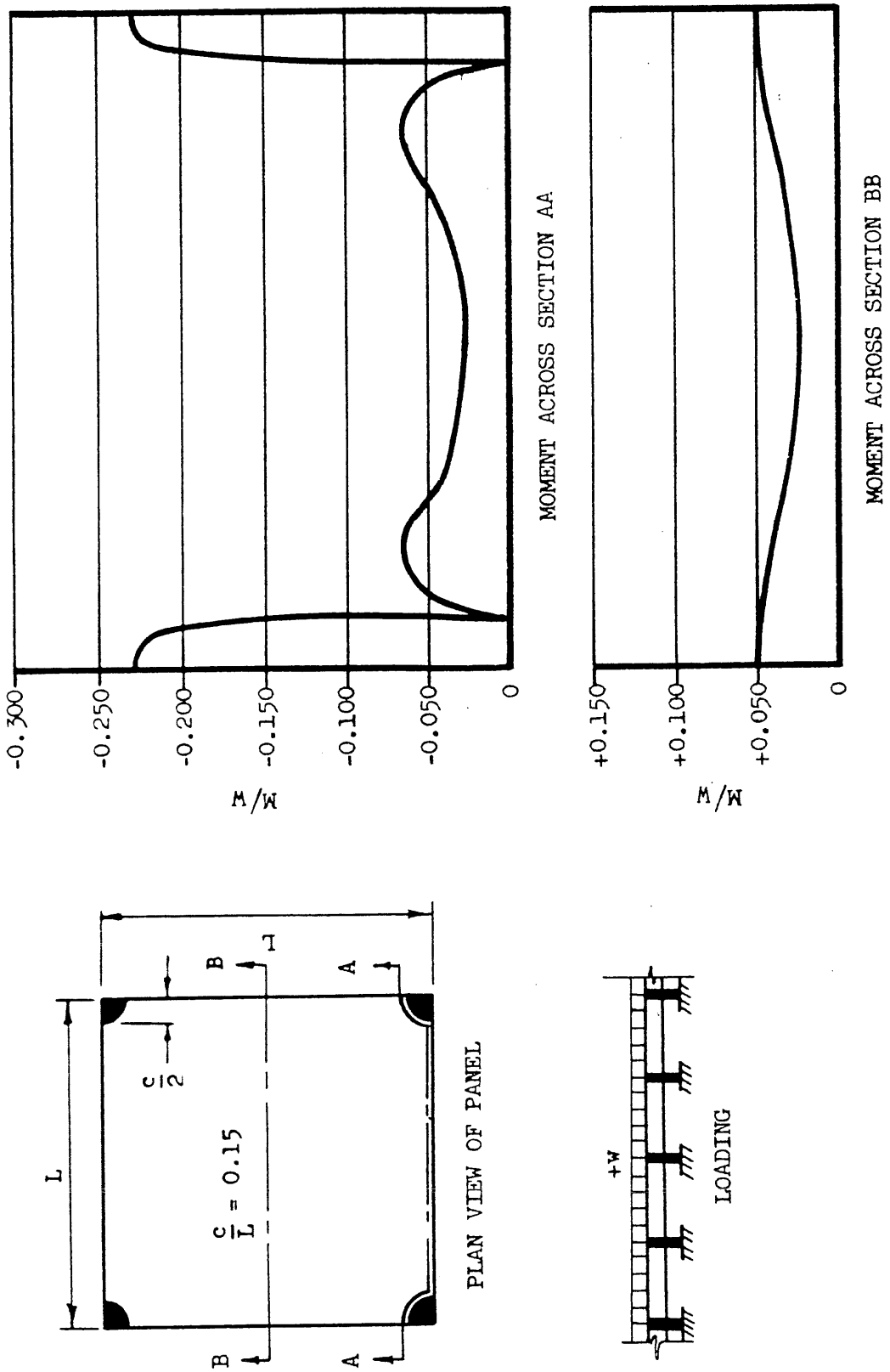

FIG. 33 MOMENTS COMPUTED BY WESTERGAARD FOR SQUARE PANELS WITH c/L = 0.15

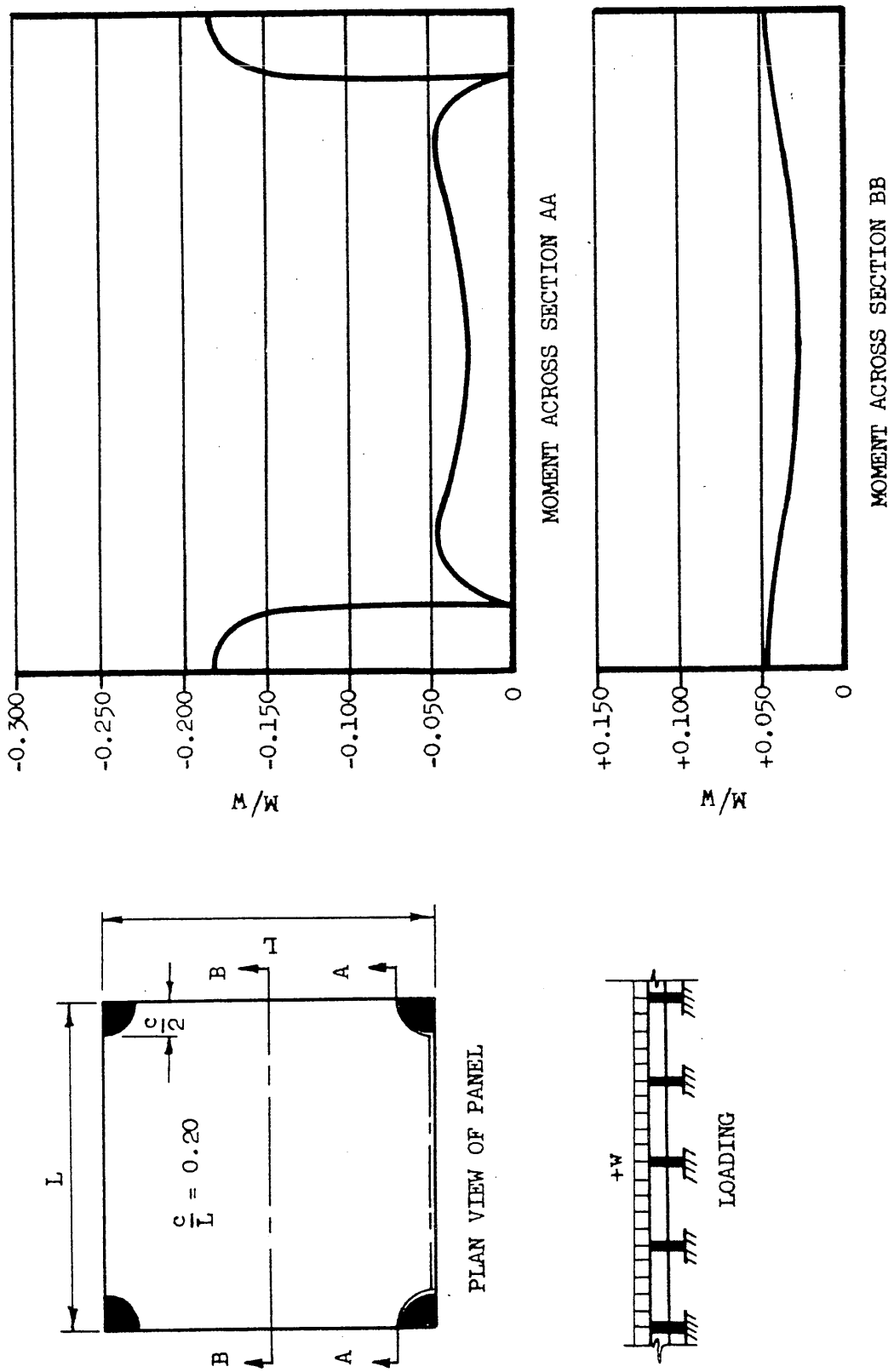

FIG. 34 MOMENTS COMPUTED BY WESTERGAARD FOR SQUARE PANELS WITH c/L = 0.20

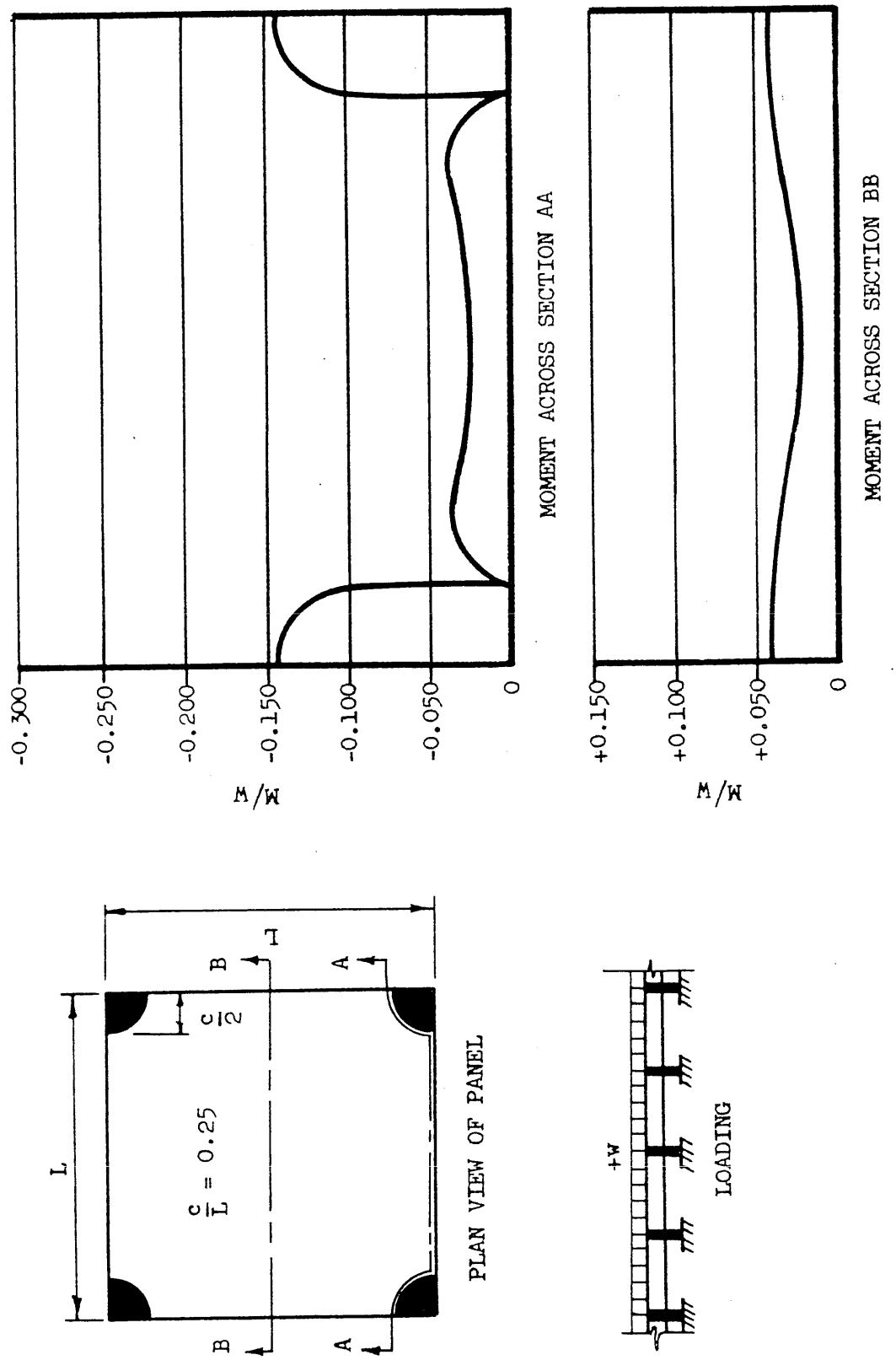

FIG. 35 MOMENTS COMPUTED BY WESTERGAARD FOR SQUARE PANELS WITH c/L = 0.25

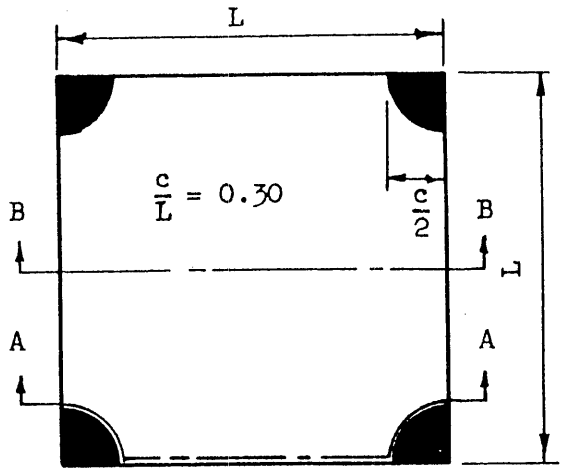

PLAN VIEW OF PANEL

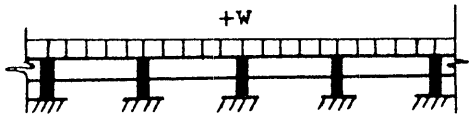

LOADING

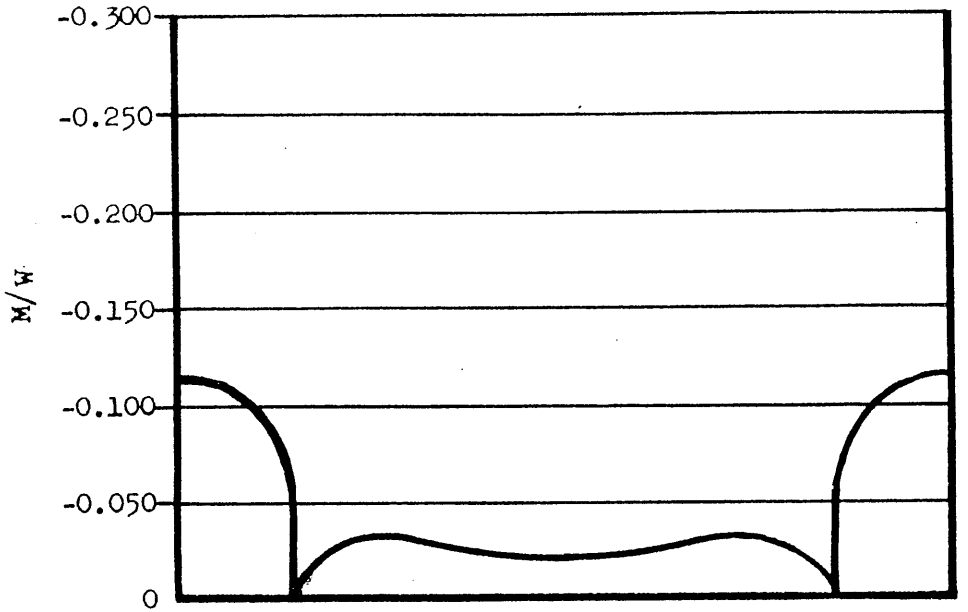

MOMENT ACROSS SECTION AA

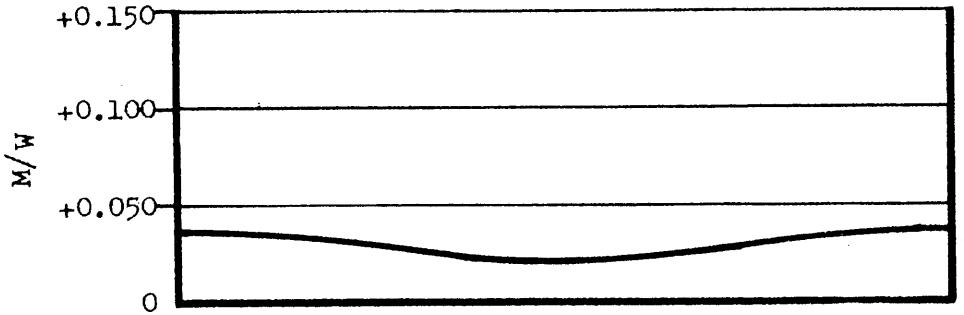

MOMENT ACROSS SECTION BB

FIG. 36 MOMENTS COMPUTED BY WESTERGAARD FOR SQUARE PANELS WITH c/L = 0.30

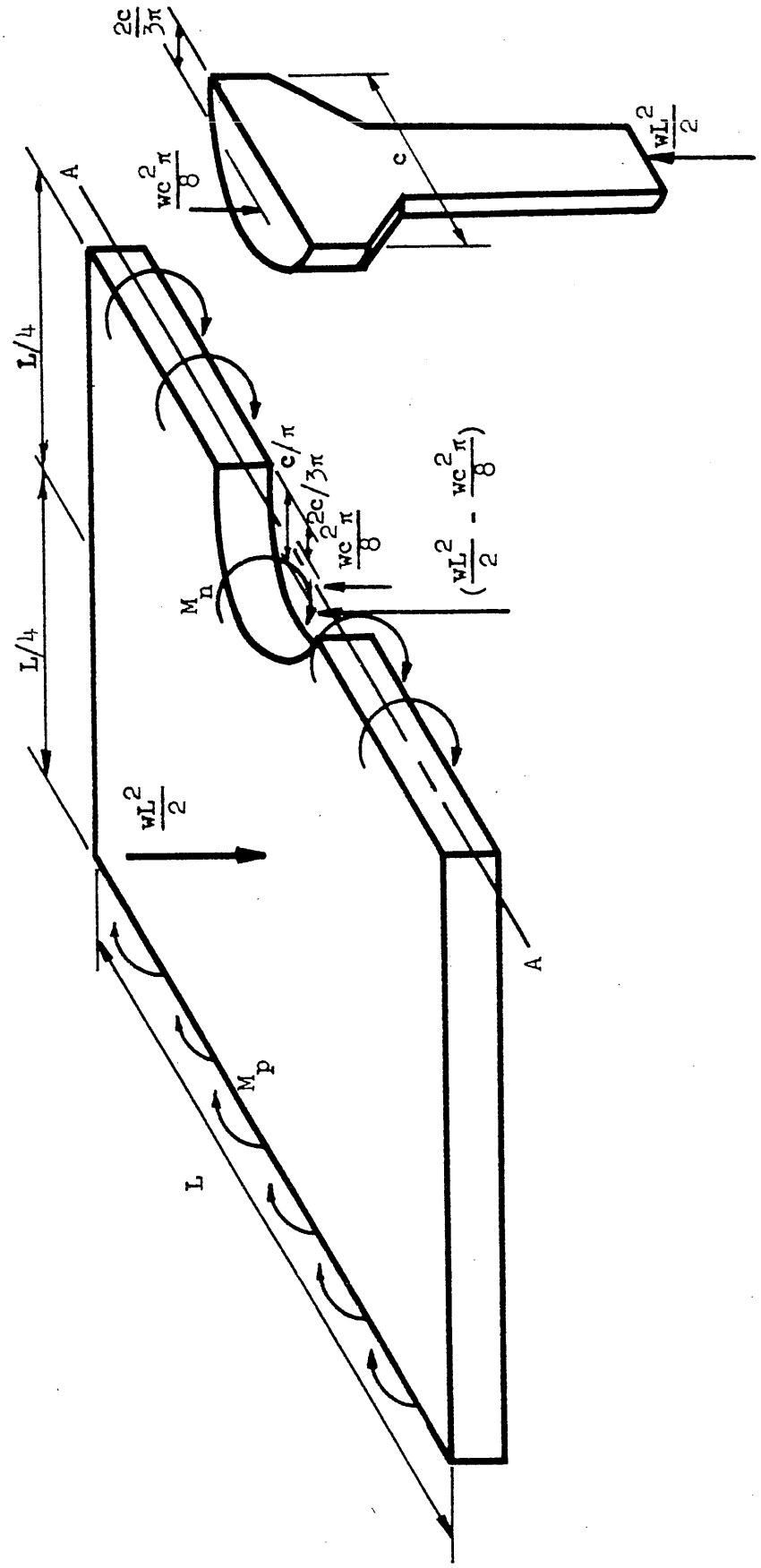

FIG. 37 FREE-BODY DIAGRAM OF ONE-HALF OF SLAB PANEL

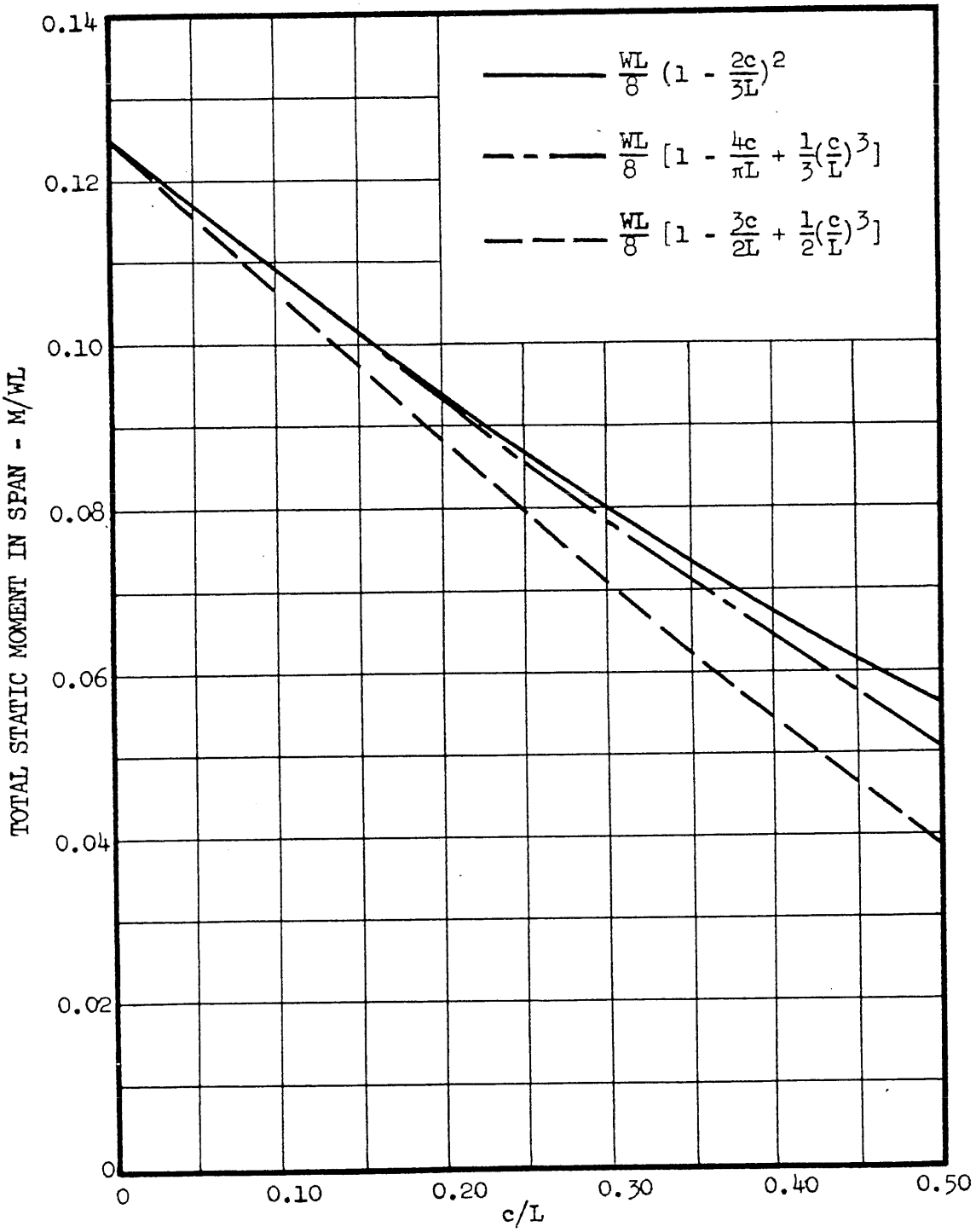

FIG. 38 COMPARISON OF EXPRESSIONS FOR TOTAL STATIC MOMENT IN SQUARE PANELS

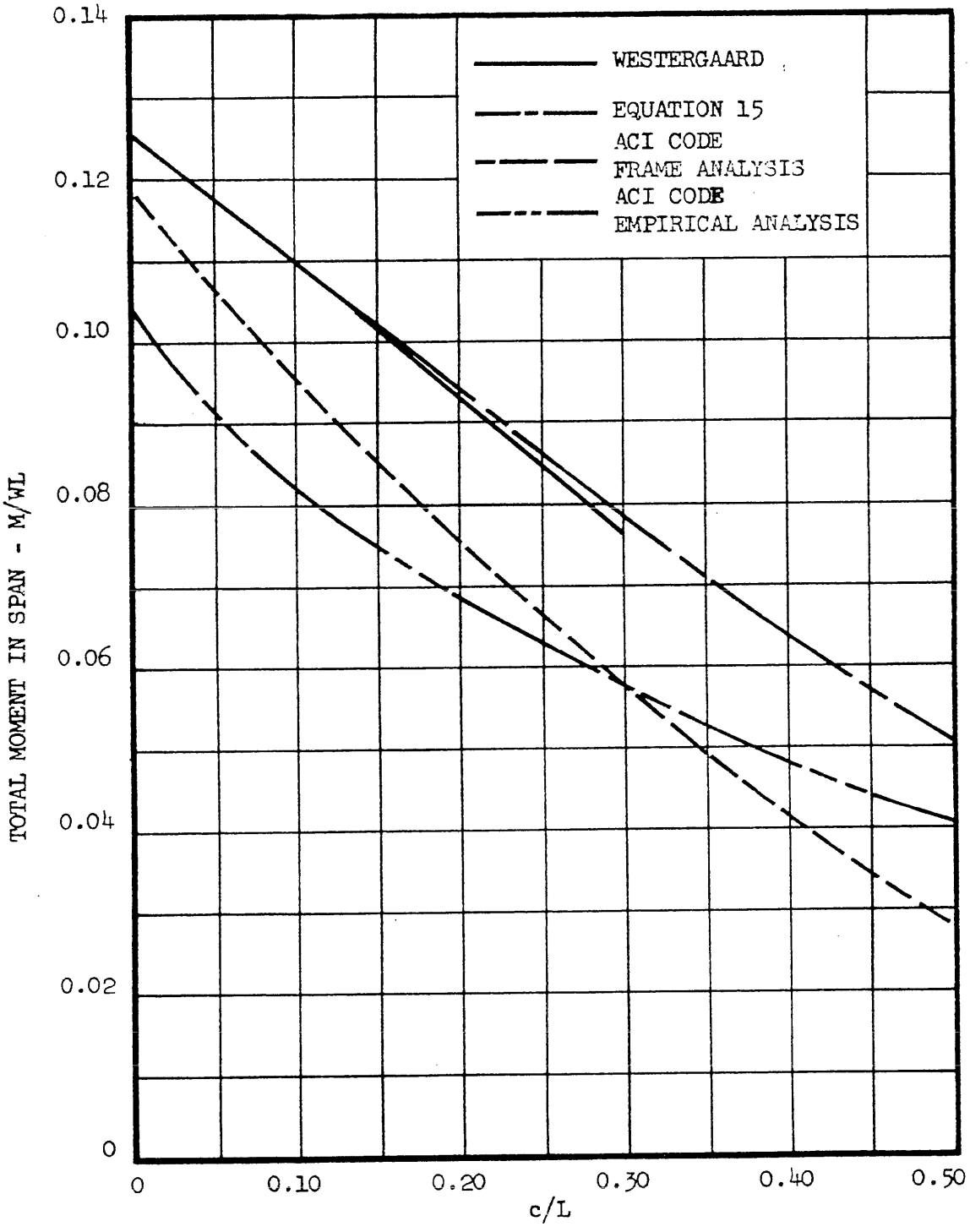

FIG. 39 TOTAL MOMENT IN SLABS SUPPORTED ON CIRCULAR COLUMN CAPITALS

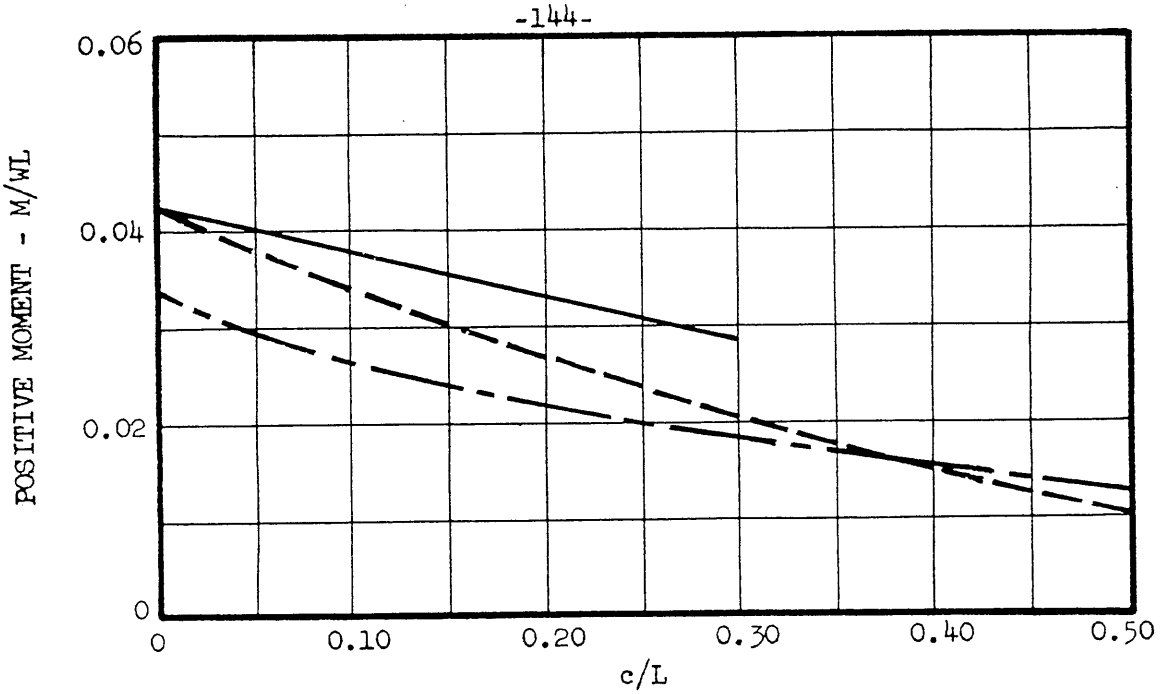

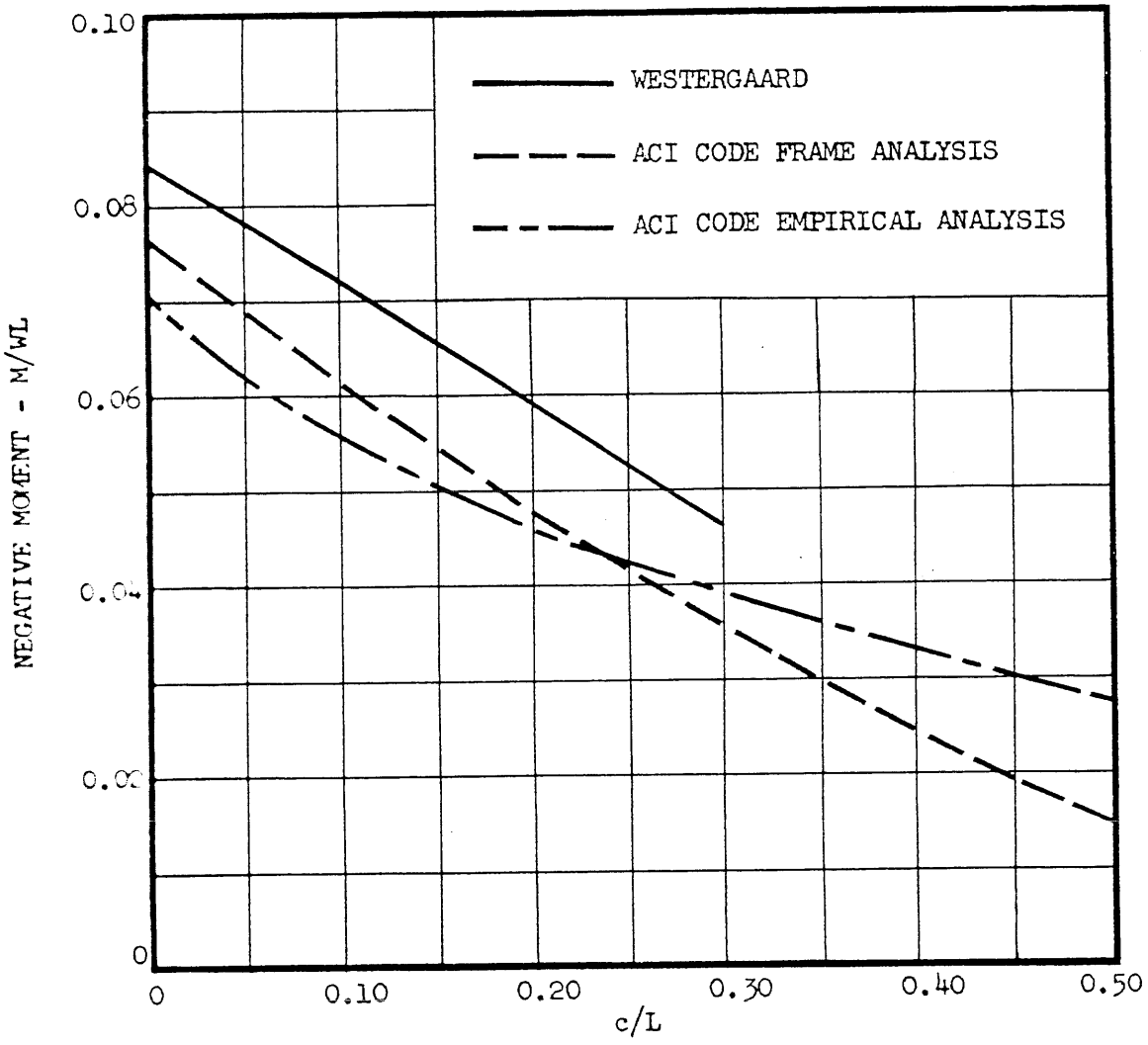

FIG. 40 MOMENTS AT DESIGN SECTIONS OF SLABS SUPPORTED ON CIRCULAR COLUMN CAPITALS

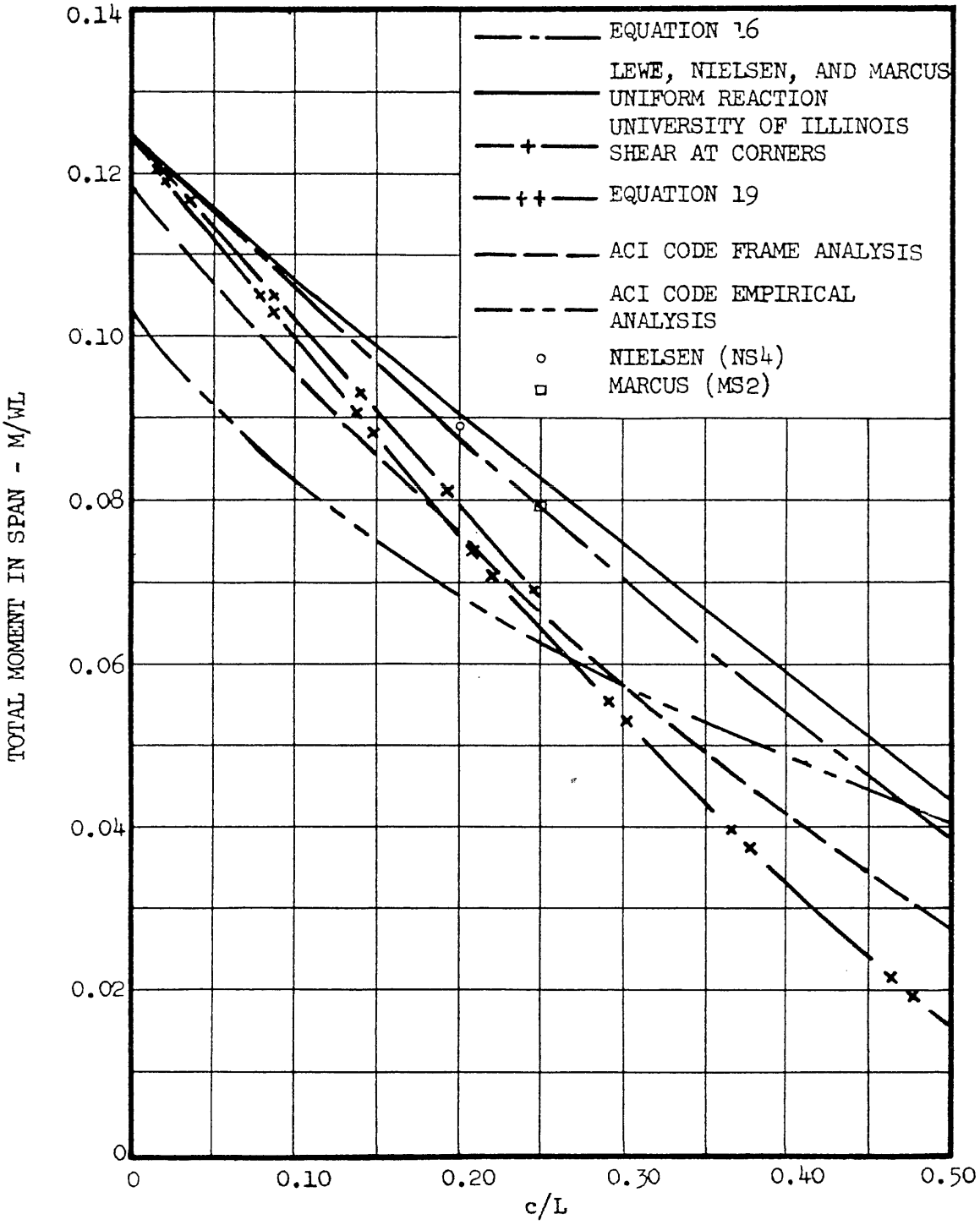

FIG. 41 TOTAL MOMENT IN SLABS SUPPORTED ON SQUARE COLUMN CAPITALS

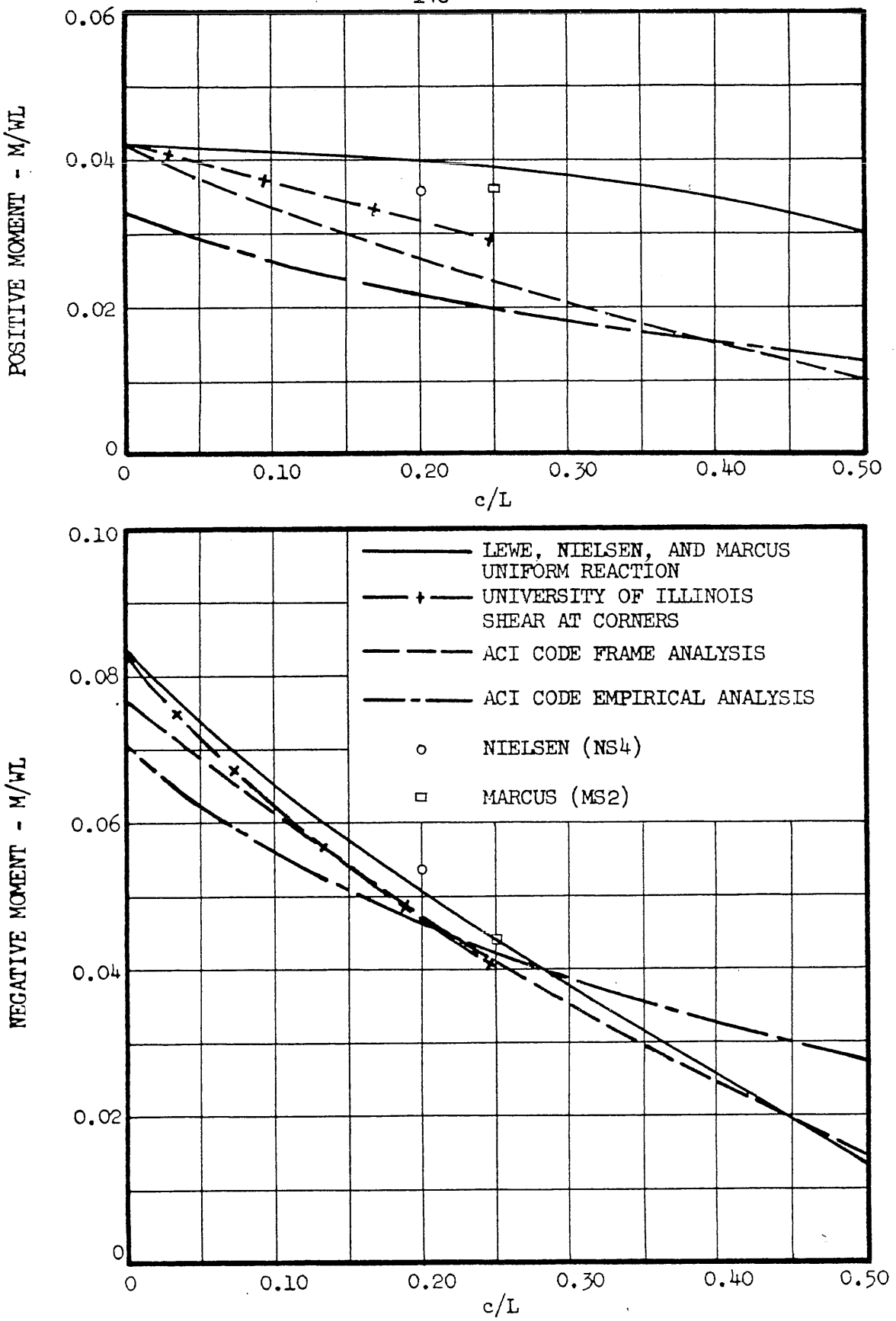

FIG. 42 MOMENTS AT DESIGN SECTIONS OF SLABS WITH SQUARE COLUMN CAPITALS

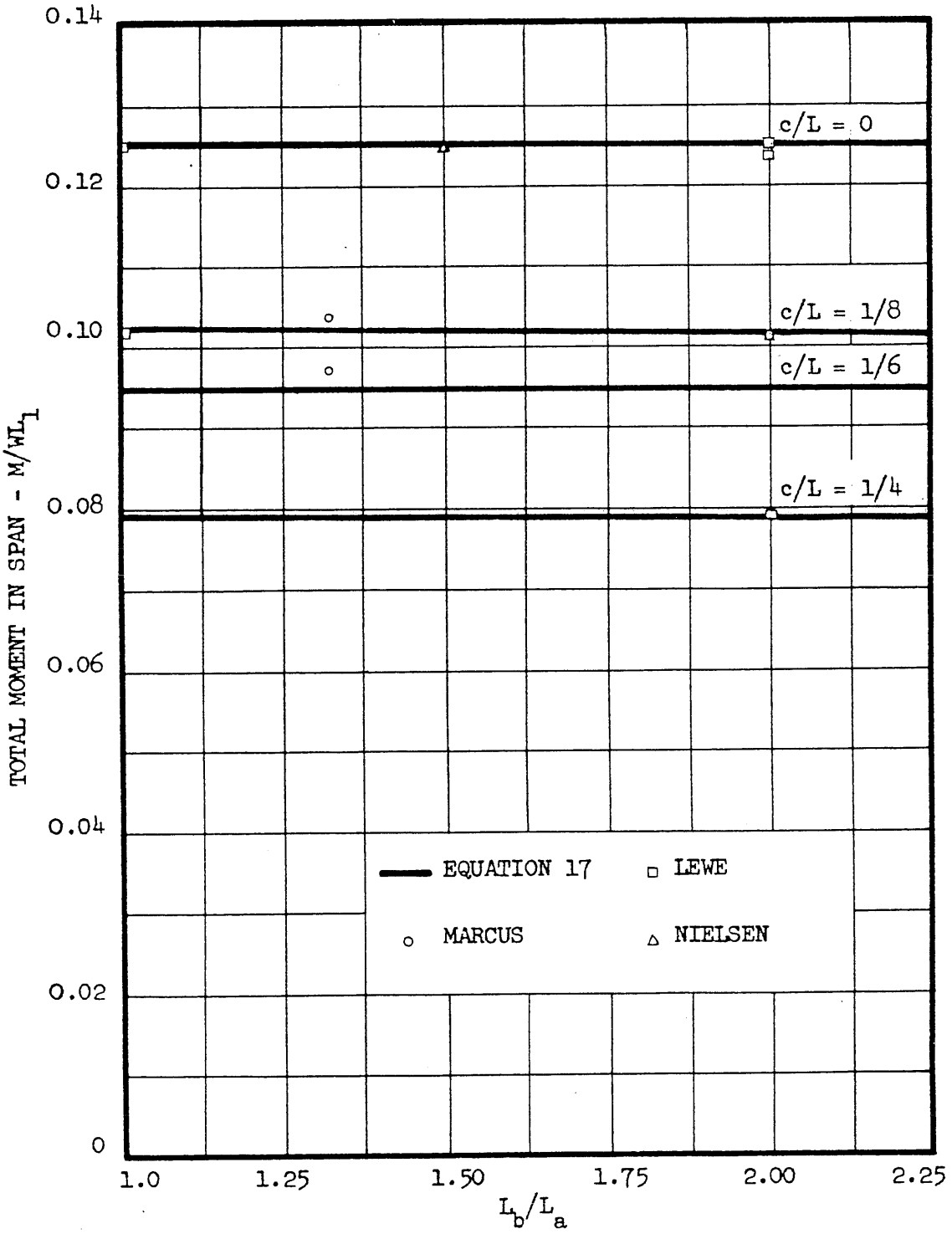

FIG. 43 TOTAL MOMENTS IN RECTANGULAR PANELS WITH SQUARE CAPITALS

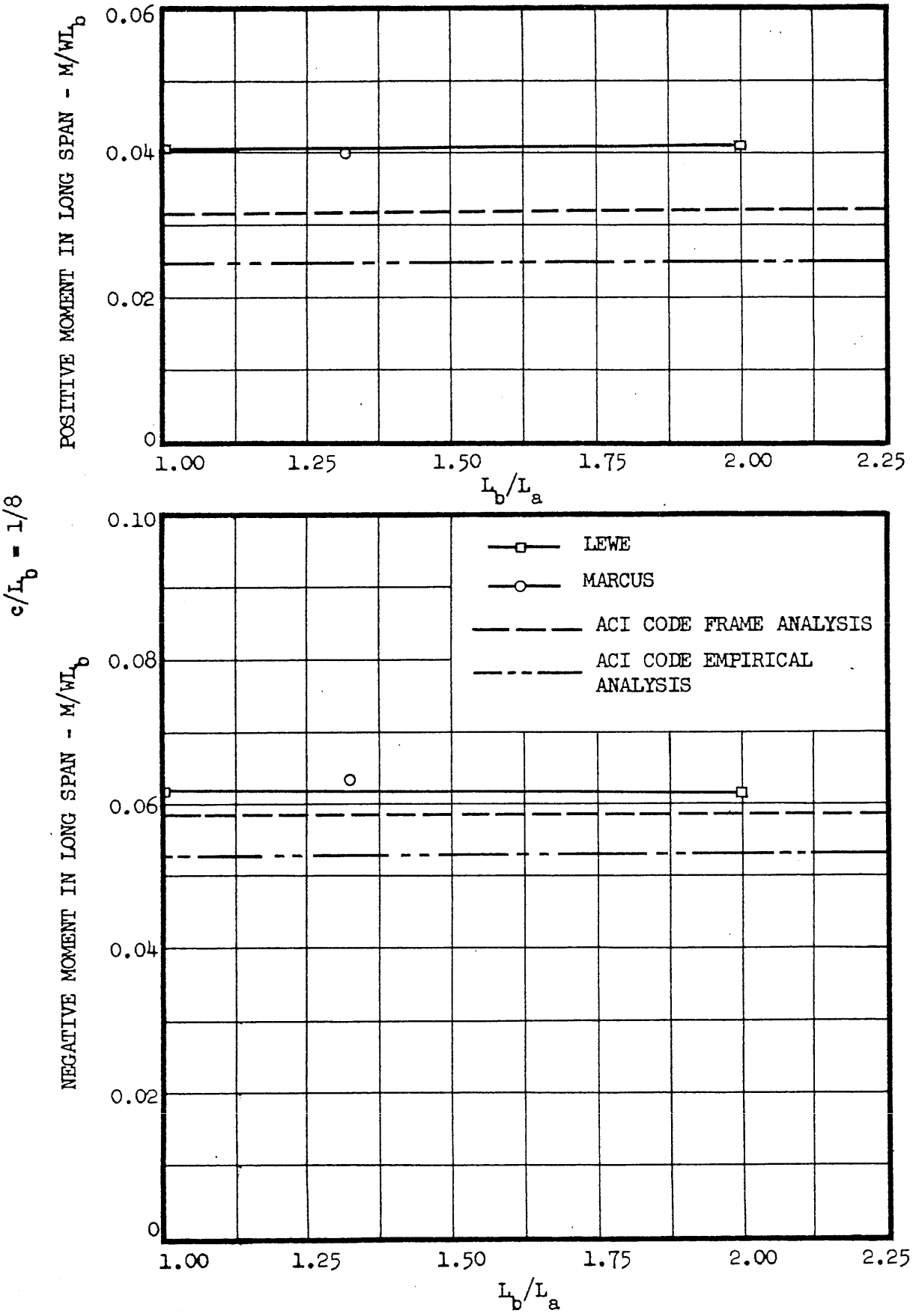

FIG. 44 MOMENTS AT DESIGN SECTIONS OF RECTANGULAR SLABS WITH SQUARE COLUMN CAPITALS

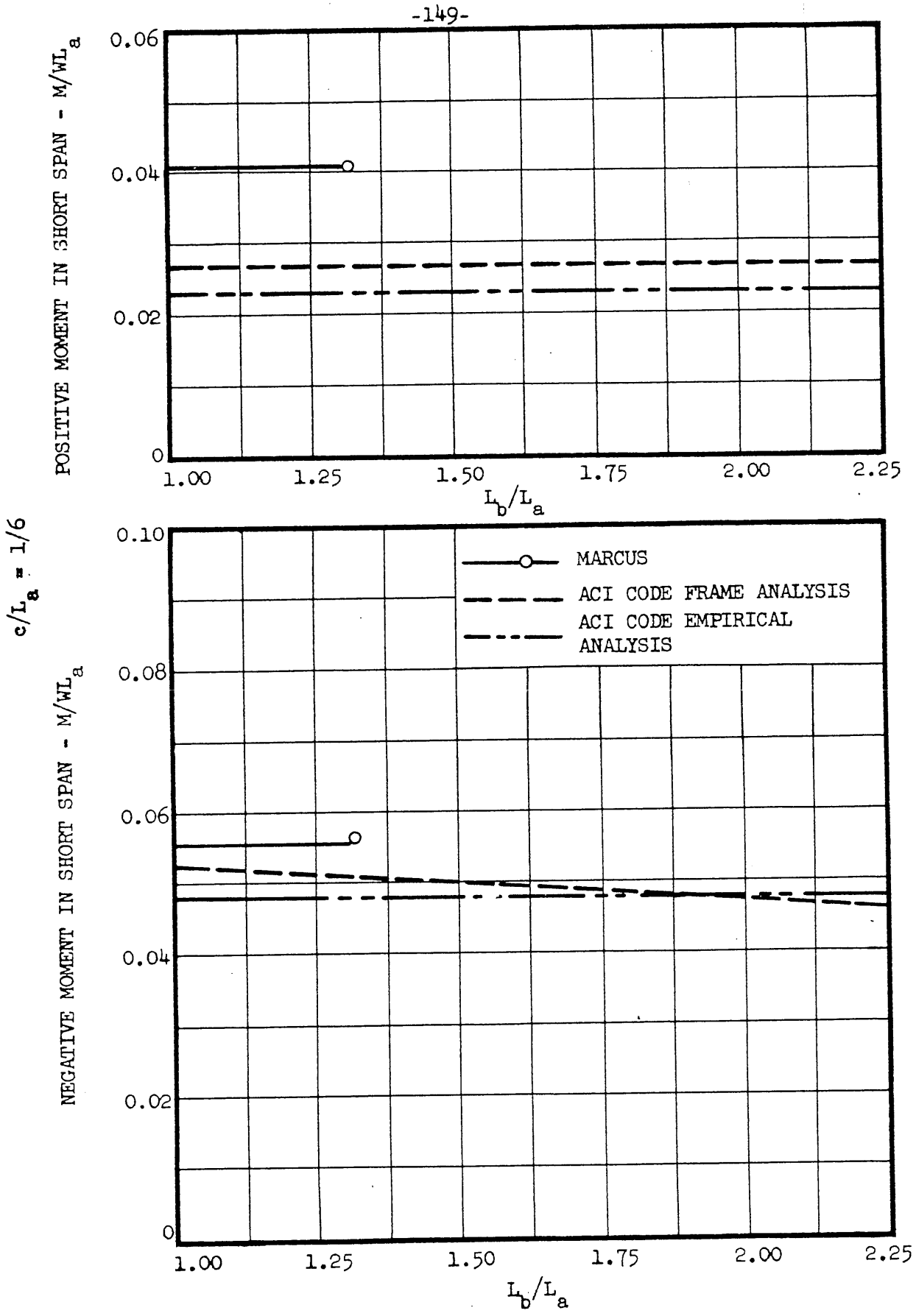

FIG. 45 MOMENTS AT DESIGN SECTIONS OF RECTANGULAR SLABS WITH SQUARE COLUMN CAPITALS

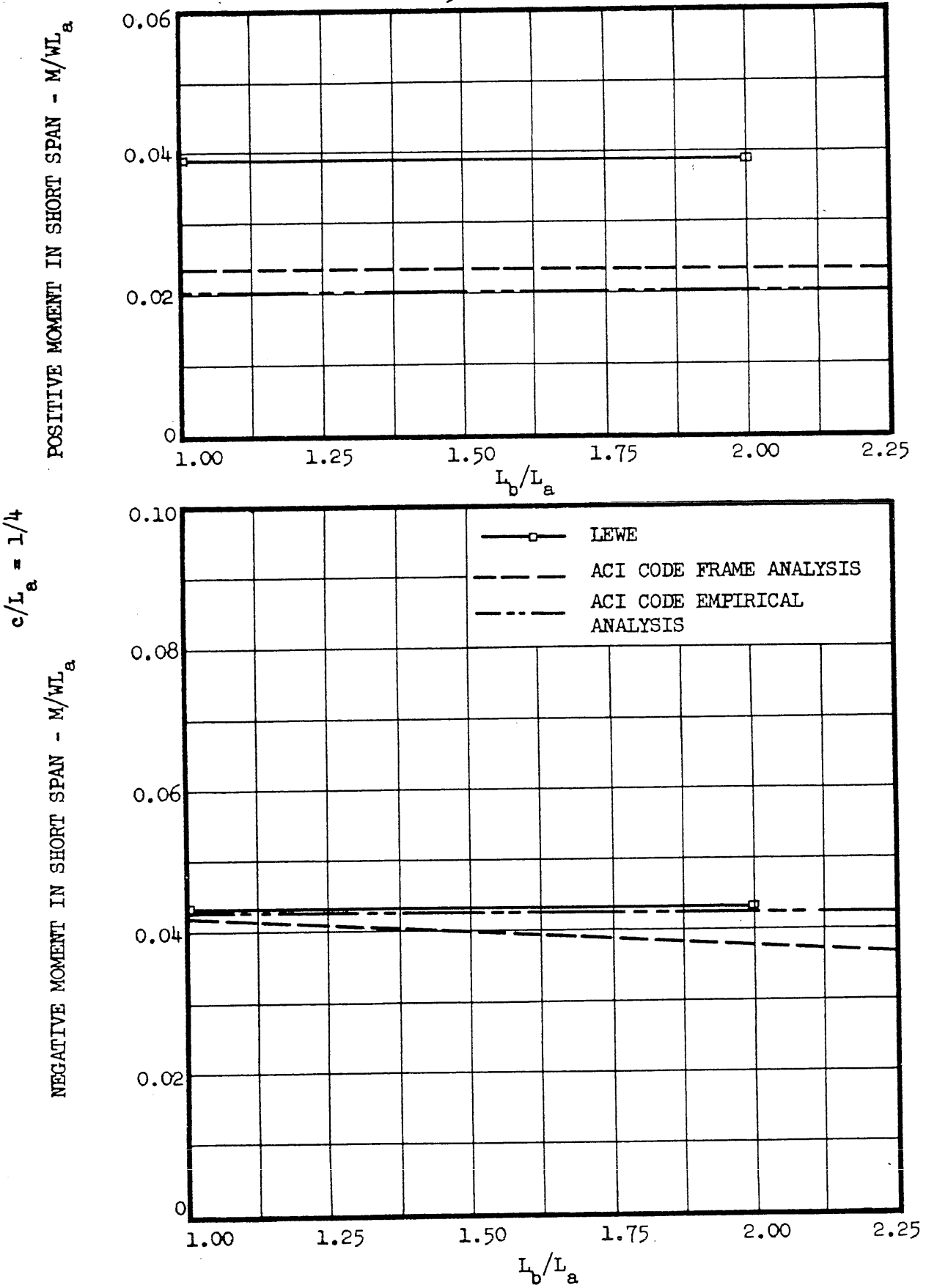

FIG. 46 MOMENTS AT DESIGN SECTIONS OF RECTANGULAR SLABS WITH SQUARE COLUMN CAPITALS

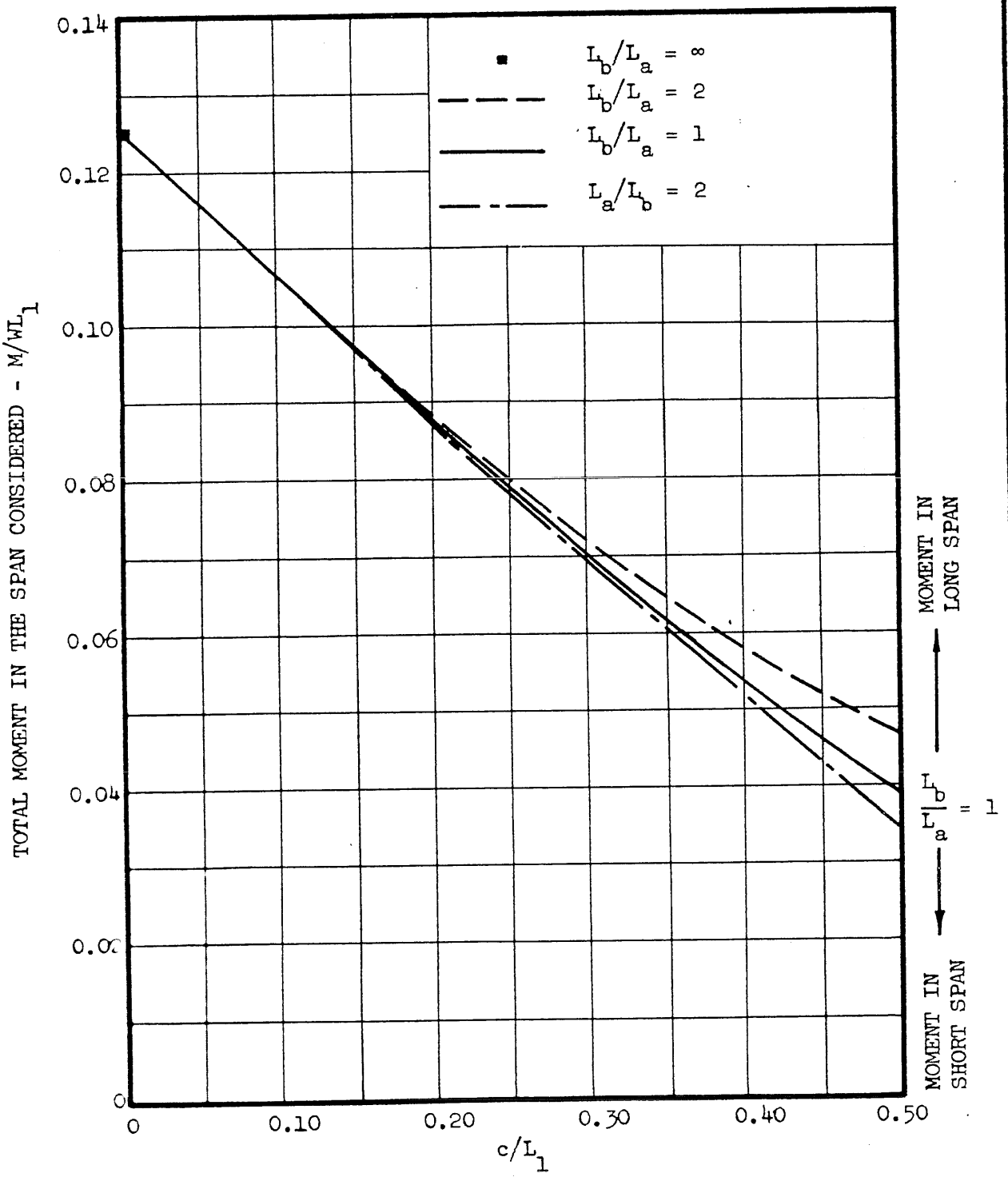

FIG. 47 TOTAL STATIC MOMENT IN RECTANGULAR SLABS WITH SQUARE COLUMN CAPITALS

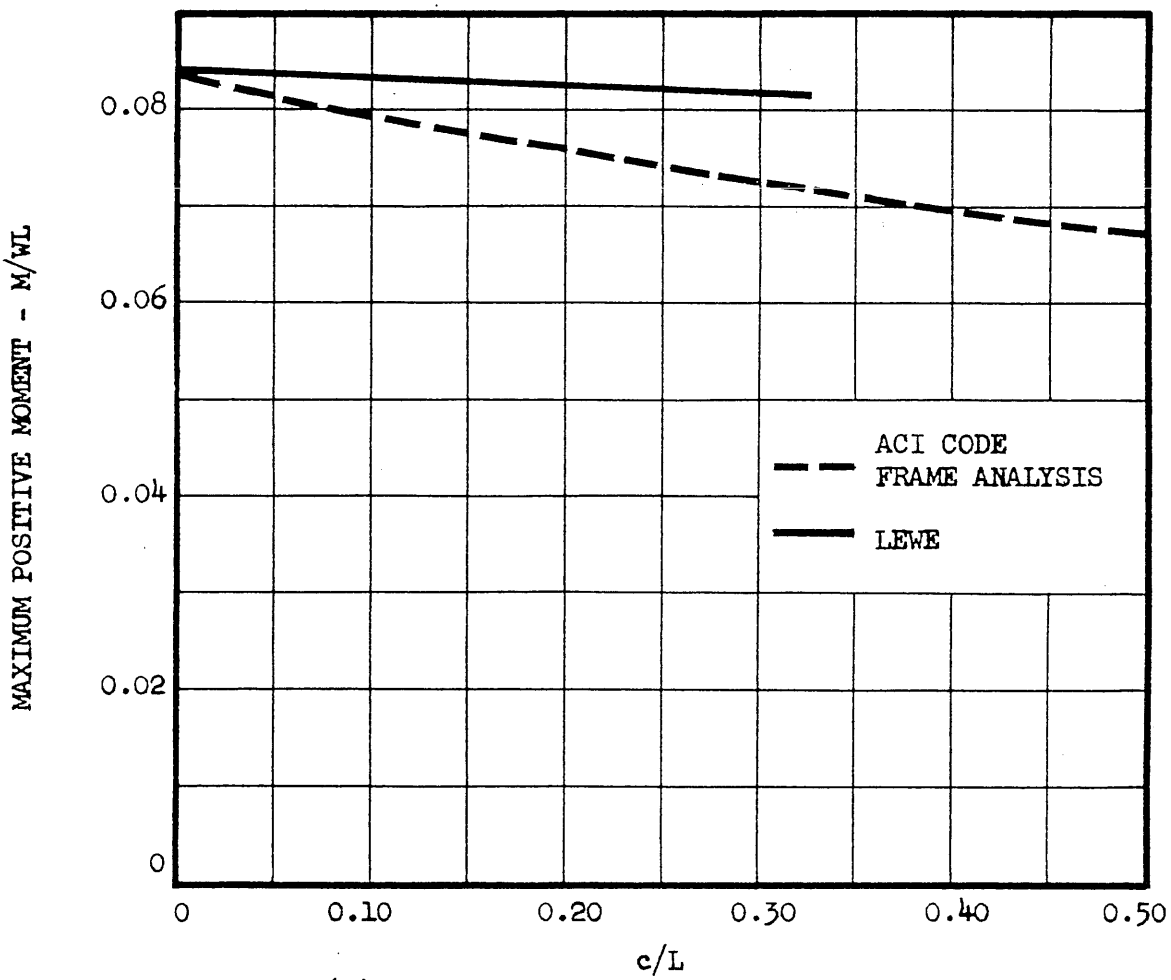

(a) COLUMN WITH ZERO FLEXURAL STIFFNESS

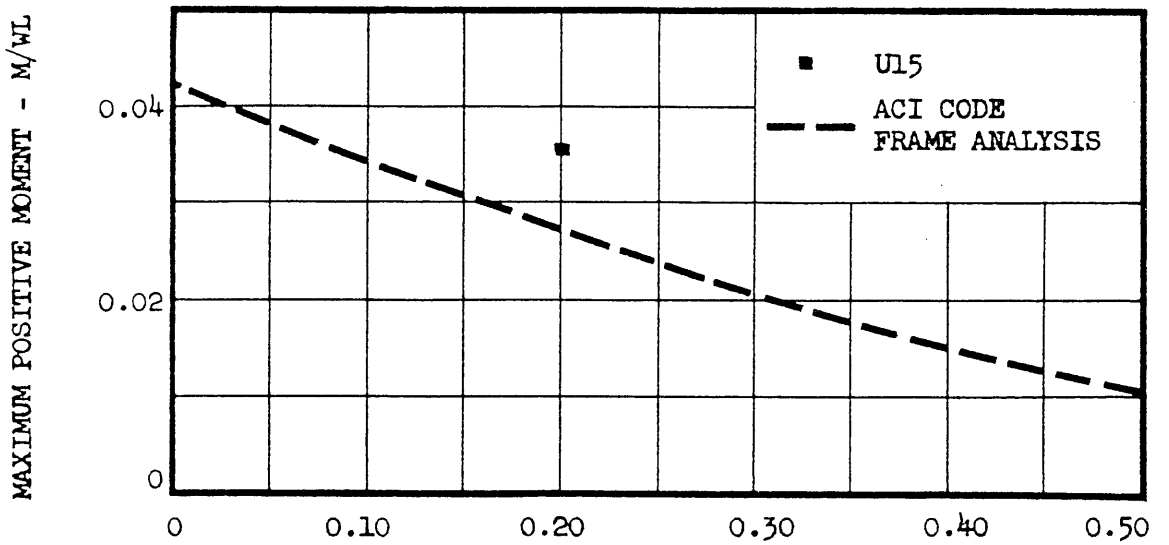

(b) COLUMN WITH INFINITE FLEXURAL STIFFNESS

FIG. 48 COMPUTED MOMENTS UNDER STRIP LOADING FOR MAXIMUM POSITIVE MOMENT

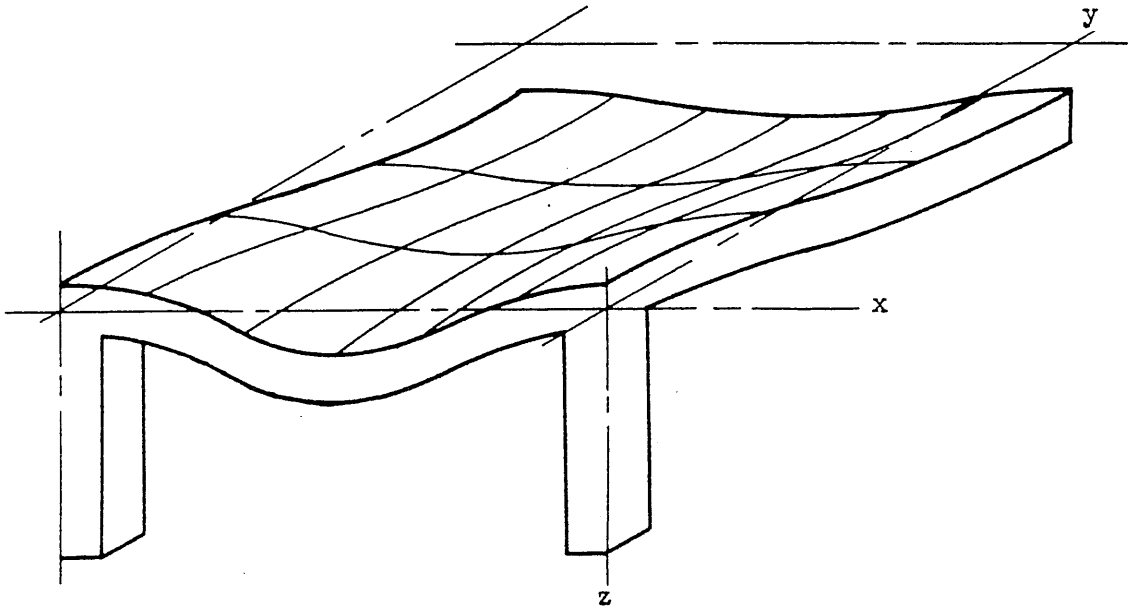

(a) DEFLECTED SHAPE OF SLAB

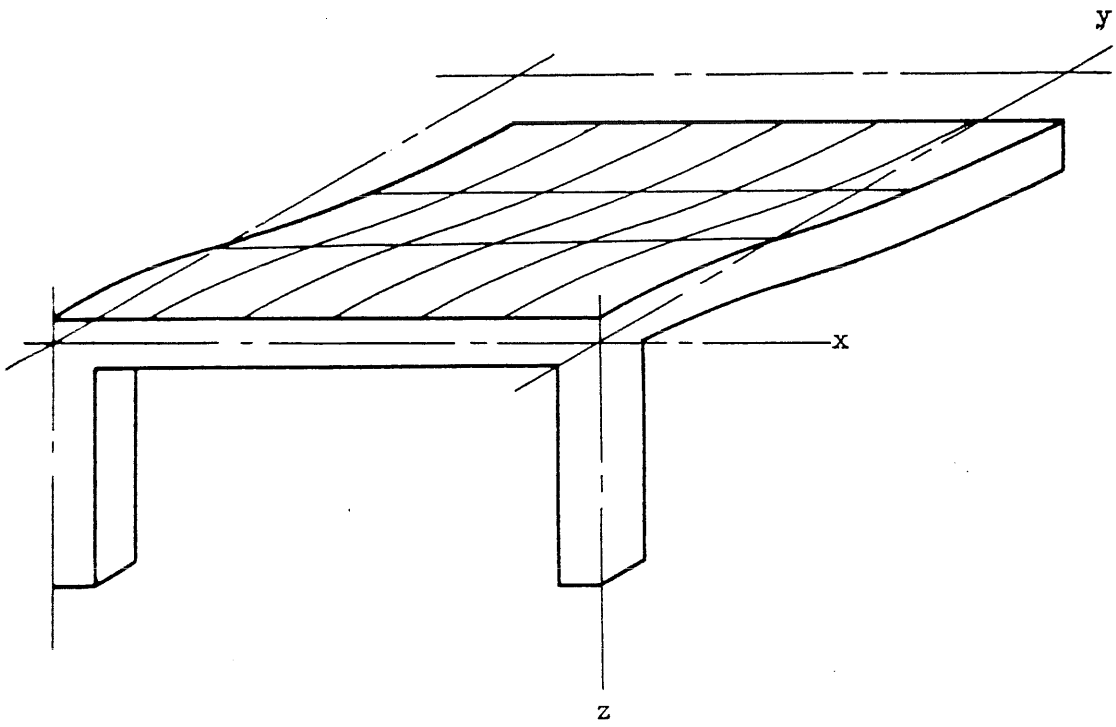

(b) DEFLECTED SHAPE OF SLAB BY ACI CODE ASSUMPTIONS

FIG. 49 DEFLECTED SHAPE OF A SLAB PANEL UNDER UNIFORM LOAD

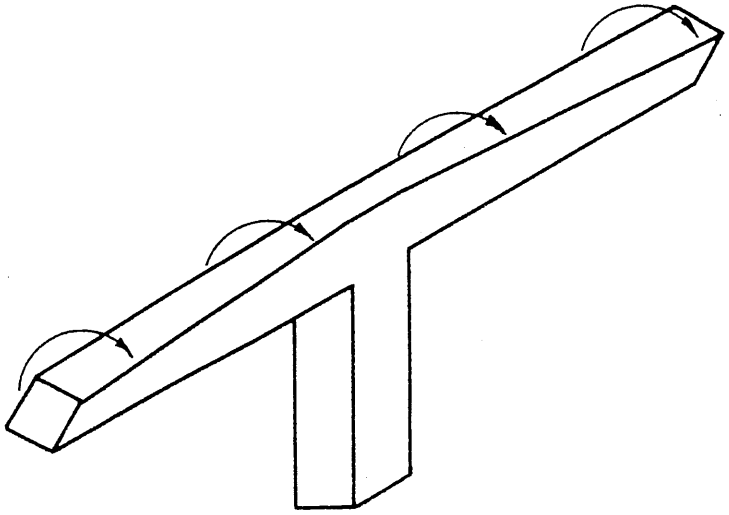

(a) DEFORMATION OF EDGE BEAM

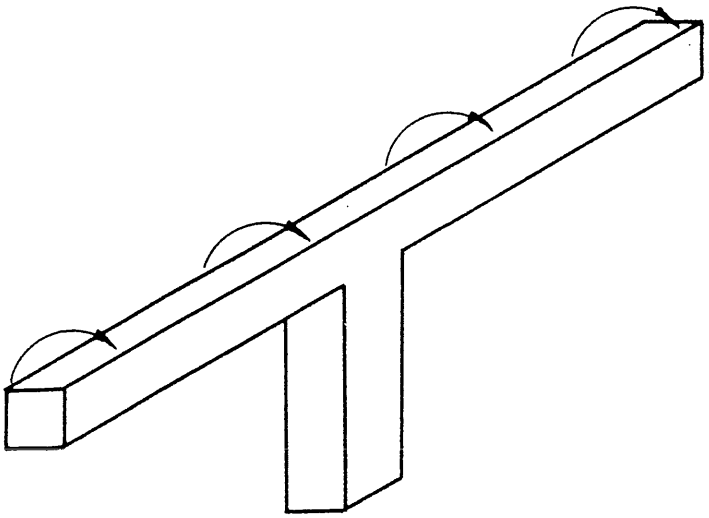

(b) "DEFORMATION" OF EDGE BEAM ACCORDING TO ASSUMPTIONS OF ACI CODE FRAME ANALYSIS

FIG. 50 ILLUSTRATION OF BEAM DEFORMATIONS CAUSED BY TWISTING MOMENT

ALTERNATE STRIPS LOADED FOR MAXIMUM POSITIVE MOMENT

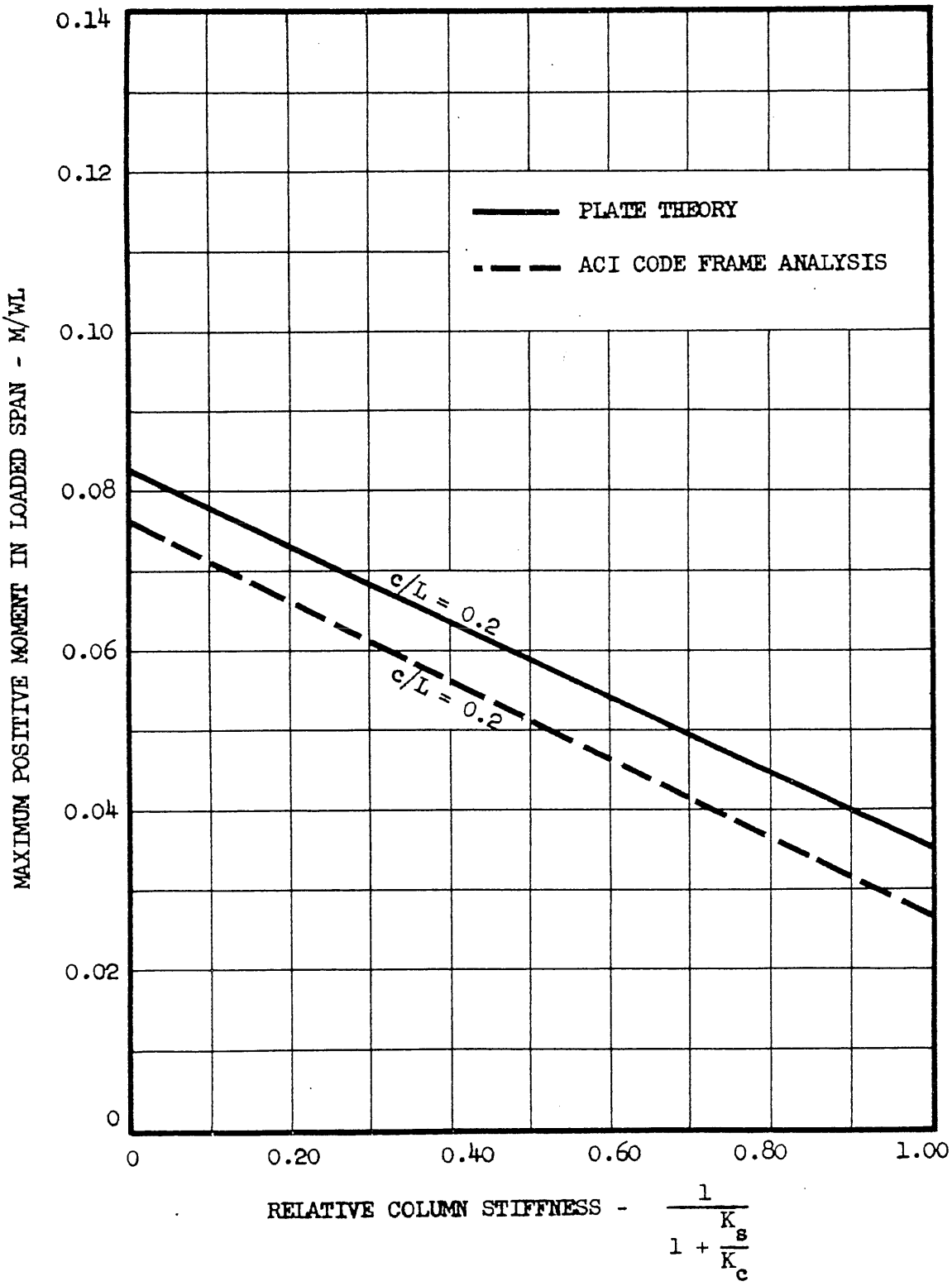

FIG. 51 INFLUENCE OF RELATIVE COLUMN STIFFNESS

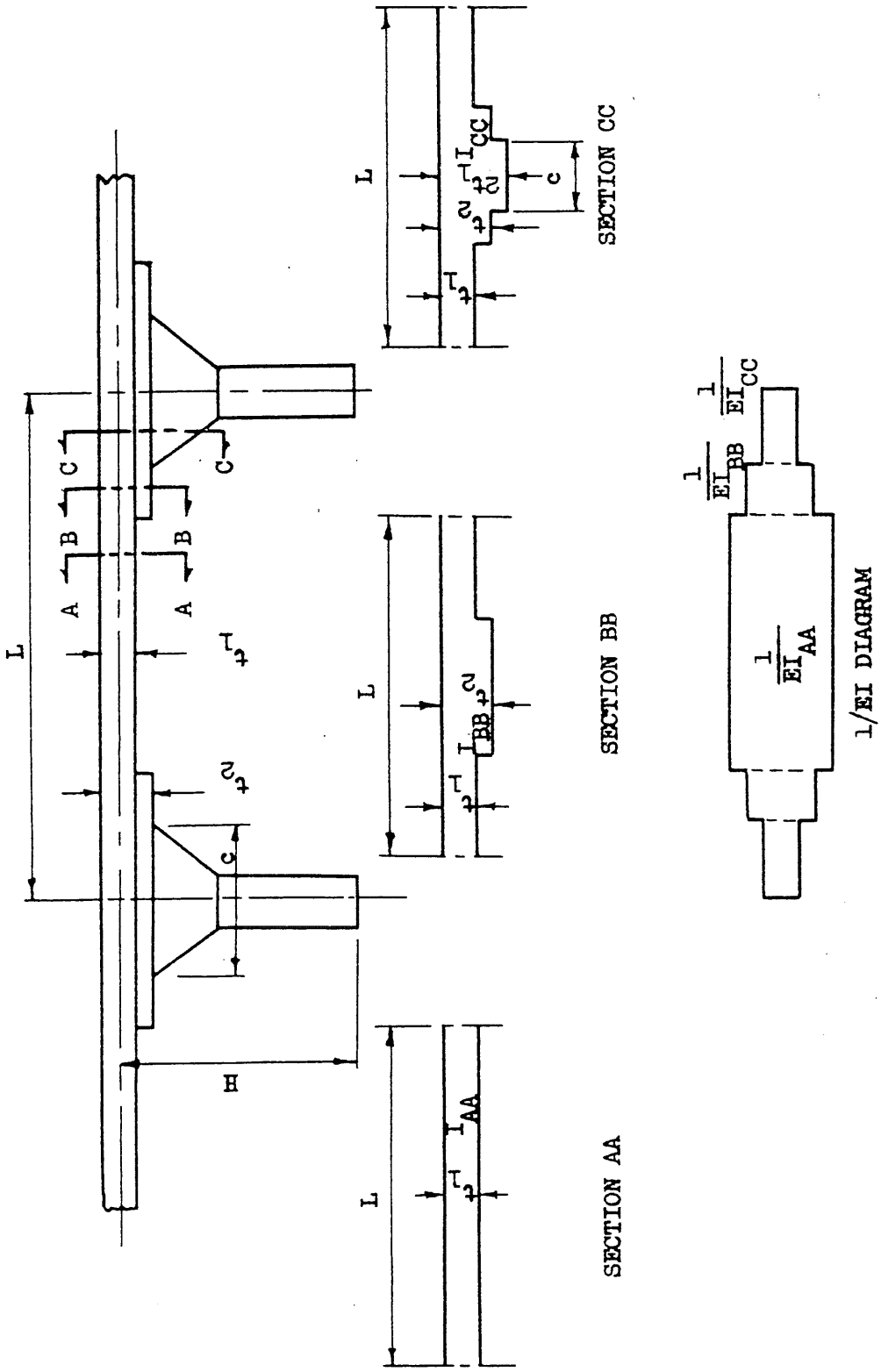

FIG. 52 DIMENSIONS OF CROSS SECTIONS USED IN PROPOSED FRAME ANALYSIS

POSITIVE MOMENTS IN INFINITE ARRAY OF UNIFORMLY LOADED PANELS

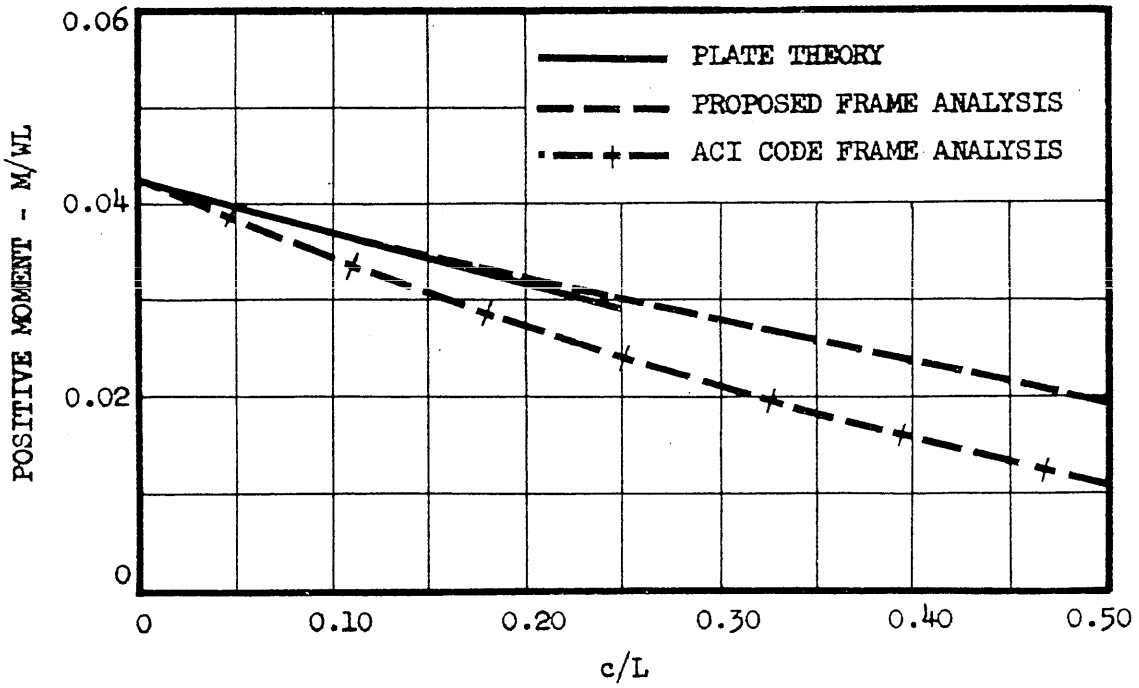

(a) PANELS WITH SQUARE COLUMN CAPITALS

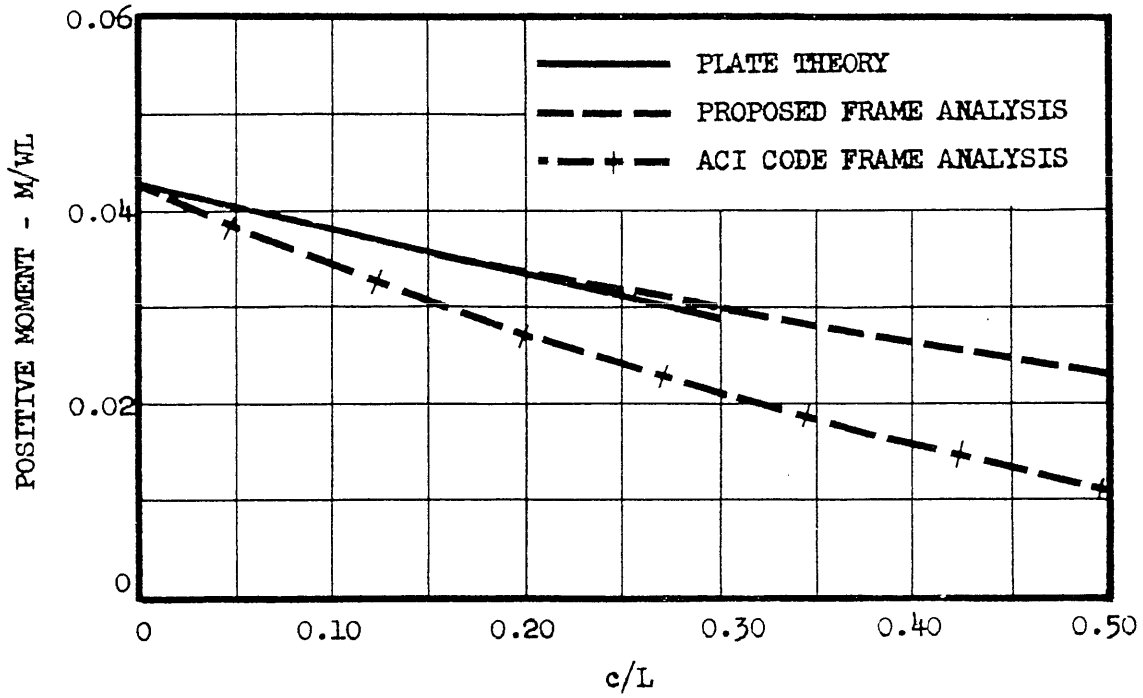

(b) PANELS WITH CIRCULAR COLUMN CAPITALS

FIG. 53 COMPARISON OF MOMENTS COMPUTED BY PROPOSED FRAME ANALYSIS WITH THOSE BY ACI FRAME ANALYSIS AND PLATE THEORY

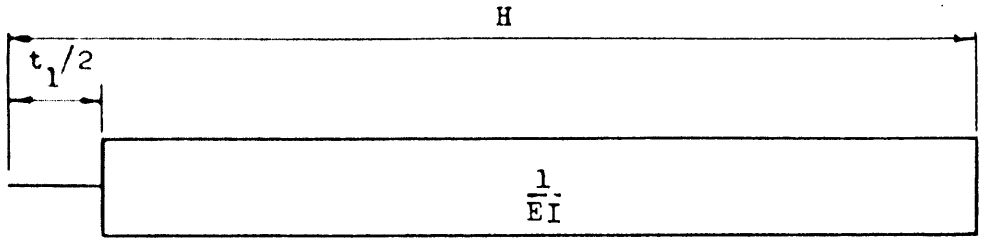

(a) 1/E I DIAGRAM OF INTERIOR COLUMN WITHOUT COLUMN CAPITALS

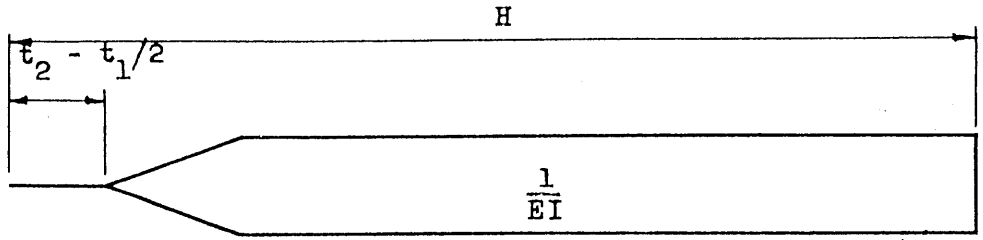

(b) IDEALIZED 1/EI DIAGRAM OF INTERIOR COLUMN WITH COLUMN CAPITALS

FIG. 54 1/EI DIAGRAMS OF INTERIOR COLUMNS WITH AND WITHOUT COLUMN CAPITALS

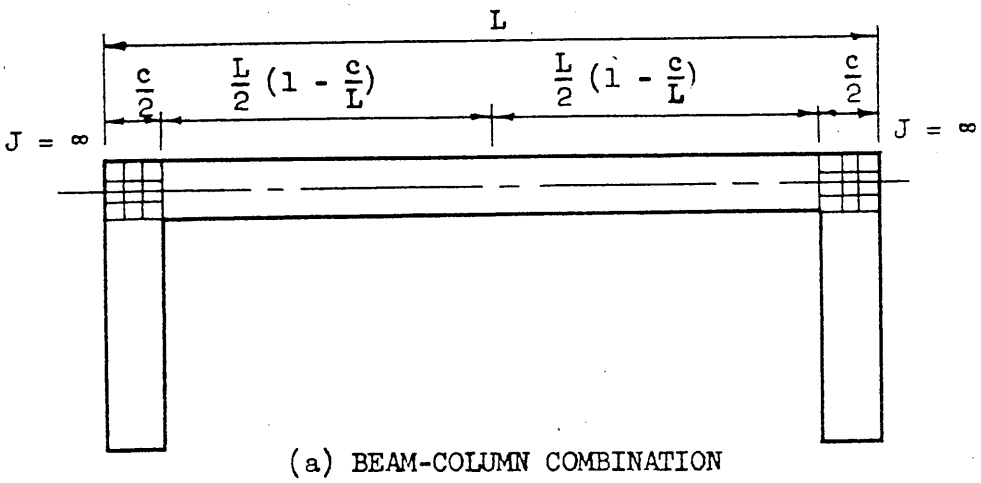

(a) BEAM-COLUMN COMBINATION

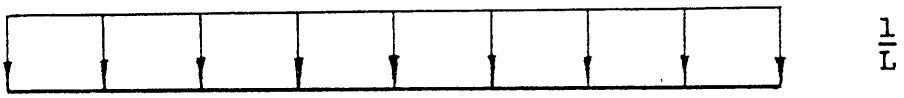

(b) TWISTING MOMENT APPLIED ALONG BEAM CENTERLINE

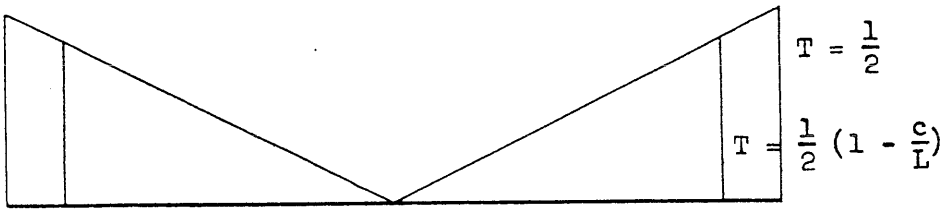

(c) TWISTING MOMENT DIAGRAM

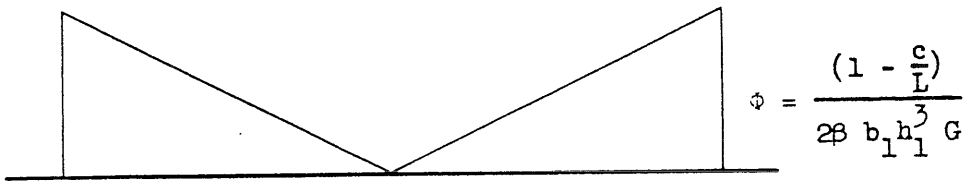

(d) UNIT ROTATION DIAGRAM

FIG. 55 ROTATION OF BEAM UNDER APPLIED UNIT TWISTING MOMENT

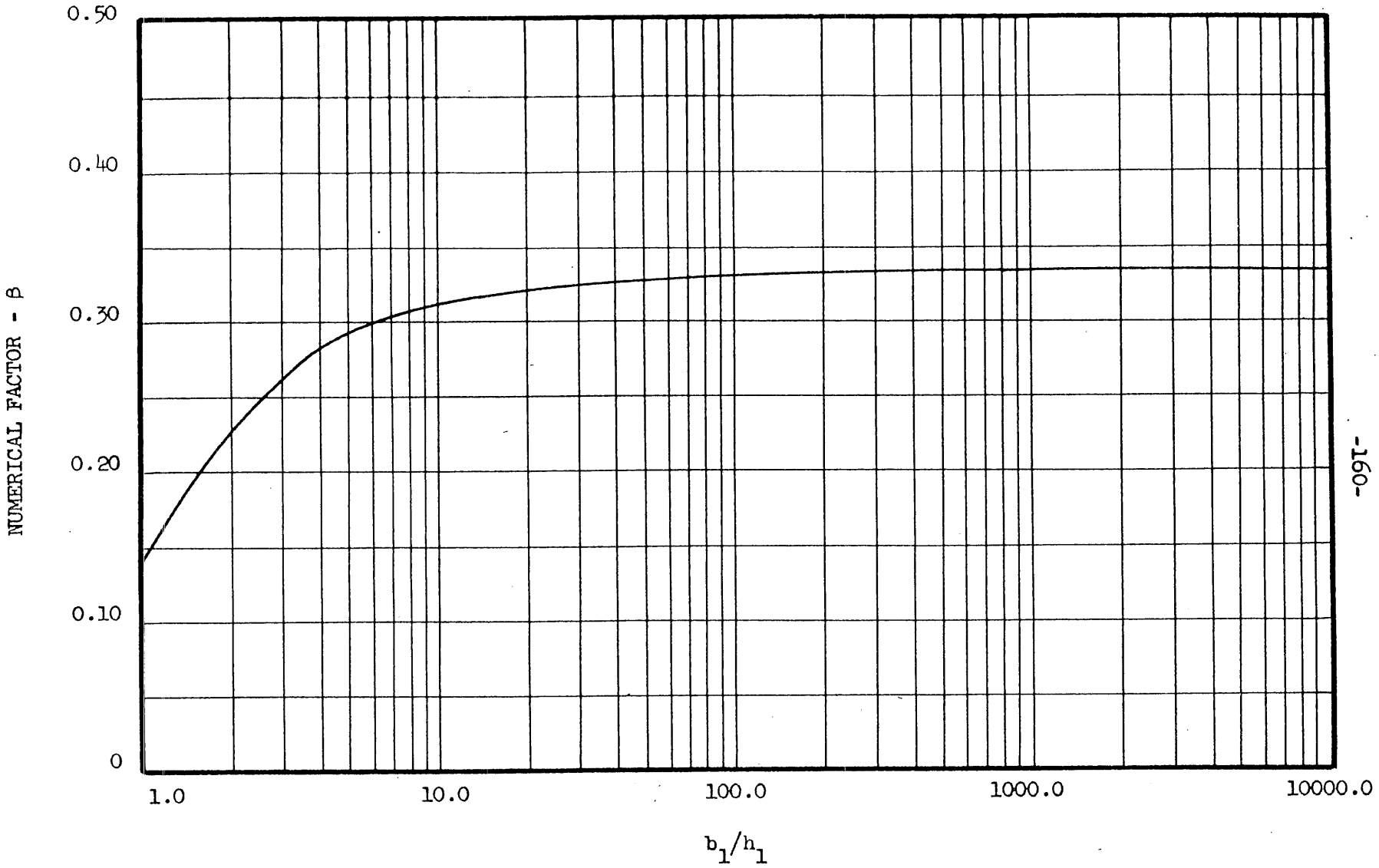

FIG. 56 CONSTANT FOR TORSIONAL ROTATION OF RECTANGULAR CROSS SECTION

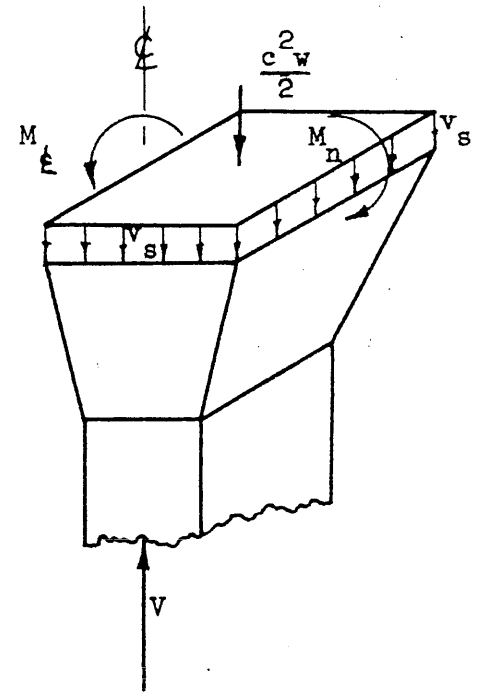

(a) TOP PORTION OF COLUMN

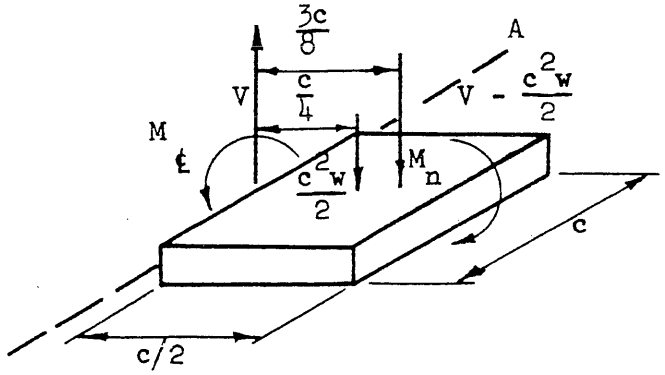

(b) FREE-BODY DIAGRAM OF CAPITAL

FIG. 57 FREE-BODY DIAGRAM FOR SQUARE COLUMN CAPITAL

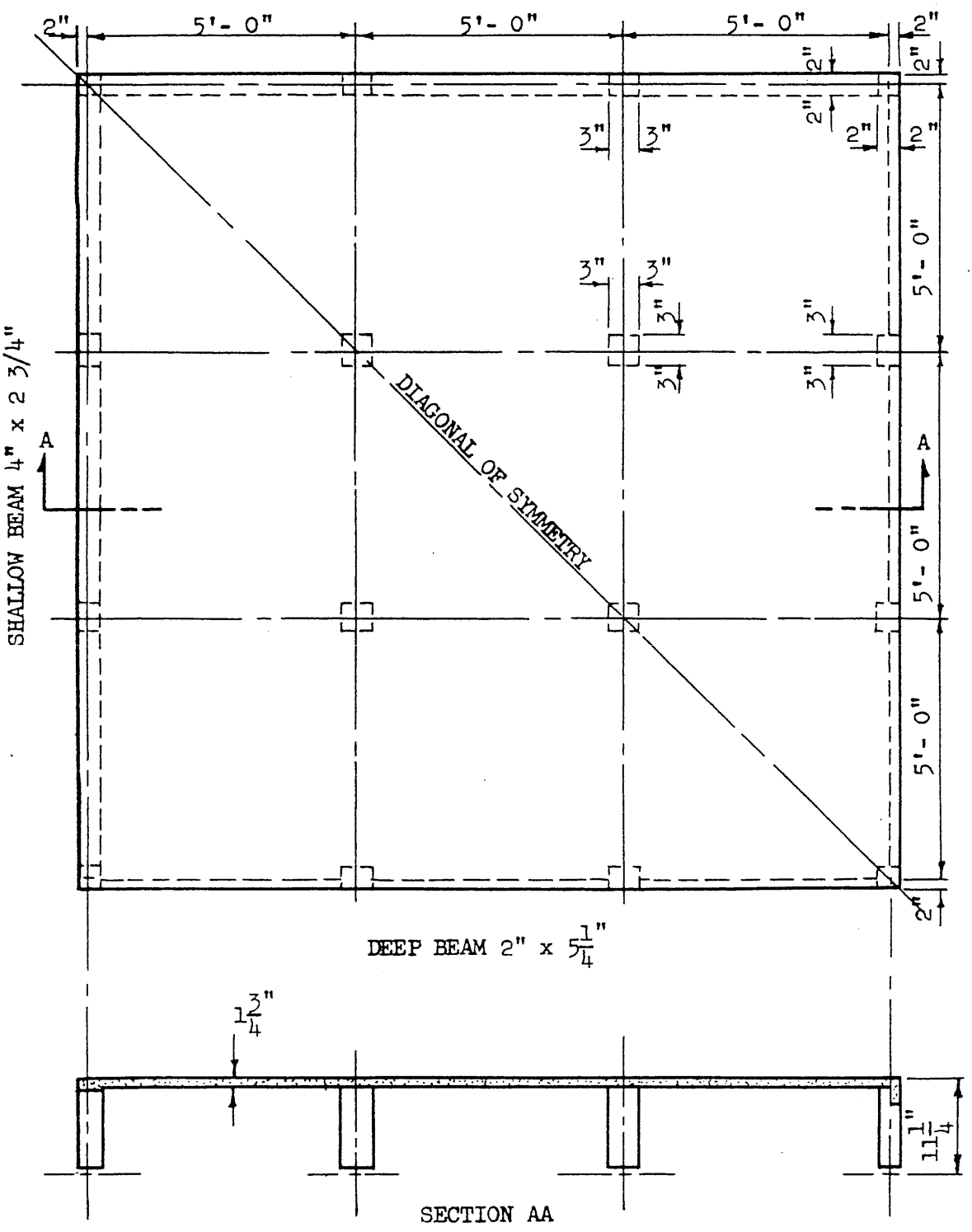

FIG. 58 LAYOUT OF NINE-PANEL REINFORCED CONCRETE FLAT PLATE

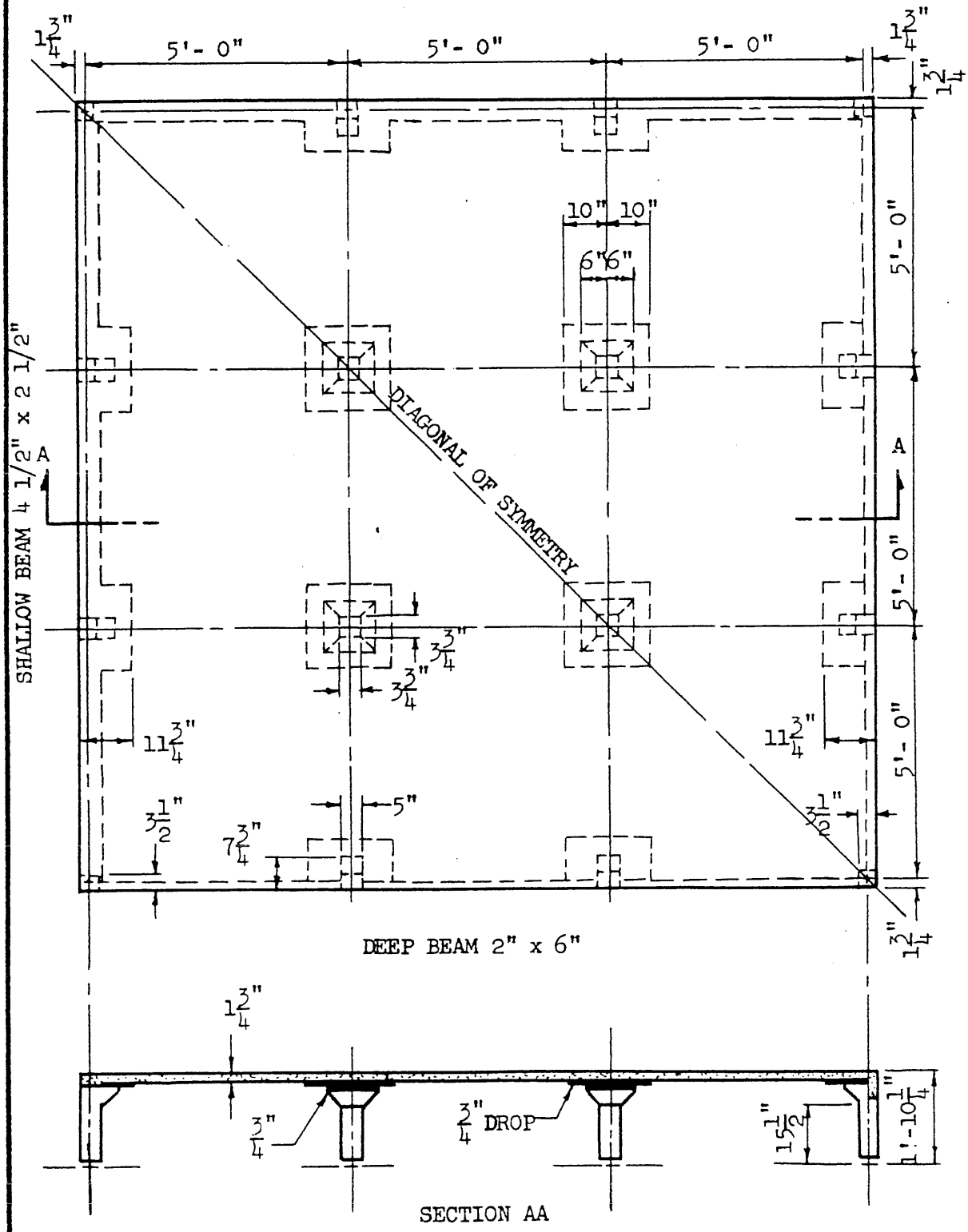

FIG. 59 LAYOUT OF NINE-PANEL REINFORCED CONCRETE FLAT SLAB

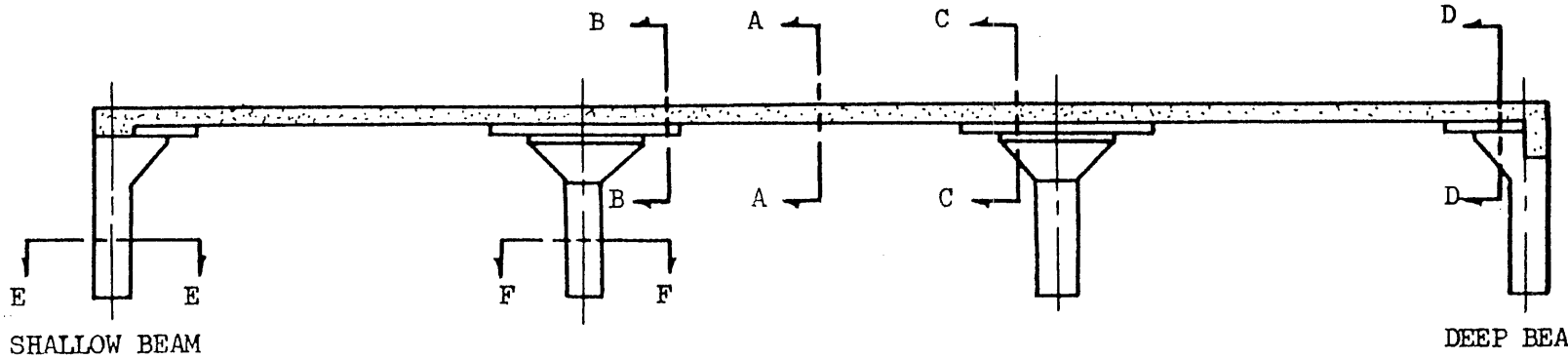

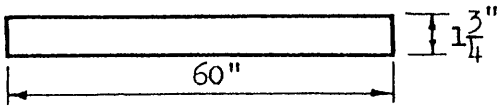

SECTION AA

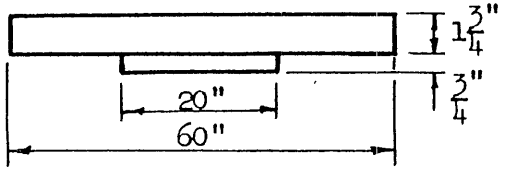

SECTION BB

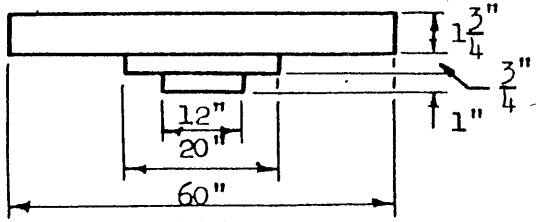

SECTION CC

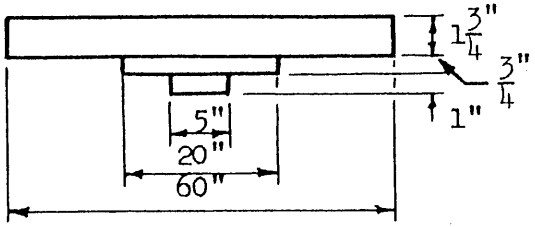

SECTION DD

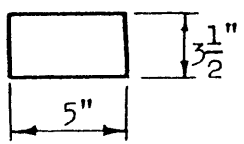

SECTION EE

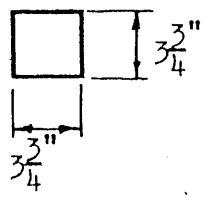

SECTION FF

FIG. 60 DIMENSIONS OF CROSS SECTIONS OF INTERIOR STRIP OF PANELS

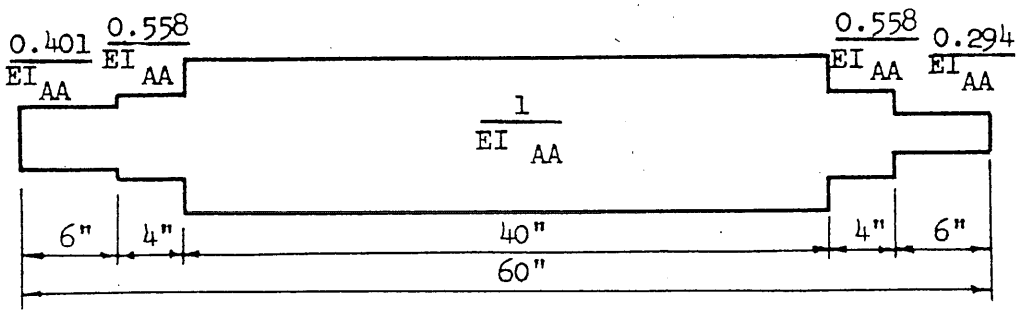

(a) EXTERIOR PANEL

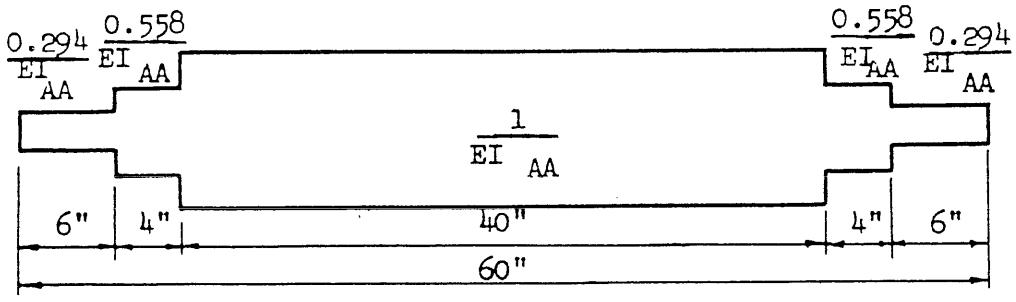

(b) INTERIOR PANEL

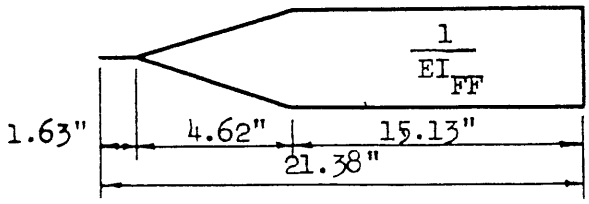

(c) INTERIOR COLUMN

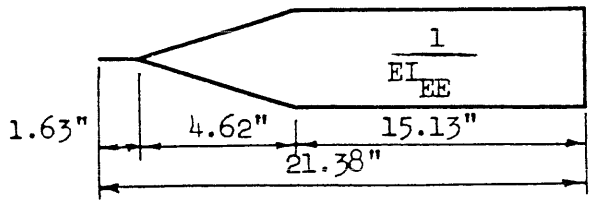

(d) EXTERIOR COLUMN

FIG. 61 1/EI DIAGRAMS FOR INTERIOR STRIP OF PANELS

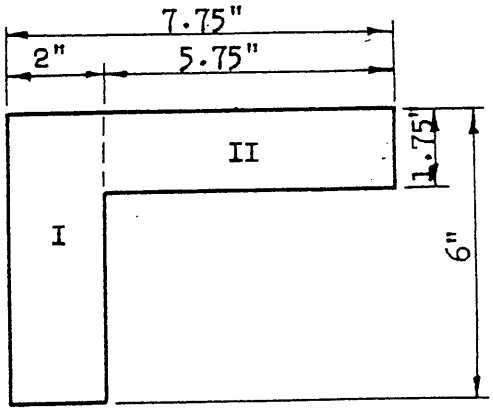

(a) DEEP BEAM

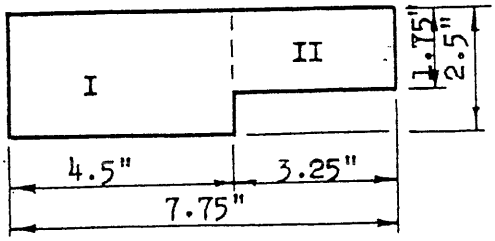

(b) SHALLOW BEAM

FIG. 62 DIMENSIONS OF CROSS SECTIONS OF EDGE BEAMS